The anti-cancer activity of extracts derived from millets and Kraalbos

Luqmaan Mohamed (MHMLUQ002)

Thesis presented for the degree of Master of Science in the Department of Human Biology

Faculty of Health Sciences
University of Cape Town

Supervisor: Professor Sharon Prince
Co-Supervisor: Professor Anwar Jardine
Co-Supervisor: Dr Suparna Chakraborty

10 February 2020

Declaration

I, Luqmaan Mohamed, hereby declare that the work on which this dissertation/thesis is based is my original work (except where acknowledgements indicate otherwise) and that neither the whole work nor any part of it has been, is being, or is to be submitted for another degree in this or any other university. I empower the university to reproduce for the purpose of research either the whole or any portion of the contents in any manner whatsoever.

Signed by candidate

Luqmaan Mohamed

10 February 2020

Acknowledgements

First and foremost, all praise is due to The Almighty for imbuing me with the strength, courage, patience and perseverance to complete this work.

Next, I would like to thank my parents for their undying love and support, especially during all the odd hours of the day and night. Indeed, their sacrifice does not go unnoticed and is by all means greatly valued.

I would also like to thank my family and friends for their continued support, encouragement and understanding. All of you have a share in this achievement as well.

It should go without saying that none of this would be possible without my supervisor, Professor Sharon Prince. It was under her able guidance that I was able to embark on this journey of learning. Her ideas and encouragement always served as a springboard to achieve new heights. Indeed her insight and passion for her work is, in my opinion, unrivalled. Thus, I would like to thank her for the opportunity she had afforded me and for seeing me through up until this point. Indeed, I am grateful to her for all this.

I would also like to thank my co-supervisor Professor Anwar Jardine for his contributions, especially with regards to the chemistry aspects of my work. His input, support, encouragement and wise words are much appreciated.

I am deeply indebted to my co-supervisor Dr Suparna Chakraborty for all her training, input and contributions. Undoubtedly, if it was not for her, I would not have been able to complete my experimental work.

There are many people who have selflessly offered their assistance along the way and I deem it necessary to acknowledge their contributions. Thus, I would like to thank Dr Lawrence Mabasa who introduced me to my project and helped me to settle in in the early days. To Desireé Bowers, for her initial training. To Dr Jade Peres, our lab manageress,

for always seeing to it that the lab was well stocked and for always being willing to assist if we needed anything. Indeed her patience knows no limits. To Kenza Sayah, for her contribution to the solubility and viability assays. To Mr Ronald Dreyer for his assistance with the FACS analysis. I would also like to thank Mrs Susan Cooper for her assistance with the microscopy work. Indeed, she is a doyen and her assistance is much appreciated. To Prof Leticia Costa-Lotufo for her invaluable feedback both in the early and late stages of my project. I would also like to thank Dr Devi Pradeep and Dr Hari Shankar for their assistance, collaboration and feedback on the millets work. I am also extremely grateful to Dr ArulJothi Nagarajan for his invaluable assistance with my experimental work and for reviewing my thesis.

I would also like to thank my lab mates. They were always willing to assist in whichever way possible and always offered their support. Indeed, my wonderful experience in the lab would not have been what it was without them. Their evolution was from unknown strangers to colleagues and finally, friends. Indeed, I owe a huge debt of gratitude to each one of them.

Finally, I would like to thank the NRF for their generous funding.

Table of contents

List of figures

List of tables

Abbreviations

°C	degrees celsius
%	percentage
ALL	acute lymphoblastic leukaemia
AMPK	5′ AMP-activated protein kinase
AMBRA1	autophagy and Beclin-1 regulator 1
AO	acridine orange
APAF1	apoptotic protease activating factor 1
ATM	ataxia telangiectasia mutated
ATR	ATM-Rad3-related
ATP	adenosine triphosphate
AU	arbitrary units
Bak	Bcl-2-antagonist/killer
Bax	Bcl-2-associated X protein
Bcl-2	B-cell lymphoma 2
Bcl-X_L	B-cell lymphoma- extra large
BRCA1	breast cancer 1
BRCA2	breast cancer 2
BSA	bovine serum albumin
CDK	cyclin dependant kinase
CDKI	cyclin dependant kinase inhibitor
CHK1	checkpoint kinase 1
CHK2	checkpoint kinase 2
cm	centimetre
cIAP1	cellular inhibitor of apoptosis protein 1
cIAP2	cellular inhibitor of apoptosis protein 2
CO_2	carbon dioxide
Cy3	cyanine 3
CYLD	cyclindromatosis
DAPI	4’,6-diamidino-2-phenylindole

DCIS	ductal carcinoma *in situ*
DDR	DNA damage response
DISC	death inducing signaling complex
DMEM	dulbecco's modified Eagle medium
DMSO	dimethyl dulfoxide
DNA	deoxyribonucleic acid
DSB	double stranded DNA breaks
EGCG	(-)-epigallocatechin-3-gallate
EGF	epithelial growth factor
EMT	epithelial to mesenchymal transition
ER	oestrogen receptor
FACS	fluorescence activated cell sorting
FADD	Fas-associated death domain
FasL	fatty acid synthetase ligand
FasR	fatty acid synthetase receptor
FBS	foetal bovine serum
FLIP	FLICE-like inhibitory protein
H & E	haematoxylin and eosin
GI	glycaemic index
GSH	glutathione
GST	glutathione S-transferase
HER2	human epidermal growth factor receptor 2
hERG	human ether-a-go-go-related gene
HPLC	high performance liquid chromatography
HPTLC	high performance thin layer chromatography
IC_{50}	half maximal inhibitory concentration
ICC	immunocytochemistry
IDC	invasive ductal carcinoma
ILC	invasive lobular carcinoma
kgbw	kilogram of body weight
LC3	microtubule-associated protein 1A/1B-light chain 3

LC-MS	liquid chromatography – mass spectroscopy
MAPK	mitogen-activated protein kinase
MLKL	mixed-lineage kinase-like protein
MOMP	mitochondrial outer membrane permeabilisation
MTT	3-(4,5-dimethylthiazol-2-yl)-2,5-diphenyl tetrazolium
M	molar
mg	milligram
ml	millilitre
mM	millimolar
mm	millmetre
mTOR	mechanistic target of rapamycin
NMR	nuclear magnetic resonance
p-p38	phosphorylated p38
PARP	poly (ADP-ribose) polymerase
PBS	phosphate buffered saline
PBST	phosphate buffered saline/tween
PCD	programmed cell death
PE	phosphatidylethanolamine
PI	propidium iodide
PI3K	phosphatidylinositol 3-kinase
PI3P	phosphatidylinositol 3-phosphate
PR	progesterone receptor
RIP1	receptor-interacting protein 1
RIP3	receptor-interacting protein 3
ROS	reactive oxygen species
RPMI	Roswell Parks Memorial Institute
SMAC	second mitochondrial-derived activator of caspases
SD	standard deviation
SDS	sodium dodecyl sulphate
SDS-PAGE	sodium dodecyl sulphate-polyacrylamide gel electrophoresis
SEM	standard error of the mean

SQSTM1	sequestosome 1
TBS	tris buffered saline
TBST	tris buffered saline/tween
TEMED	N,N,N’,N’,-tetramethyl-1-,2-diaminomethane
TLC	thin layer chromatography
TN	triple negative
TNF	tumour necrosis factor
TNFR	tumour necrosis factor receptor
TRADD	TNFR1 associated death domain
TRAF2	TNFR associated factor 2
TRAF5	TNFR associated factor 5
ULK1	Unc-51-like autophagy-activating kinase-1
ULK2	Unc-51-like autophagy-activating kinase-2
UV	ultraviolet
γH2AX	phosphorylated histone 2AX
µg	microgram
µl	microlitre
µM	micromolar

Abstract

Breast cancer is the second most commonly diagnosed cancer and the leading cause of cancer deaths in women. Several factors, such as the costs of anti-cancer drugs, drug resistance and relapse, make it difficult to treat this disease effectively. In the South African context this is exacerbated by poor socio-economic conditions. Thus, there is a dire need to develop novel anti-breast cancer drugs which are safe, effective and cheap. In this regard, natural products serve as a highly exploitable medicinal resource and indeed, many successful commercially available drugs have been derived from natural products. Plants, especially those used as food or medicine, are a particularly robust source of beneficial phytochemicals. Thus, this study investigated the anti-cancer effects of extracts derived from three varieties of African millets as well as from the indigenous Kraalbos plant, *Galenia africana*, against the MCF-7 oestrogen receptor positive and the MDA-MB-231 triple negative breast cancer cell lines.

The millet extracts tested were derived from *Sorghum bicolor* (Enforcer), *Pennisetum glaucum* (Babala) and *Eragrostis tef* (Tef) using both a reflux-based and a cold extraction procedure. MTT assays reveal that the millet extracts derived from the reflux-based extraction show no short-term cytotoxicity against both breast cancer cell lines tested. Extracts derived from the cold extraction were subjected to fractionation using HPTLC. Results from these extracts show that only the methanol fractions of the Babala and Enforcer millets exhibited short-term cytotoxic activity against the MCF-7 and the MDA-MB-231 breast cancer cell lines.

Five Kraalbos extracts (KB1, KB2, KB3, KB4 and KB5) were tested for their short-term cytotoxicity against the MCF-7 and MDA-MB-231 breast cancer cell lines. KB2 was found to display the most potent activity and its anti-cancer activity was characterized further. Clonogenic assays revealed that KB2 also displayed long-term cytotoxicity against breast cancer cells but not normal breast epithelial cells. Scratch motility assays and western blotting with antibodies to epithelial to mesenchymal transition markers showed that KB2 inhibited the migratory ability of breast cancer cells. To understand the mechanism(s)

underpinning the anti-cancer activity of KB2, ROS-Glo™ H_2O_2 and GSH-Glo™ Glutathione assays were performed and the results revealed that KB2 induced the production of reactive oxygen species. Furthermore, western blotting with antibodies to γH2AX showed that KB2 induced double strand DNA breaks in breast cancer cells. Flow cytometry and western blotting with antibodies to p53, p21, cyclin A and cyclin B1 further revealed that KB2 causes breast cancer cells to arrest in the S and G2/M phases. A sub-G1 peak, indicative of cell death, was also observed in the flow cytometry analyses. Indeed, using western blotting with antibodies to markers of apoptosis (caspases 3, 7, 8, and 9 and PARP) and necroptosis (p-MLKL and p-RIP3) KB2 was found to induce cell death via the intrinsic and extrinsic apoptotic pathways and necroptosis. Western blotting and immunocytochemistry with an antibody to LC-3 also showed that KB2 induces autophagy in the breast cancer cells but whether it functions as a pro-death or pro-survival mechanism remains to be elucidated.

Taken together, this study demonstrates that extracts derived from millets and Kraalbos show anti-cancer activity against oestrogen receptor positive and triple negative breast cancer cells and that KB2 is worth progressing to pre-clinical studies.

Chapter 1: Literature Review

1.1 Introduction

The global burden of cancer is so great that it has been dubbed the emperor of all maladies (Mukherjee, 2010; Reyes-aldasoro, 2017). In 2008 alone it was estimated that 7.6 million cancer deaths occurred and this figure rose to 8.2 million in 2012 (Jemal, Bray and Ferlay, 2011; Torre *et al.*, 2016). Similarly, the rate of cancer incidence has increased from 12.7 million new cancer cases in 2008 to 14.1 million new cases in 2012 (Jemal, Bray and Ferlay, 2011; Torre *et al.*, 2016). The latest estimates indicate that in 2018 there were 18.1 million new cancer cases and 9.6 million cancer deaths (Bray *et al.*, 2018). Thus, the global cancer burden is an ever increasing one. South Africa is no exception to this global epidemic. Despite the prevalence of diseases such as HIV/AIDS and tuberculosis, cancer is still ranked as the second leading cause of death in the country (Stefan, 2015). However, in the South African context the burden of cancer is exacerbated by poor socio-economic conditions. Although adequate treatment might be available, factors such prohibitive costs and lack of infrastructure result in preventable cancer deaths (Vanderpuye and Yarney, 2014). The true impact of cancer in South Africa, and indeed Africa, may not yet be fully realized due to poor implementation of cancer surveillance systems (Parkin *et al.*, 2014; Stefan, 2015). In addition to this, it should also be considered that cancer has a knock-on effect on social and economic conditions.

This literature review provides a general overview of key areas of research relevant to the focus of this thesis.

1.2 Breast cancer

Breast cancer is the second most commonly diagnosed cancer in women globally and it is the most commonly diagnosed cancer as well as the leading cause of cancer deaths in women in Africa (Parkin *et al.*, 2014; Torre *et al.*, 2016; Bray *et al.*, 2018). Although breast cancer may affect both women and men, it occurs far more frequently in women. Of

concern, there is a disparity between breast cancer incidence in developed and developing countries. Although incidence and mortality due to breast cancer are decreasing in developed countries, they are increasing in developing countries (Jemal, Bray and Ferlay, 2011; Ferlay *et al.*, 2015). These disparities exist primarily due to poor socio-economic conditions which are associated with a lack of public awareness, early detection services and well-equipped hospitals.

1.2.1 Risk factors for breast cancer

Various factors, often linked to hormones and reproduction, can place a woman at risk of breast cancer. These include a long menstrual history, nulliparity, use of postmenopausal hormone therapy and contraceptives, late age of first birth, late age of menopause and early menarche (Jemal, Bray and Ferlay, 2011; Anderson, Schwab and Martinez, 2014; Sun *et al.*, 2017). Family history is also an important risk factor as a women's risk of contracting breast cancer doubles if she has a first-degree relative (mother, sister or daughter) with breast cancer. The most common cause of hereditary breast cancer is mutations in the breast cancer 1 and 2 (BRCA1 and BRCA2) genes (de Jong *et al.*, 2002; Sun *et al.*, 2017; Feng *et al.*, 2018). Mutations in several other genes such as TP53, CHEK2, PTEN, ATM and HRAS have also been implicated in breast cancer etiology (de Jong *et al.*, 2002; Balmana, Diez and Castiglione, 2009; Skol, Sasaki and Onel, 2016). Several lifestyle factors could aid in mitigating the risk of breast cancer diagnosis such as maintaining a healthy weight, not smoking, physical activity and moderate alcohol consumption (Torre *et al.*, 2016).

1.2.2 The structure of the breast

The breast is made up of a dense matrix of connective and fatty tissues which contain and support the mammary glands and it has a rich supply of blood and lymphatic vessels **(figure 1.1)**. The glandular tissue of the breast consists of lobes made up of lobules which in turn are made up of clusters of alveoli which are lined by mammary secretary epithelial cells. The alveoli drain into a network of ducts which exit onto the skin at the nipple. Each

duct is also lined with mammary secretary epithelial cells and is surrounded by an outer layer of myoepithelial cells which possess contractile properties. The breast adipose tissue is situated between lobes (Ali and Coombes, 2002; Zucca-matthes, Urban and Vallejo, 2016).

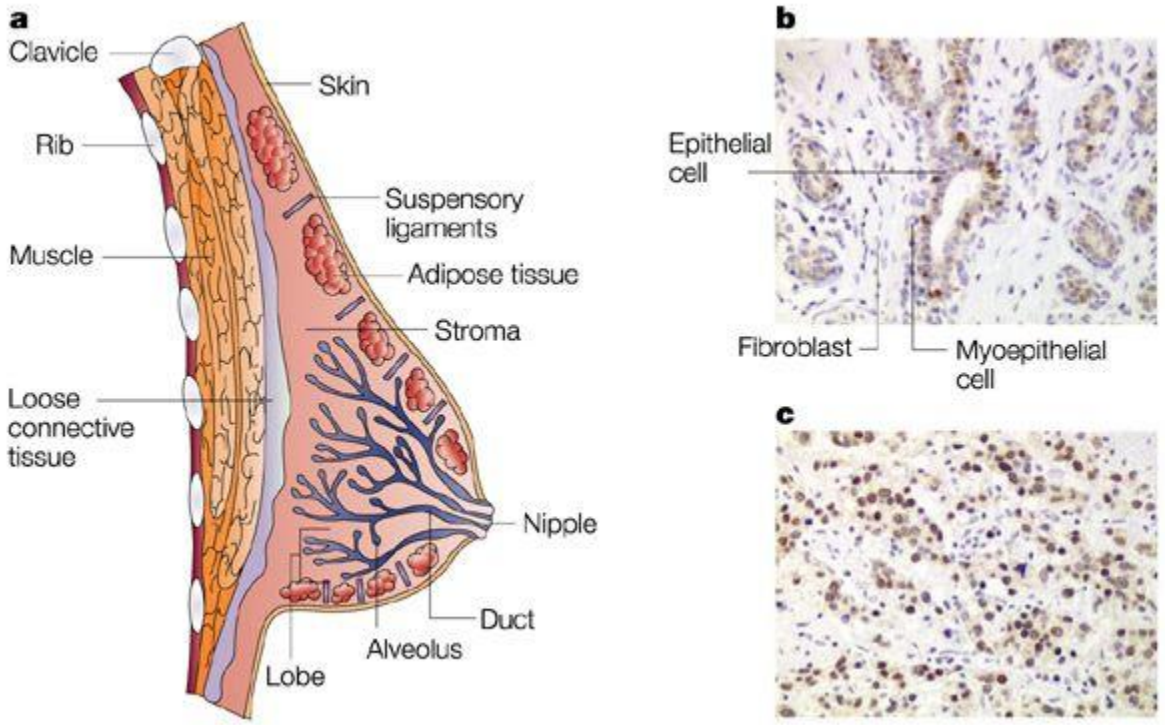

Figure 1.1: The structure of normal and malignant breast tissue. (A) The mammary glands, embedded in the connective and fatty tissues in the breast, are made up of clusters of alveoli which form lobes. The lobes are separated by adipose tissue and rain into a network of ducts which exit onto the skin at the nipple. **(B)** Each duct is also lined with mammary secretary epithelial cells and is surrounded by an outer layer of myoepithelial cells, which possess contractile properties, and embedded in the fibroblast stroma. **(C)** The normal structure of the breast breaks down in cancer and gives rise to an epithelial mass. Figure taken from Ali and Coombes (2002).

1.2.3 Classification of breast cancer

Breast cancers can be classified according to where in the breast they originate and their level of invasiveness as well as the expression of surface receptors **(figure 1.2)**. Ductal

carcinoma *in situ* (DCIS) originates within the ducts of the breast and is generally non-invasive. Invasive ductal carcinoma (IDC) and invasive lobular carcinoma (ILC) spread outside of the ducts and lobes into the surrounding stromal tissue and have the potential to become metastatic. Metastatic or advanced breast cancers are late stage cancers in which the cancer spreads from the breast tissue to other parts of the body, most commonly the bones, liver, lymph nodes, lungs and brain (Feng *et al.*, 2018).

The classification of breast cancer based on the expression of certain cell surface receptors is useful for the purposes of screening, managing and treating the disease. Indeed, breast cancer can be divided into the oestrogen receptor positive (ER+), human epidermal growth factor receptor 2 positive (HER2+) and triple negative (TN) subtypes. ER+ breast cancers can be further divided into luminal A and luminal B with luminal A being the more common and less aggressive. Unlike the ER+ and HER2+ subtypes, the TN subtype (also known as basal-like) lacks hormone receptors and is therefore not amenable to hormone therapy. Of all breast cancer subtypes, ER+ is associated with the best clinical outcome and TN is associated with the worst clinical outcome (Dent *et al.*, 2007; Anderson, Schwab and Martinez, 2014).

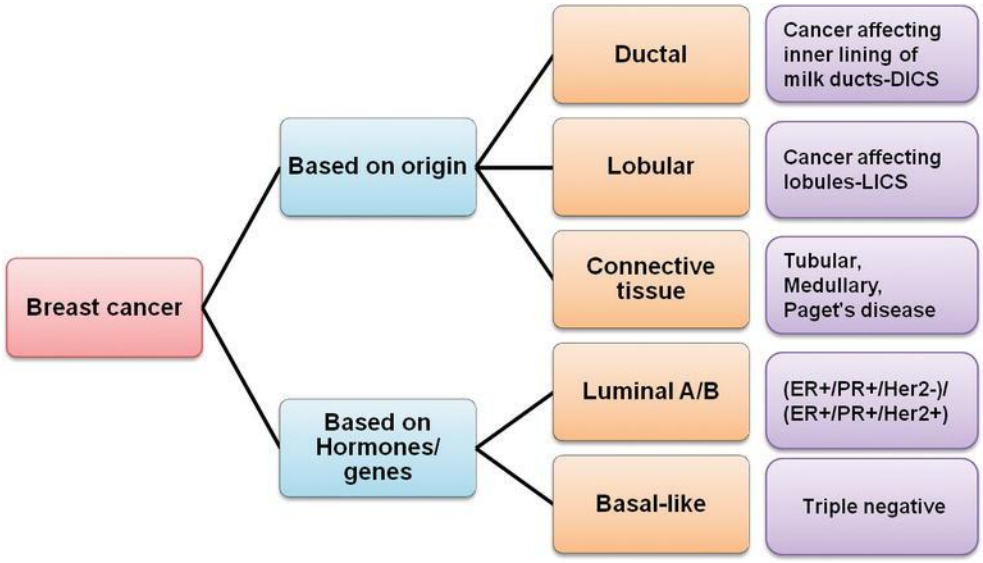

Figure 1.2: The classification of breast cancer based on its origin and hormone receptors. Breast cancer can be classified according its origin in the breast i.e. the ducts, lobes or connective tissue. Similarly, breast cancer can also be classified by the presence or absence of the oestrogen, progesterone and human epidermal growth factor 2 receptors. Figure taken from Aiyengar, Chiranjeevi and Rani (2017).

1.2.4 Current therapies to treat breast cancer

Although treatment for breast cancer is dependent on the type and stage of the cancer, common treatments involve surgery, chemotherapy, hormone therapy, immunotherapy and radiotherapy (Majeed *et al.*, 2014). For non-metastatic cancers, the aims of therapy are to eradicate the tumours from the breast as well as the regional lymph nodes to avoid recurrence. However, metastatic breast cancers are not easily treated and treatment is administered as a palliative measure (Waks and Winer, 2019).

The classification of breast cancer according to hormone receptor status has proven clinically useful for treatment and prognosis (Osborne *et al.*, 1980). For example, tamoxifen is used to treat ER+ breast cancers, as it acts as an antagonist to the oestrogen receptor. Similarly, letrozole, anastrozole and exemestane are used to treat ER+ breast cancers and act by blocking the production of oestrogen (Condorelli and Vaz-luis, 2018). Trastuzumab (Herceptin) and pertuzumab are monoclonal antibodies which are used to

treat HER2+ breast cancers (Charlton and Spicer, 2015; Bettaieb *et al.*, 2017). TN metastatic breast cancer is treated using a chemotherapy regimen consisting of a combination of drugs such adriamycin, cyclophosphamide, docetaxel and paclitaxel (Waks and Winer, 2019).

Targeted therapy refers to any therapeutic which interferes with a specific molecule(s) that is critical for the survival of cancer cells and which promotes drug resistance (Mishra and Parikh, 2006). The advent of targeted therapy has made it possible to not only treat breast cancer according to hormone receptor status but has also led to personalized treatment approaches based on the genetic makeup of individual cancer tumours. This can be achieved by targeting key pathways within cancer cells such as the phosphoinositide 3-kinase (PI3K)/protein kinase B (AKT)/ mechanistic target of rapamycin (mTOR) pathway. For example, the use of ONC201, an AKT inhibitor, has been shown to induce cell death in many cancers including TN breast cancer (Chan, Tan and Dent, 2019). Such therapies are advantageous as it specifically attacks cancerous cells with minimal toxicity to normal cells. However, intratumoral and intertumoral heterogeneity pose a great challenge for precision therapy and has prevented it from becoming widespread (Bettaieb *et al.*, 2017; Zhang, Yang and Zhang, 2019). Furthermore, off target effects are a major concern. For example trastuzumab is associated with cardiotoxicity as cardiac myocytes also express HER2 (Suter, Cook-bruns and Barton, 2004). Therefore, there is a need to develop new drugs which are effective in eradicating breast cancer with little to no side effects.

1.3 Natural products

The idea of looking towards nature in order to treat disease is by no means new. Indeed, the natural world can be viewed as a vast reservoir of potentially useful compounds because it has an outward diversity which is underpinned by chemical diversity. The potential of this reserve is largely unrealised and thus a need exists to mine the natural world for such compounds. Natural products are a known source of medicinal agents which are often associated with less side effects than synthetic drugs (A. K. Singh *et al.*,

2017; Banerjee *et al.*, 2018). They are secondary metabolites which may be produced by plants, bacteria and marine organisms. As secondary metabolites they are not essential to the survival of these organisms but may display activity in other biological systems. The biological targets of natural products are often evolutionarily conserved, enabling molecules produced in one biological setting to exert an effect in another (Paterson and Anderson, 2005). However, given the current landscape of drug discovery and treatment viz. high throughput screening and personalised medicine, the relevance of screening natural products is often questioned. Furthermore, pharmaceutical companies prefer rational drug design and screening pre-existing libraries for new applications as opposed to the slow process of identifying complex novel structures derived from natural products (Bailly, 2009; Li and Vederas, 2009). However, the screening of libraries often produce multitudes of hits which still require biological validation (Rishton, 2008). Importantly, natural products may also display targeted activities with few side effects and thus may still be a good source of therapeutics for use in targeted medicine (Bailly, 2009).

Several commonly used medications such as morphine, from the opium plant, and penicillin, from the penicillium mould, are natural products. Furthermore, natural products have served as templates for the rational design of drugs. For example, the structure of salicylic acid, from willow bark, has been modified to form aspirin. Similarly, the analgesic medications codeine and oxycontin have been modelled after the structure of morphine (Rishton, 2008; Li and Vederas, 2009). Thus, the avenue of using natural products as a springboard to find anti-cancer drugs is likely to be successful. Indeed, the screening of the natural world for anti-cancer drugs has already yielded success. For example, the vinca alkaloids vincristine and vinblastine, used to treat a broad range of cancers, have been derived from the Madagascan periwinkle plant (*Catharanthus roseus*) (Kumar, 2016). Similarly, trabectedin (Yondelis), used to treat sarcomas, was isolated from the sea squirt *Ecteinascidia turbinate* (Cuevas and Francesch, 2009). Furthermore, the widely used cancer drugs paclitaxel (isolated from the bark of the Pacific Yew tree *Taxus brevifolia*) and docetaxel (synthesised from needles of the European Yew tree *Taxus baccata*) are also natural products and are used to treat both early stage and metastatic

breast cancers (Crown, O'Leary and Ooi, 2004; Saloustros, Mavroudis and Georgoulias, 2008).

Plants are especially important as foods and medicines because they are a robust source of beneficial phytochemicals such as saponins, phenolics and anthocyanins, all of which have known health benefits (Verhoeckx *et al.*, 2015; Ibidapo *et al.*, 2019). Thus, this review will focus on the health benefits of millets, which are a staple food in many countries, and Kraalbos, an indigenous South African plant used in traditional medicine.

1.4 Millets

Millets are small-seeded crops which belong to the family *Poaceae* and are farmed as a subsistence crop in parts of Africa and Asia **(figure 1.3)**. They are a popular food in many African and Asian countries where they are often milled into flours and used in the production of several varieties of flatbreads and the like (Singh and Sarita, 2016). Although they are commonplace in the Africa and the Orient, in the western world millets are regarded as 'health food' or 'super food' and is often incorporated into special diets or used as a supplement to other 'health foods' such as Goji berries, quinoa, etc. Indeed, millets are known for their health benefits such as lowering blood pressure and decreasing the risk of cardiovascular disease (Amadou, Gounga and Le, 2013; Taylor and Duodu, 2015; Singh and Sarita, 2016). Coupled to this, millets are known to be a source of beneficial phytochemicals, such as phenols, tannins, flavonoids and saponins, which are known antioxidants and some exhibit anti-cancer activities (Rao, Nagasampige and Ravikiran, 2011; Mathanghi, 2012). Despite the presence of such compounds in millets, evidence is limited that the consumption of millets provides any net benefit to overall health (Driessche, Plat and Mensink, 2018).

This review will focus on the health benefits of three African varieties of millets viz, *Sorghum bicolor* (Enforcer), *Pennisetum glaucum* (Babala) and *Eragrostis tef* (Tef).

<u>Figure 1.3:</u> Examples of different varieties of millet crops (A) and their seeds (B).

1.4.1 Enforcer

Enforcer (also known as sorghum or great millet) is an African millet which is farmed in tropical and subtropical regions and commonly used as in the preparation of food, animal feed and ethanol production **(figure 1.4)**. Enforcer has been shown to be a rich source of beneficial phytochemicals, especially 3-deoxyanthocyanins, tannins and polycosanols (Moraiscardoso *et al.*, 2017). Indeed, 3-deoxyanthocyanins are peculiar to Enfocer millets and have been shown to exhibit cytotoxicity against breast cancer cells (Suganyadevi, Saravanakumar and Mohandas, 2013; Rao *et al.*, 2018). The consumption of Enforcer has also been shown to reduce the risk of colorectal cancer in mouse models (Yang *et al.*, 2019). Furthermore, polyphenol rich extracts derived from Enforcer have shown antimutagenic properties in *Salmonella typhimurium* and *Drosophila melanogaster* models (Grimmer, Parbhoo and Mcgrath, 1992). Thus, Enforcer has properties which would make it suitable for both chemopreventative and chemotherapeutic applications.

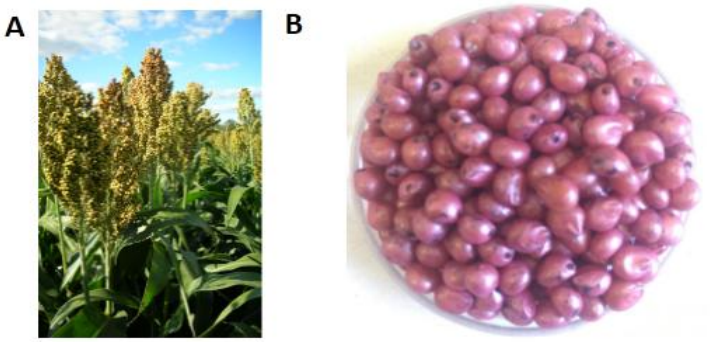

<u>Figure 1.4:</u> The Enforcer (*Sorghum bicolor*) crop (A) and its seeds (B)

1.4.2 Babala

Babala (also known as pearl millet) is a drought tolerant crop which is cultivated and consumed in West Africa and India **(figure 1.5)**. It is a known source of dietary antioxidants, such as flavonoids and phenolics, which have been associated with numerous health benefits including anti-aging and protection against cardiovascular and neurodegenerative diseases (Nambiar *et al.*, 2012; Siroha and Sandhu, 2017). In addition to its phytochemical content, Babala also has a high fibre content, low glycaemic index (GI) and is gluten free and is therefore recommended in the treatment and management of constipation, diabetes and celiac disease (Nambiar *et al.*, 2011). Indeed, Nani *et al.* (2015) showed polyphenols and lipids from Babala to exhibit immunosuppressive effects suggesting its use in the treatment of autoimmune diseases. Furthermore, extracts derived from Babala have been shown to exhibit anti-proliferative properties against HT-29 colon cancer cells (Chandrasekara and Shahidi, 2011a, 2011b). Given these and other properties of Babala, it has gained attention in the public eye as a dietary supplement for the treatment of certain diseases and the improvement of general health (Siroha and Sandhu, 2017; Ibidapo *et al.*, 2019).

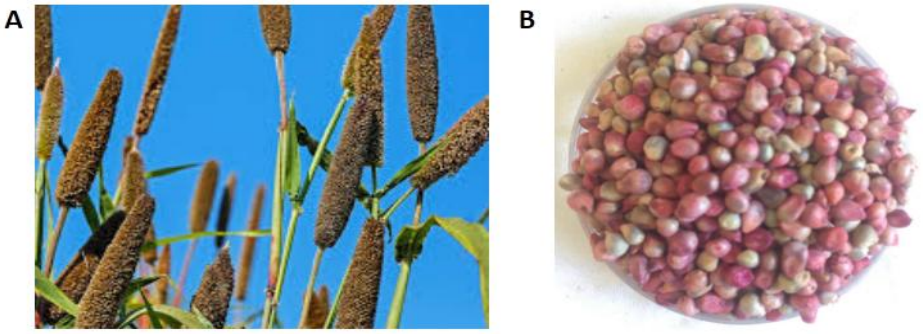

<u>Figure 1.5:</u> The Babala (*Pennisetum glaucum*) crop (A) and its seeds (B)

1.4.3 Tef

Tef is an important staple crop in Ethiopia and Eritrea and its seeds are used in the preparation of flatbreads (e.g. injera) and alcoholic beverages (e.g. tella). Like other millets, Tef is a reservoir of phenolic compounds with ferulic, vanillic, cinnamic, coumaric and protocatechuic acids being the most predominant (Dykes and Rooney, 2007; Gebremariam, Zarnkow and Becker, 2014). Furthermore, Tef has a high protein and fibre content and is gluten free and is therefore often used in nutrient fortified gluten free foods (Gebremariam, Zarnkow and Becker, 2014). Interestingly, Tef has a high iron content and the low incidence of anaemia in Ethiopia has been attributed to the consumption of Tef (Satheesh and Fanta, 2018). Hydroalcoholic Tef extracts have also displayed antimutagenic effects and this may be due to its high mineral, amino acid and fatty acid content (Goerch *et al.*, 2019). Although these show value of Tef as a dietary supplement in the context of several disease, its anti-cancer effects have not previously been investigated.

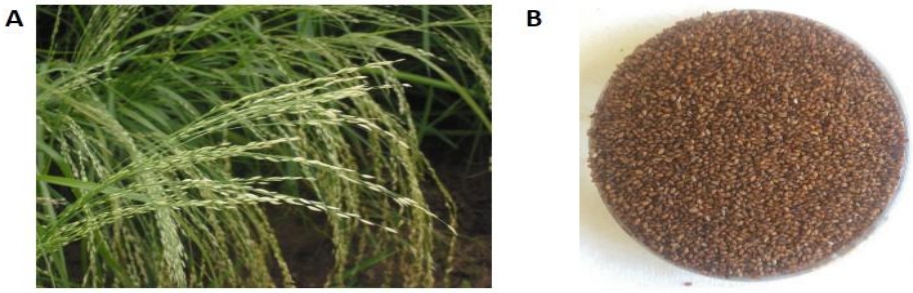

Figure 1.6: The Tef (*Eragrostis tef*) crop (A) and its seeds (B)

1.5 Kraalbos

The South African landscape is replete with indigenous plants which hold great cultural and medicinal value. Among these plants is the *Galenia africana* shrub **(figure 1.7)**, more commonly known as Kraalbos or Geelbos. Kraalbos is a perennial shrub belonging to the *Aizoaceae* family, is indigenous to southern Africa and is found mainly in the Namaqualand and Karoo regions (De Beer and Van Wyk, 2011). It is thought to have several medicinal properties and has been traditionally used to treat a variety of ailments such as skin rashes, eye infections, dandruff and dry scalp, coughs and wounds (Van Wyk, De Wet and Van Heerden, 2008; De Beer and Van Wyk, 2011). The Kraalbos plant is also a known analgesic used to treat toothaches and has even been used to treat respiratory conditions such as asthma and tuberculosis (Mativandlela *et al.*, 2008, 2009; De Beer and Van Wyk, 2011). This versatility in the traditional use of Kraalbos shows its value as a medicinal agent. Indeed, the panacea like status of Kraalbos among the indigenous people has been the impetus for the investigation of its medicinal properties and several studies have demonstrated the activity of Kraalbos extracts against a broad variety of biological pathogens. For example, Elbagory *et al.* (2017) reported that gold nanoparticles encasing an aqueous Kraalbos extract exhibited anti-microbial properties against *Pseudomonas aeruginosa*. Kraalbos was also shown to exhibit antimycobacterial effects against both *Mycobacterium smegmatis* and *Mycobaterium turberculosis* (Mativandlela *et al.*, 2008, 2009). Similarly, Kraalbos has been reported to display antifungal activity against a the fungal pathogen *Botrytis cinerea*, a common cause of

food spoilage (Vries *et al.*, 2005; Fielding *et al.*, 2015). Thus, the anecdotal value of Kraalbos as a medicinal agent seems to have growing pool of scientific literature to support such claims. However, there are only two studies which have reported on the anti-cancer activity of Kraalbos (Shoko, 2010; Ng'uni, 2017).

Figure 1.7: The Kraalbos plant (*Galenia africana*)

1.6 The DNA damage response

The integrity of DNA is essential for the survival and propagation of cells and therefore when a cell's DNA is damaged, the cell will either attempt to repair it or initiate a program of cell death (Giglia-mari, Zotter and Vermeulen, 2011; Shaltiel *et al.*, 2015). Hence, the response mounted by cells in the event of DNA damage lies upstream of cell death pathways. Many anti-cancer drugs take advantage of this by causing DNA damage, either directly or indirectly. For example, metal-based drugs such as cisplatin damage DNA directly by chelating DNA to its metal center. Other modes of DNA damage exerted by anti-cancer drugs can be more subtle and may involve the production of reactive oxygen species (ROS) (Lord and Ashworth, 2012).

Double strand DNA breaks (DSBs) are a common form of DNA damage and many anti-cancer compounds exert their activity by inducing DSBs (Jekimovs *et al.*, 2014). The DNA damage response (DDR) is mediated through the activation of ataxia telangiectasia mutated (ATM), in the case of double strand breaks, and ATM-Rad3-related (ATR), in the case of single strand breaks **(figure 1.8)**. These drive the accumulation of the

phosphorylated version of the histone variant H2AX, referred to as γH2AX, at the site of DNA damage and therefore γH2AX is considered a robust marker of DNA damage (Valdiglesias *et al.*, 2013). ATM phosphorylates H2AX thereby amplifying the DNA damage signal (Tšuiko *et al.*, 2019). Furthermore, ATM acts as a transducer which facilitates the activation of the checkpoint kinase CHK2 and they both converge on the tumour suppressor p53 which mediates the decision of the cell to either repair the damaged DNA or to initiate programmed cell death if the damage is too severe (Shaltiel *et al.*, 2015). The p38 mitogen activated protein kinase (MAPK) is also phosphorylated in response to DSBs. This allows for its nuclear localization and activation of its substrates which include cell cycle checkpoints and DNA repair. Phosphorylated p38 (p-p38) also activates p53, amplifying the DDR (Wood *et al.*, 2009). The cyclin dependent kinase inhibitor (CDKI) p21 is a key downstream target of p53. It plays a multifunctional role in the cell and is known to inhibit cell cycle progression by inhibiting cyclin/cdk complexes (Johnson and Walker, 1999). This results directly in the arrest of the cell cycle and may eventually lead to cell death.

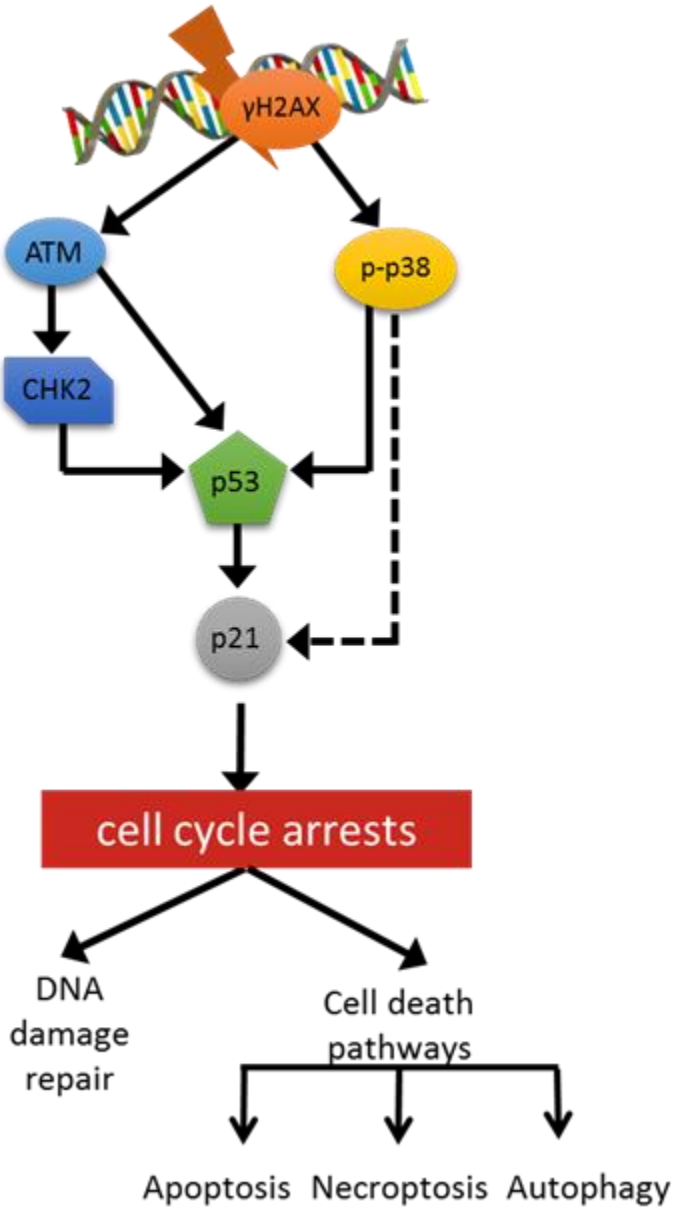

Figure 1.8: An overview of the cascade of events in response to DNA damage. Figure adapted from the PhD thesis of Bleloch (2019).

1.7 Cell death

There are different modes of cell death including apoptosis, autophagy and necrosis, and those induced by anti-cancer therapies are of pharmacological importance. Indeed, it is becoming increasingly apparent that to be effective cancer therapies need to induce

multiple modes of programmed cell death (Aguadé-gorgorió and Bornhauser, 2016). Cell death pathways have been classed according to distinct morphological **(figure 1.9)** and molecular features. For example, apoptosis and autophagy have been classed as type I and type II programmed cell death pathways respectively (Galluzzi *et al.*, 2007; Ouyang *et al.*, 2012). In contrast to apoptosis and autophagy, necrosis was initially thought of as an accidental mode of cell death. However, evidence has emerged that necrosis can also be a programmed mode of cell death, with one example being necroptosis, which has been classed as type III programmed cell death (Galluzzi *et al.*, 2007; Ouyang *et al.*, 2012). Although other modes of cell death have been described, this review will focus on apoptosis, autophagy and programmed necrosis (necroptosis).

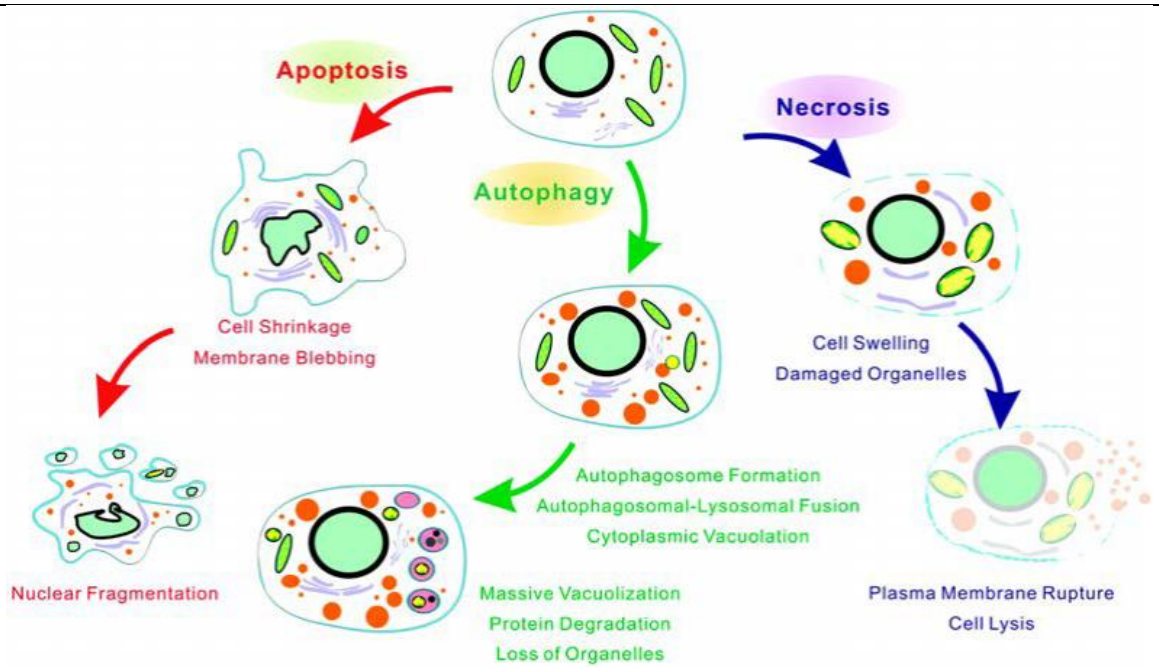

Figure 1.9: Morphological features of apoptosis, autophagy and necrosis. Figure taken from (Tan *et al.*, 2014) and highlights the distinguishing morphological features of the different modes of programmed cell death.

1.7.1 Apoptosis

Apoptosis is a Greek word which denotes leaves falling from a tree. In cell biology, apoptosis describes a mode of programmed cell death in which the cell is broken down into apoptotic bodies **(figure 1.9)**. Apoptosis occurs naturally and plays an important role in the development and maintenance of the human body. Examples of this are apoptosis occurring in embryonic development to form the interdigital spaces and apoptosis causing the regression of the mammary glands after weaning (Ali and Coombes, 2002; Suzanne and Steller, 2013). Apoptosis may also occur when cells acquire infection, or their DNA is irreparably damaged. Cancer cells acquire mechanisms to evade apoptosis to confer upon them a survival advantage and resistance to anti-cancer agents (Hanahan and Weinberg, 2011). Many clinical drugs induce apoptosis in cancer cells to control tumour growth and prevent its spread. Apoptotic cell death is sought after in clinical drugs as apoptosis does not cause an inflammatory or immune response (Walsh, 2014; Heckmann, Tummers and Green, 2019).

Morphologically apoptosis is characterized by cell shrinkage, membrane blebbing, chromosome condensation and nuclear fragmentation **(figure 1.9)** (Galluzzi *et al.*, 2007; Ernest, Habela and Sontheimer, 2009). At a molecular level, apoptosis is mediated by certain caspases (cysteine proteases) which degrade cellular components. These caspases can irreversibly be activated via one of two pathways, the intrinsic or the extrinsic pathway **(figure 1.10)**. The intrinsic (or mitochondrial) pathway is activated by internal stressors such as DNA damage, lack of nutrients or oxidative stress and is controlled by the B-cell lymphoma (Bcl-2) family of proteins. Some members of the Bcl-2 family, such as Bax, Bak and Bcl-X_S, are pro-apoptotic whereas other members, such as Bcl-2 and Bcl-X_L, are anti-apoptotic (Ouyang *et al.*, 2012). The activation of pro-apoptotic Bcl-2 family proteins results in mitochondrial outer membrane permeabilisation (MOMP). This triggers the release of the pro-apoptotic protein cytochrome c from the mitochondrial intermembrane space into the cytosol. Cytochrome c binds the apoptotic protease activating factor 1 (APAF1) to form the apoptosome. The apoptosome in turn activates caspase 9 which directly cleaves and activates the effector caspases 3 and 7.

The DNA repair protein poly (ADP-ribose) polymerase (PARP) is directly cleaved by these effector caspases and serves as a biomarker of apoptosis (Ricci and Zong, 2006; Pistritto *et al.*, 2016).

The extrinsic pathway proceeds via transmembrane death receptors which form part of the tumour necrosis factor (TNF) family and the cytoplasmic component of these receptors, known as the death domain, plays a crucial role in initiating this pathway. This is best understood using the fatty acid synthetase ligand and receptor (FasL/FasR) as a model. Upon the binding of FasL to FasR, the adapter protein FADD (Fas-associated death domain) is recruited to the death domain. FADD then associates with procasapse-8, which results in the formation of the death inducing signaling complex (DISC). This results in the auto-catalytic activation of procaspase 8. The active from of caspase 8 subsequently cleaves the effector caspases 3 and 7 (Elmore, 2007; Ouyang *et al.*, 2012).

The intrinsic and extrinsic apoptotic pathways thus both converge at the level of the effector caspases 3 and 7 and can be distinguished by the presence of either active caspase 9 or caspase 8 respectively. Although these pathways are independent of each other, cross talk between them can occur at the level of caspase 8 which could lead to an intensification of the death signal (Elmore, 2007). Since either of these pathways may be bypassed in certain cancers, many drugs aim to activate apoptosis via both these pathways(Fernald and Kurokawa, 2014; Pistritto *et al.*, 2016).

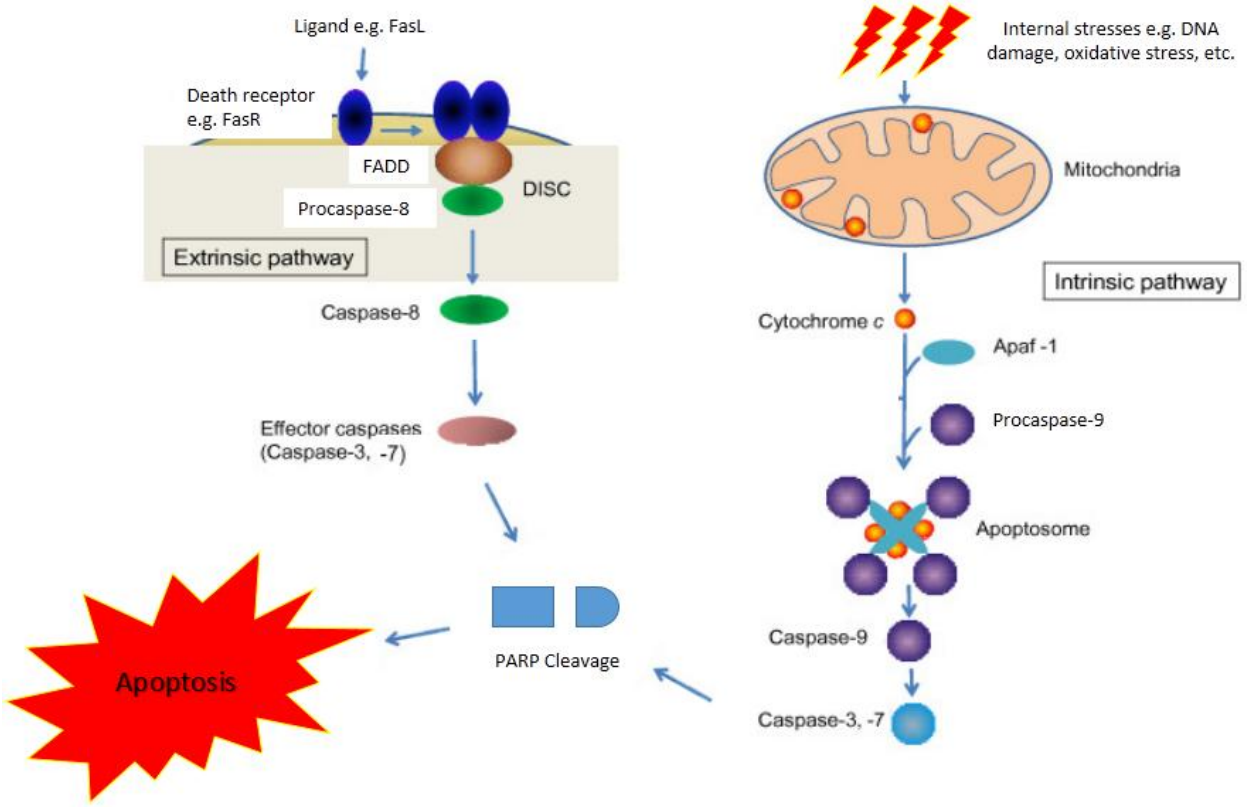

Figure 1.10: A biochemical overview of the intrinsic and extrinsic apoptotic pathways. Figure adapted from Li and Sheng (2012).

1.7.2 Autophagy

Autophagy is a biological process by which cells recycle their own contents into reusable units and it plays an important role in regular cell maintenance. Under nutrient poor or stress conditions, autophagy enables the cell to survive until conditions improve (Su, Mei and Sinha, 2013; Mathiassen, Zio and Cecconi, 2017). Morphologically, autophagy is characterized by the formation of double membrane vesicles, known as autophagosomes, which engulf misfolded proteins, damaged organelles and other cellular contents which have been targeted for degradation **(figure 1.9)** (Galluzzi *et al.*, 2007). In the cancer context, autophagy may assist in meeting the energy demands of established tumour cells but has also been implicated in cell death (Hanahan and Weinberg, 2011; Su, Mei and Sinha, 2013). Indeed, the induction of autophagy by anti-cancer drugs has been shown to play either a pro-death or pro-survival role, depending

on the context. For example, cisplatin induced autophagy was shown to play a pro-survival role in esophageal cancer cells (Liu *et al.*, 2011). On the other hand, autophagy induced by the palladacycle AJ-5 was shown to play a pro-death role in melanoma and breast cancer cells (Aliwaini *et al.*, 2013, 2015).

The molecular mechanisms which drive autophagy are complex **(figure 1.11)**. The induction of autophagy can occur in stressful situations such as when nutrients, oxygen or energy is low. Under favorable conditions the serine/threonine kinase mechanistic target of rapamycin (mTOR), when activated by class 1 phosphatidylinositol 3-kinases (PI3Ks), negatively regulates autophagy. Under these conditions, the mTOR complex 1 (mTORC1) inhibits autophagy by preventing the activation of Unc-51-like autophagy-activating kinase-1 and kinase-2 (ULK1 and ULK2) via phosphorylation. Under stress conditions, the 5' AMP activated protein kinase (AMPK) activates ULK1 as well as the TSC1/2 complex which negatively regulates mTOR. One of the earliest events in autophagy is phagophore formation which occurs when the ULK1 complex translocate to the phagophore, promoting the formation of the class 3 PI3K complex. This complex comprises Vps34, p150, Beclin-1, Atg14L and autophagy and Beclin-1 regulator 1 (AMBRA1) and produces an autophagosome-specific pool of phosphatidylinositol 3-phosphates (PI3Ps) that recruit downstream effectors which drive the nucleation of the isolation membrane (Su, Mei and Sinha, 2013; S. S. Singh *et al.*, 2017; Dikic and Elazar, 2018). Next, the isolation membrane is elongated, and the cargo is sequestrated inside this membrane. It is during this elongation step in which microtubule-associated protein 1A/1B-light chain 3 1 (LC3-I), the cytosolic form of LC3, is conjugated by phosphatidylethanolamine (PE) to form LC3II, the autophagosome membrane bound form of LC3. As LC3II remains bound to the autophagosome membrane, it is widely used as a marker of autophagy. The closure of this membrane results in the formation of the double membrane autophagosome. Autophagosomes later fuse with hydrolase containing lysosomes, to form the single membrane autolysosome (Su, Mei and Sinha, 2013; Klionsky, Eskelinen and Deretic, 2014; Dikic and Elazar, 2018). This results in the degradation of the cargo and the release of usable biomolecules into the cytosol (S. S. Singh *et al.*, 2017). Certain cargo may be marked for degradation by autophagy via

ubiquitination. Adaptor proteins bind to ubiquitinated cargo at one end and to LC3 at the other end, ensuring that the cargo is engulfed by the autophagosome. Thus, adaptor proteins such as p62 serve as reliable markers of autophagy (Corcelle, Puustinen and Jäättelä, 2009; Hansen and Rubinsztein, 2018).

The process of autophagy is multi-stepped and encompasses everything from the formation of the autophagosome, its maturation, its fusion with lysosome, the degradation of its cargo and release of macromolecules into the cytosol. Collectively these steps are referred to as autophagic flux. The rate of flux will determine the turnover of cellular components via autophagy (S. S. Singh *et al.*, 2017). Although markers such as LC3II and p62 can determine whether autophagy is occurring, the change in these markers over time can be monitored to yield data on autophagic flux.

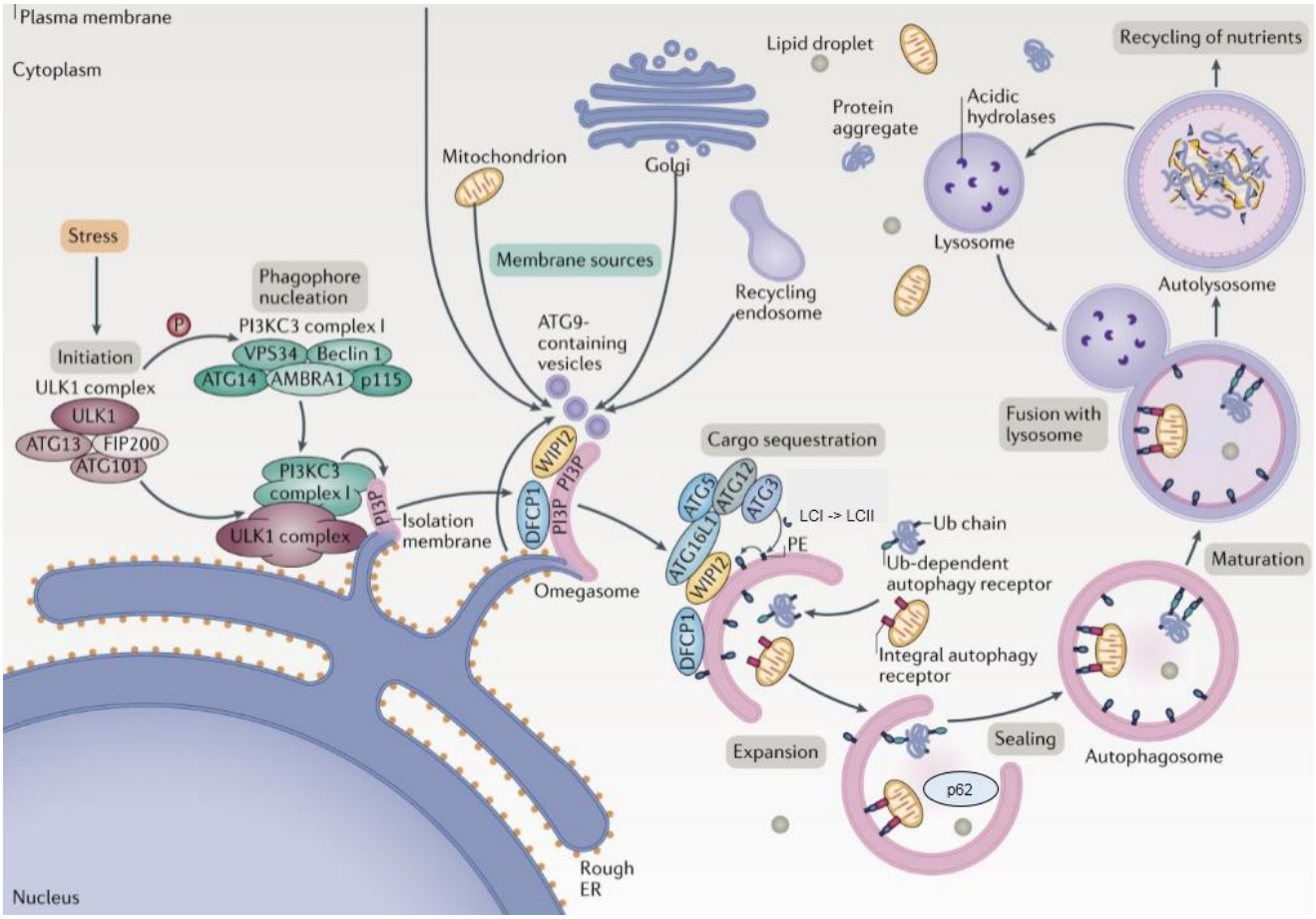

Figure 1.11: An overview of autophagy. Figure adapted from Dikic and Elazar (2018).

1.7.3 Necroptosis

Necrosis is a form of cell death characterized by the permeabilisation of the cell membrane, resulting in the swelling of the cell, damage of its organelles and ultimately cell lysis **(figure 1.9)** (Galluzzi *et al.*, 2007). It has classically been thought of as an unregulated mode of cell death which occurs in response to environmental stressors (Coimbra *et al.*, 2011). However, evidence has emerged that necrosis can be a programmed cell fate (Ouyang *et al.*, 2012; Wang *et al.*, 2018). Thus necroptosis, a form of programmed necrosis, has emerged as a potential targeted cell death pathway in the treatment of cancer and other maladies (Fulda, 2018).

The most well characterized molecular pathway for necroptosis is triggered by TNF **(figure 1.12)**. The binding of the TNF ligand to its receptor TNFR1 results in TNFR1 recruiting various proteins to form complex I. This complex consists of receptor interacting protein kinase 1 (RIP1 also known as RIPK1), TNFR1 associated death domain (TRADD), cellular inhibitor of apoptosis protein 1 and 2 (cIAP1 and cIAP2) as well as TNFR associated factor 2 and 5 (TRAF2 and TRAF5). RIP1 dissociates from complex I when it is deubiquitinated by cyclindromatosis (CYLD) (Berghe *et al.*, 2014; He, Huang and Shen, 2016). This results in the formation of the DISC (also known as complex IIa) which consists of RIP1, RIP3, TRADD, FADD, and FLICE-like inhibitory protein (FLIP). When caspase 8 is active, it inactivates RIP1 and RIP3. However, when caspase 8 is inactive, RIP1 associates with RIP3 which results in their autophosphorylation, transphosphorylation and the formation of the necrosome. RIP3 then recruits and phosphorylates mixed lineage kinase domain-like protein (MLKL). This results in the oligomerisation and membrane translocation of MLKL (Berghe *et al.*, 2014; He, Huang and Shen, 2016). Here MLKL binds to phosphatidylinositol phosphates to form membrane disrupting pores which results in the influx of Na^+ and Ca^{2+} into the cell, causing a rise in osmotic pressure and the eventual rupture of the cell membrane i.e. necroptosis (X. Chen *et al.*, 2013). The phosphorylation of RIP1, RIP3 and MLKL are hallmarks of necroptosis and are widely used as biomarkers for its detection (He, Huang and Shen, 2016).

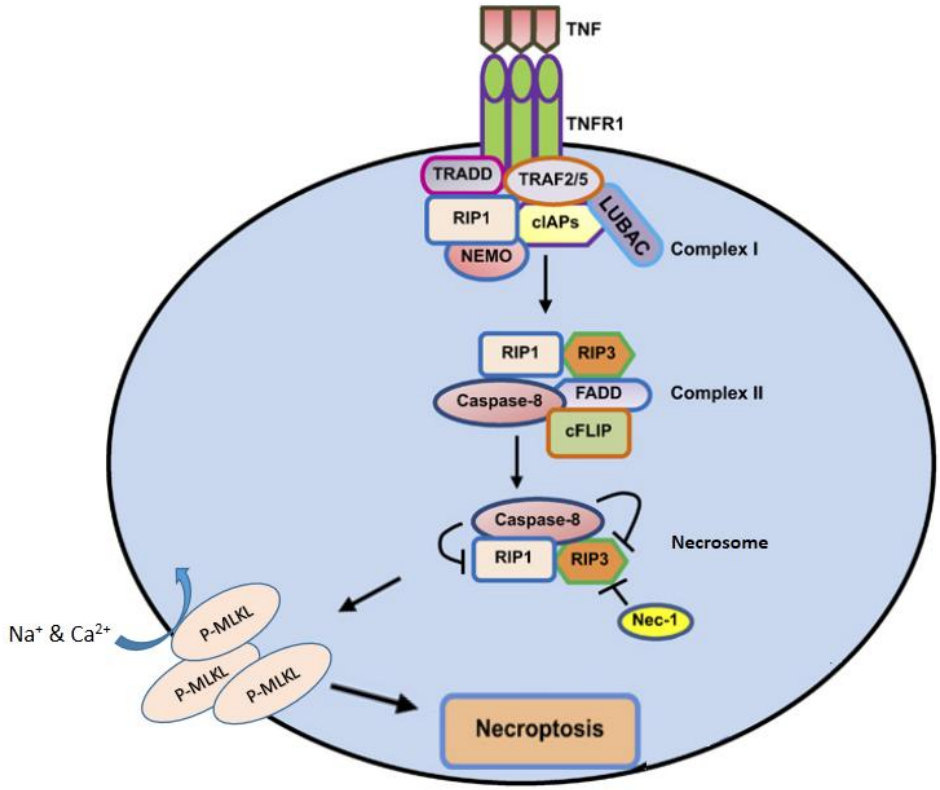

Figure 1.12: A biochemical overview of necroptosis. Figure adapted from Aziz, Jacob and Wang, 2014

1.8 Aims of this study

Breast cancer is the most common cancer in women, and it is also the principal cause of death from cancer among women globally. To reduce this burden, there is a pressing need to find effective therapies that exhibit minimal adverse effects. Accumulating evidence suggests that plant-derived compounds may prove extremely beneficial in the development of chemotherapy to treat a wide spectrum of cancers (Bonam *et al.*, 2018). The broad aim of this study was to investigate the anti-breast cancer activity of extracts derived from two independent sources, namely sub-Saharan millet varieties and the indigenous Kraalbos plant. To achieve this the following specific aims and objectives were carried out in MCF-7 oestrogen receptor positive and MDA-MB-231 triple negative breast cancer cell lines:

Aim 1: To determine the cytotoxicity of extracts derived from three varieties of African millets in breast cancer cells

(a) To prepare extracts from *Sorghum bicolor* (Enforcer), *Pennisetum glaucum* (Babala) and *Eragrostis tef* (Tef) using reflux-based and cold extraction procedures

(b) To determine the solubility of the millet extracts in various solvents in order to identify a suitable solvent for use in cell culture

(c) To test the cytotoxicity of the extracts prepared above in breast cancer cells

(d) To derive the active fraction of the millet extracts which exhibit anti-cancer activity

Aim 2: To identify and characterize the anti-cancer activity of ethanolic Kraalbos extracts obtained from BioPharm (Cape Town, South Africa) in breast cancer cells

(a) To identify a suitable solvent for testing the Kraalbos extracts in cell culture

(b) To investigate the cytotoxicity of 5 ethanolic Kraalbos extracts and to further characterise the most potent extract (referred to as KB) as described below

(c) To investigate the selectivity of the KB extract for breast cancer cells

(d) To explore the long-term effect of the KB extract on breast cancer cell survival

(e) To explore the effect of the KB extract on breast cancer cell migration

(f) To determine whether the mechanism by which the KB extract executes its anti-cancer activity involves ROS production and double strand DNA damage

(g) To explore the effects of the KB extract on cell cycle progression

(h) To investigate if the KB extract induces apoptosis, necroptosis and autophagy

Chapter 2: Materials and methods

2.1 Millets extraction

2.1.1 Reflux-based extraction

Extracts were derived from three varieties of millets (Agricol, Brackenfell, Cape Town, South Africa), namely *Pennisetum glaucum* (Babala), *Sorghum bicolor* (Enforcer) and *Eragrostis tef* (Tef), using the method described by Pradeep and Sreerama (2015). An overview of the reflux based extraction is shown in **figure 2.1**.

2.1.1.2 Processing of millets

Briefly, 20g of millet seeds were soaked overnight in distilled water in a ratio of 1:3 (w: v) and thereafter allowed to germinate at 30°C for 48 hours. During the germination period, moisture was constantly applied to the millet seeds to prevent them from drying out. Germinated seeds were then dried at 40°C for 48 hours to obtain a moisture content of 40-60%. The dried germinated seeds were then milled into flour and passed through a sieve to remove lumps. This flour was then defatted using hexane treatment (1:5 w: v) for 2 hours and this was repeated three times at room temperature. After air drying, defatted millet powder was stored at -20°C.

2.1.1.3 Extraction of millets

The extraction was carried out by refluxing 5g of defatted millet powder in 50ml acidified methanol (1% 10M HCl) for 30 minutes. Acidified methanol was used as it was reported to be the most efficient solvent for extracting polyphenols from millets (Chethan and Malleshi, 2007). The extracts were then centrifuged for 10 minutes at 4000g. The supernatants were collected, and the extraction was repeated two more times. The supernatants collected after each round of extraction were pooled and concentrated

under vacuum using a rotatory evaporator (Rotavapor R-210, Buchi, Switzerland), then weighed and resuspended in 6ml methanol.

2.1.1.4 Processing of extracts

Extracts were once again centrifuged for 10 minutes at 4000g (Digtor 21, Orto Alresa, Madrid, Spain). The supernatant was collected and aliquoted into 1ml aliquots. One aliquot was used at a time and the remaining aliquots were stored at 4°C until needed. The extract was then neutralized using Na_2CO_3 and centrifuged at 10 000g for 5 minutes (Prism R, Labnet, New Jersey, United States). The supernatant and pellets were separated and each fraction was oven dried at 60°C overnight.

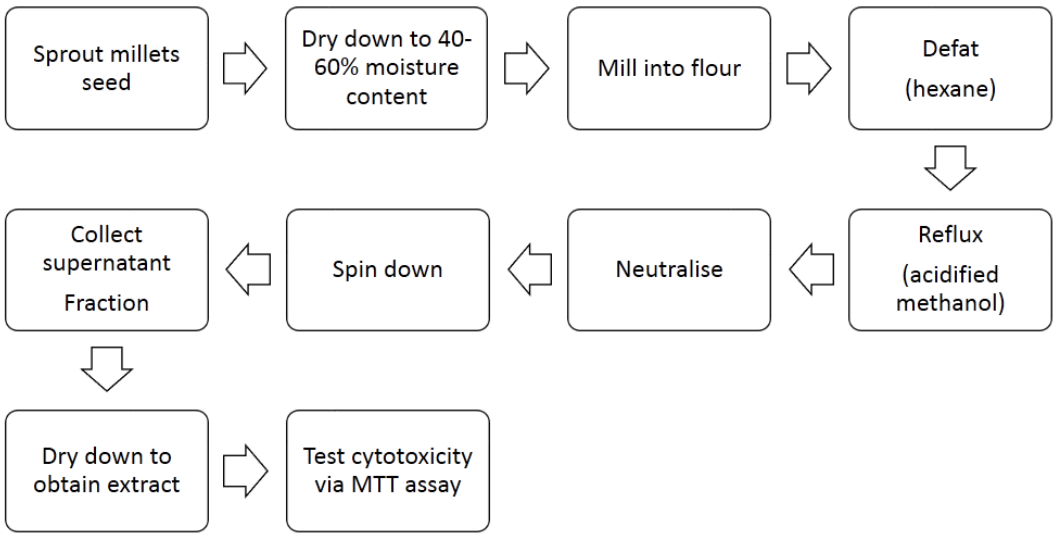

Figure 2.1: An overview of the reflux-based extraction procedure for millets. Millets seeds were sprouted and subsequently dried down to reduce their moisture content. The millets sprouts were then ground down and defatted using hexane. The defatted millet powder was the subjected to a reflux extraction using acidified methanol. The residual acid present in the extracts obtained were then neutralized, spun down and the supernatant was dried to obtain the final extract. The cytotoxicity of this extract towards breast cancer was then determined using the MTT assay.

2.1.2 Cold extraction

An overview of the cold extraction procedure is shown in **figure 2.2**. Briefly, millet seeds were ground into a fine powder using an electronic grinder (Sunbeam, Florida, USA). Approximately 25g of each powder was weighed out and defatted in 100ml n-hexane (HPLC grade) (catalogue no. 104391, Merck, New Jersey, United States) at 27°C with shaking for 3 days. Thereafter the hexane was removed and the powder was air dried at room temperature. Once dry, the cold extraction was carried out by adding 100ml of methanol (HPLC grade) (catalogue no. 106035, Merck, New Jersey, United States) to the defatted powder and incubating at 27°C with shaking for 5-7 days. Samples were subjected to ultracentrifugation (Digtor 21, Orto Alresa, Madrid, Spain) for 15 minutes to pellet undissolved material. The supernatant was removed and concentrated under vacuum using a rotatory evaporator (Rotavapor R-210, Buchi, Switzerland). After complete evaporation of solvent, the remaining extracts were weighed and resuspended in 6ml methanol. This sample was subjected to fractionation using high performance thin layer chromatography (HPTLC) plates.

2.1.3 Fractionation

2.1.3.1 High performance thin layer chromatography (HPTLC) fractionation

High performance thin layer chromatography (HPTLC) plates (C_{18} silica gel matrix) (product no. Z265365, Sigma, Missouri, USA) were used to fractionate the methanol millet extracts. For each methanol millet extracts 50mg were loaded onto HPTLC plates. A mobile phase solvent of 50:50 water methanol mixture was used and the plate was run until approximately 2cm before the edge of the plate. Coloured bands were used to monitor if adequate separation had occurred. Non-coloured bands were visualised under UV light (365nm). Bands were scraped off the glass plate. Thereafter, the solid silica was separated from the liquid phase by microfiltration. The solvent was evaporated off at 60°C to yield a powder. This powder was then re-dissolved for subsequent treatment of cells.

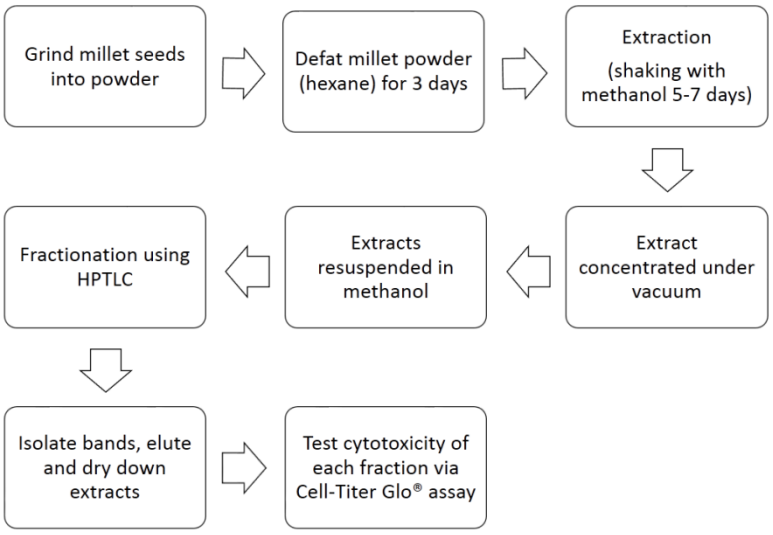

Figure 2.2: An overview of the cold extraction procedure for millets. Millets seeds were ground down and defatted using hexane. Methanol was then added to the defatted millet powder and it was incubated with shaking for 5-7 days. Thereafter the methanol (containing the extract) was removed and the extract was concentrated down under vacuum. This extract was then fractionated using HPTLC plates. The resulting fractions were then tested for their cytotoxic activity towards breast cancer cells using the Cell-Titer Glo® assay.

2.2 Preparation of Kraalbos extracts

The Kraalbos extracts KB1, KB2, KB3, KB4, and KB5 were supplied to the Prince lab by the company BioPharm (Cape Town, South Africa). These extracts were obtained from the leaves of the Kraalbos plant using proprietary extraction procedures. Extracts were prepared for use in cells by using DMSO to obtain a 20mg/ml stock. In order to dissolve the extract, the solution was subjected to several cycles of vortexing and heating at 65°C. This stock was serially diluted using the appropriate medium to a working stock of 1mg/ml. This working stock was used to make up the respective treatment concentrations. A fresh stock was made for each experiment as the stability of the extracts in solution was not known.

2.3 Solubility assays

The solubility of the millets and Kraalbos extracts were not known, hence it was necessary to test their solubility in various solvents. Briefly, 1mg of extract was dissolved in 500µl of either acetone, ethanol, DMSO, water, or 1x phosphate buffered saline solution (PBS). The extract was then solubilised by subjecting it to several cycles of vortexing and heating at 65°C for 30 seconds. Any colour change in the solution was noted. The solutions were then centrifuged at 10 000rpm for 5 minutes in order to pellet all undissolved matter. The supernatant was then removed, and the pellets were dried at 60°C overnight prior to being weighed. The mass of the dry pellet was then compared to the initial amount of extract added and the percentage of extract dissolved was calculated.

2.4 Cell culture

MCF-7 human breast adenocarcinoma cells were maintained in Roswell Park Memorial Institute (RPMI) 1640 medium (Gibco®, Life Technologies, New York). MDA-MB-231 human breast adenocarcinoma and FG0 normal human fibroblast cells were maintained in Dulbecco's Modified Eagle's Medium (DMEM) (Gibco®, Life Technologies, New York). MCF-12A non-malignant mammary epithelial cells were maintained in a 1:1 mixture of DMEM and Ham's F12 medium (Gibco®, Life Technologies, New York) supplemented with cholera toxin (100ng/ml) (catalogue no. C8052-1MG, Sigma-Aldrich, Missouri, USA), epidermal growth factor (EGF) (20ng/ml) (catalogue no. E9644-2MG, Sigma-Aldrich, Missouri, USA), hydrocortisone (500ng/ml) (catalogue no. 3867, Calbiochem, California, USA), and insulin (10µg/ml) (catalogue no. 707927001, Novo Nordisk, Bagsværd, Denmark). All media were supplemented with 10% foetal bovine serum (FBS) (Gibco®, Life Technologies, New York) to provide growth factors. Likewise, the antibiotics penicillin (100U/ml) (catalogue no. P3032-25MU, Sigma-Aldrich, Missouri, USA) and streptomycin (100µg/ml) (catalogue no. S9137-25G, Sigma-Aldrich, Missouri, USA) were added to all media to prevent bacterial infection. For MCF-12A cells, all supplements were withdrawn from the media 48 hours prior to commencing experiments. Furthermore, cells were only handled under sterile conditions in order to prevent contamination and infection. All cells

were maintained in a 95% air humidified incubator at 37°C and 5% CO_2. Cells were passaged once a week or as needed. Medium was changed every two to three days. All cells were regularly subjected to mycoplasma testing and only mycoplasma free cells were used for experiments.

2.5 Mycoplasma staining

Cells were seeded onto coverslips and grown in antibiotic free medium for at least 48 hours. At approximately 60% confluence, cells were fixed using 1ml fixative solution (3:1 methanol: glacial acetic acid) for 10 seconds. Next, the cells were rinsed with deionised water and subsequently fixed again as described above. Excess fixative was then rinsed off with deionised water. Thereafter, coverslips were air dried at room temperature. DNA was then stained using 1ml 0.5µg/ml Hoechst 33258 (Invitrogen, California, USA) for 10 seconds. Excess stain was washed off with deionised water prior to mounting. Coverslips were mounted using mounting fluid **(appendix 1.3.1)**. Stained cells were viewed under the Zeiss Axiovert 200M inverted fluorescent microscope (Zeiss, Germany) using the DAPI channel in order to visualise stained DNA.

2.6 Cell viability assays

2.6.1 3-(4,5-dimethylthiazol-2-yl)-2,5-diphenyl tetrazolium (MTT) assays

In order to assess the short-term cytotoxicity of millet extracts against breast cancer cells, 3-(4,5-dimethylthiazol-2-yl)-2,5-diphenyl tetrazolium (MTT) assays were performed. The MTT assay is a colorimetric assay which measures the ability of cells to reduce the tetrazolium salt 3-(4,5-dimethylthiazol-2-yl)-2,5-diphenyl-trazolium bromide to formazan via the mitochondrial succinate dehydrogenase enzyme **(figure 2.3)**. This reaction is associated with a colour change from yellow to purple. As this process only occurs in living cells, the change in colour is representative of the population of live cells. Thus, this colour change is used to determine the number of viable cells. Briefly, cells (3000 - 4500 cells per well) were seeded in quadruplicate in a 96 well plate. Cells were treated at

approximately 60% confluence with either vehicle or extracts for 48 hours. Thereafter 10µl of 5mg/ml MTT solution (Sigma-Aldrich, Missouri, USA) was added to each well and the plate was incubated at 37°C in the dark for 4 hours. Next, 100µl of solubilisation buffer (10% SDS in 0.01M HCl) **(appendix 1.2.2)** was added to each well and the plate was further incubated at 37°C in the dark overnight. As the purple formazan crystals accumulate intracellularly, the solubilisation buffer is added to lyse cells and draw these crystals into solution. The plate was then read using a spectrophotometer (RT-2100C Microplate Reader, Rayto, China) at a wavelength of 595nm. A blank well, containing only extract and medium, was included as a control to account for any inherent absorbance or interference of the extracts with the MTT salt. In order to plot cell survival, readings were blanked to the extract only control and cell survival was measured as a percentage of the vehicle treated control. GraphPad Prism version 6 software (GraphPad software, California, USA) was used to determine IC_{50} concentrations.

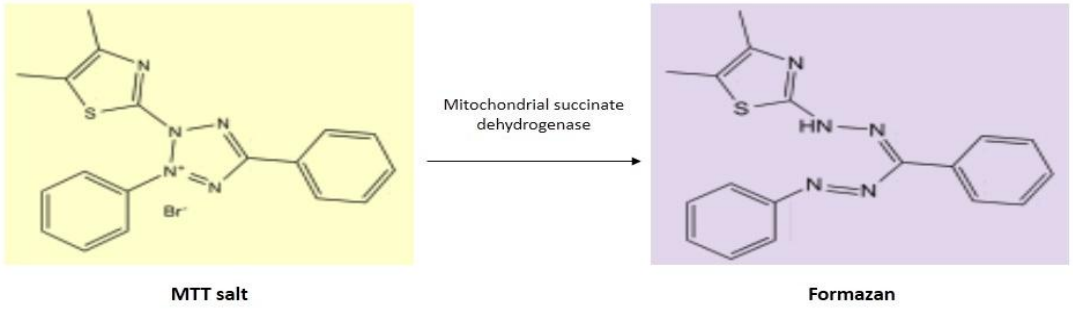

Figure 2.3: The conversion of MTT to formazan. The yellow MTT salt is reduced to the purple formazan by the mitochondrial succinate dehydrogenase. This reaction forms the basis of the MTT assay as it can only occur in living cells. Hence the change in colour represents the population of live cells.

2.6.2 Cell-Titer Glo® assay

The Cell-Titer Glo® Luminescent Cell Viability Assay (catalogue no. G7571, Promega, Wisconsin, USA) was used to determine the cytotoxicity of the millet and Kraalbos extracts against breast cancer cells. The Cell-Titer Glo® Assay contains a proprietary luciferase and luciferin, which react in the presence of ATP to produce light **(figure 2.4)**.

This ATP is provided by the lysate of living cells and thus the amount of light emitted corresponds to ATP levels and thus cell survival. The Cell-Titer Glo® Assay was used as per manufacturer's instructions. Briefly, cells (3000 - 4500 cells per well) were seeded in quadruplicate in a 96 well plate. Cells were treated at approximately 60% confluence with either vehicle or extracts for 48 hours. After treatment, the plate was allowed to equilibrate to room temperature before adding 100µl of the Cell-Titer Glo® reagent (made by adding 10ml Cell-Titer Glo® buffer to the lyophilised Cell-Titer Glo® substrate) to each well. This was mixed for two minutes on an orbital shaker to induce cell lysis. Thereafter, the plate was incubated at room temperature for five minutes to allow the luminescent signal to stabilise. Luminescence was read using the Luminoskan Ascent luminometer (Thermo Fisher Scientific, Massachusetts, USA) or the GloMax® Explorer machine (Promega, Wisconsin, USA). A blank well, containing only extract and media, was included in order to account for any background luminescence. In order to plot cell survival, readings were blanked to the extract only control and cell survival was measured as a percentage of the vehicle treated control. The GraphPad Prism version 6 software was used to determine the IC_{50} concentrations.

Based on the outcome of the cell viability assays, it was determined that KB2 was the most effective of all the Kraalbos extracts. Thus, only KB2 was further characterised in term of its anti-cancer activity and mechanism of action. Hence, all subsequent experiments were only carried out using the KB2 extract.

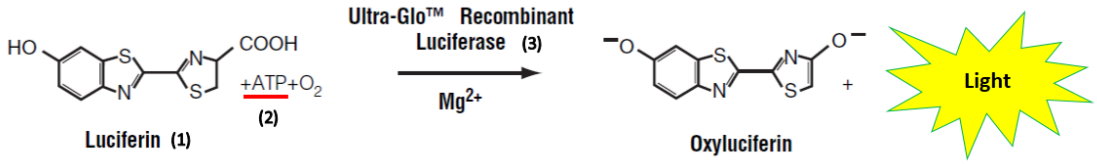

Figure 2.4: An overview of the Cell-Titer Glo® assay. Luciferin **(1)** reacts with the Ultra-Glo™ recombinant luciferase **(3)**, in the presence of ATP **(2)**, to produce light. As the ATP is supplied by living cells, the light output is a direct measure of cell viability. Adapted from the Cell-Titer Glo® Luminescent Cell Viability Assay product manual.

2.7 Cell morphology

In order to observe the effects of KB2 on breast cancer cells, the morphology of the cells was captured after treatment with either vehicle or KB2. Briefly, cells were seeded and allowed to reach 60-70%confluence. Thereafter cells were treated with either vehicle or KB2 at the respective ½IC_{50} and IC_{50} concentrations for 24 and 48 hours. The morphology of the cells was captured using the Evos® FL microscope (Thermo Fisher Scientific, Massachusetts, USA).

2.8 Clonogenic assays

Clonogenic assays were carried out in order to determine the long-term survival of MCF-7, MDA-MB-231 and MCF-12A cells after treatment with the KB2 extract. Briefly, cells were plated (5000 – 10 000 cells per dish) in 6cm dishes and subsequently treated with either vehicle or KB2 at the respective ½IC_{50} or IC_{50} concentrations for 24 hours. Thereafter cells were trypsinized, spun down and resuspended. This cell suspension was replated at a density of 500 – 1000 cells in 35mm dishes. Cells were left to grow in the absence of KB (5-7 days for MDA-MB-231 cells and 14-21 days for MCF-7 and MCF-12A cells), with medium changed every 3-5 days, until colonies reached a size of 50 or more cells. Prior to staining, cells were gently washed with 1xPBS solution to remove excess media and fixed using 750µl fixative solution (3:1 methanol: acetic acid) for 15 minutes. Excess fixative was removed, and cells were washed with 1xPBS solution prior to being stained with 750µl 0.5% crystal violet **(appendix 1.4.1)** (Sigma-Aldrich, Missouri, USA) for 15 minutes. Excess stain was washed off using 1xPBS solution and subsequently dishes were gently emerged in distilled water. Dishes were photographed and images were analysed using the ColonyArea plugin for ImageJ (Guzmán *et al.*, 2014). Cell survival was expressed relative to the vehicle treated control.

2.9 *In vitro* cell migration assay

In order to test the effect of KB2 on cell migration, a two-dimensional *in vitro* scratch motility assay (also referred to as a wound healing or scratch assay) was performed. Briefly, cells (2 - 4x10^5 cells per well) were seeded in 12 well plates and allowed to reach 100% confluence. Thereafter, a linear artificial wound was created using a 10µl pipette tip. The medium was then aspirated off and replaced to remove floating cells. Cells were then treated with vehicle or KB2 at the respective IC_{50} or ½IC_{50} concentrations. Simultaneously, cells were treated with 10µg/ml Mitomycin C (Sigma-Aldrich, Missouri, USA) in order to block proliferation. Three markings were made along the scratch line and these were used as reference points. The wound was monitored and photographed using the Evos® XL Core microscope (Thermo Fisher Scientific, Massachusetts, USA) at 3-hour intervals for up to 24 hours. The area of the wound were measured using the ImageJ software. The area of the wound at each time point was measured and subtracted from the area at time zero to yield the area migrated.

2.10 Flow cytometry analysis

In order to determine if KB2 induced a cell cycle arrest in breast cancer cells, fluorescence-activated cell sorting (FACS) analysis was carried out. Cells were plated in 6cm dishes and were treated at a confluence of approximately 60% with either vehicle or KB2 at the respective ½IC_{50} and IC_{50} concentrations for 24 or 48 hours. After treatment, cells were harvested. Briefly, medium was removed from the cells and the cells were trypsinized. Cells were then pelleted, resuspended in 2ml 1xPBS solution and subsequently repelleted. In order to fix the cells, they were resuspended in 3ml chilled 70% ethanol. Cells were stored at -20°C, for no longer than 2 weeks, prior to FACS analysis. Immediately prior to FACS analysis, cells were pelleted, and fixative was aspirated off. Cells were resuspended in 500µl of FxCycle™ PI/RNase Staining Solution (catalogue no. F10797, Life Technologies, California, USA) and incubated at room temperature in the dark for 15-30 minutes. The propidium iodide (PI) stains the DNA present in the cells. Subsequent flow cytometry analysis measures the intensity of PI

staining, indicating the amount of DNA present in the cells and hence the phase of the cell cycle. For the flow cytometry individual samples were subjected to a Becton Dickinson FACSCalibur flowcytometer (Becton Dickinson, New Jersey, USA) with a 488nm Coherent laser (Santa Clara, California, USA). A minimum of 20 000 cells was used per sample. The Cellquest Pro version 5.2.1 software was used for data acquisition. The cell population was identified and gated on a forward scatter (FSC) vs. side scatter (SSC) dot plot in acquisition mode. Fluorescent Channel 2 (FL2) at 575nm was used for PI detection. A dot plot of FL2A (area) vs FL2W (width) was used to identify single cells and thus eliminating doublets. A histogram plot of FL2A was used to enumerate G1/G0, S-phase and G2 populations. The combined parameters FSC, SSC, FL2A and FL2W display the results. A threshold of 52 on the FSC channel was set to remove sample debris. Nile Red fluorescent particles were used for instrument standardization, stability and reproducibility. Analysis and results obtained from the acquired data was done with Modfit version 3.3 software.

2.11 Reactive oxygen species (ROS) detection assays

2.11.1 ROS-Glo™ H_2O_2 assay

When cells undergo oxidative stress, the intracellular levels of reactive oxygen species (ROS) rises. Among the many ROS produced, H_2O_2 is the most stable. Thus, in order to determine whether KB2 induced oxidative stress in breast cancer cells, the levels of H_2O_2 were measured using the ROS-Glo™ H_2O_2 assay kit (catalogue no. G8820, Promega, Wisconsin, USA). This assay contains an H_2O_2 substrate which reacts with H_2O_2 to produce a luciferin precursor. This precursor, in the presence of the ROS-Glo™ detection solution, is converted to luciferin which then reacts with luciferase to produce light **(figure 2.5)**. This luminescence output thus corresponds to the amount of H_2O_2 present. Briefly, cells (3000 – 4500 cells per well) were seeded in opaque 96 well tissue culture plates. Cells were treated for 24 hours with either vehicle or KB2 in a volume of 80µl per well. After 18 hours of incubation, 20µl H_2O_2 Substrate Solution (prepared by mixing 25µl H_2O_2 substrate with 2ml H_2O_2 Substrate Solution Buffer) was added to each well. After 24 hours

of incubation 100µl ROS-Glo™ Detection Solution (prepared by mixing 10ml Luciferin Detection Reagent, 100 µl D-Cysteine and 100 µl Signal Enhancer Solution) was added to each well and incubated at room temperature for 20 minutes. After incubation the luminescence was read using the GloMax® Explorer machine (Promega, Wisconsin, USA).

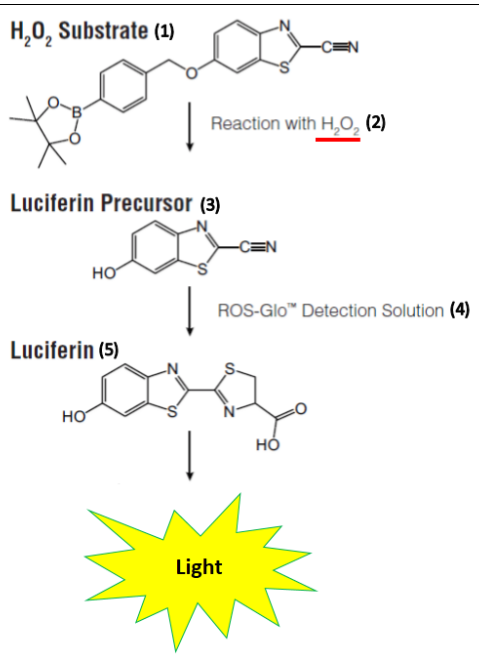

Figure 2.5: An overview of the ROS-Glo™ H_2O_2 assay. An H_2O_2 substrate **(1)** reacts with H_2O_2 **(2)** in order to yield a luciferin precursor **(3)** which in the presence of the ROS-Glo™ detection solution **(4)** produces luciferin **(5)** which is converted to light by luciferase. As the H_2O_2 is the only reagent supplied by the cells, the light output is a measure of the H_2O_2 produced by the cells. Adapted from the adapted from the ROS-Glo™ H_2O_2 assay product manual.

2.11.2 GSH-Glo™ Glutathione assay

As the levels of ROS rise within the cell, they are neutralised by antioxidants. Hence, the rise of the levels of ROS causes a decrease in the levels of antioxidants. Thus, to confirm the presence of intracellular ROS, the levels of the antioxidant glutathione (GSH) was measured using the GSH-Glo™ Glutathione assay kit (catalogue no. V6911, Promega,

Wisconsin, USA). The GSH-Glo™ Glutathione assay contains a luciferin precursor, which is converted into luciferin in the presence of glutathione and glutathione S-transferase. This luciferin then reacts with luciferase to produce light, which is measured as an output of glutathione levels **(figure 2.6)**. Briefly, cells (3000 – 4500 cells per well) were seeded in opaque 96 well tissue culture plates. Cells were treated for 24 hours with either vehicle or KB2. Thereafter, the cell culture medium was removed by aspiration. Next, 100µl of 1X GSH-Glo™ Reagent (prepared using Luciferin-NT substrate and Glutathione S-Transferase each diluted 1:100 in GSH-Glo™ Reaction Buffer) was added to each well. The plate was then mixed briefly on a shaker and incubated for 10 minutes at room temperature. Thereafter, 100µl reconstituted Luciferin Detection Reagent (prepared by adding the Reconstitution Buffer to the lyophilised Luciferin Detection Reagent) was added to each well. The plate was then incubated for 15 minutes at room temperature in order to stabilize the luminescence signal. The plate was read using the GloMax® Explorer machine (Promega, Wisconsin, USA).

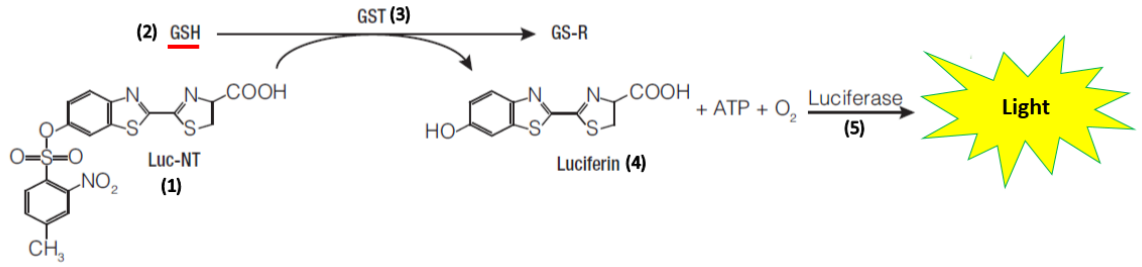

Figure 2.6: An overview of the GSH-Glo™ Glutathione assay. A luciferin precursor **(1)** is converted to luciferin in the presence of glutathione (GSH) **(2)** via glutathione S-transferase (GST) **(3)**. The luciferin **(4)** then reacts with luciferase **(5)** to produce light. As the GSH supplied by the cells are required for these reactions to take place, the amount of light produced is a measure of the amount of GSH present. Adapted from the GSH-Glo™ Glutathione assay product manual.

2.12 Western Blotting

Western blot analysis was carried out in order to detect changes in expression levels of proteins of interest in response to treatment.

2.12.1 Harvesting of protein

Cells were seeded in 6cm dishes and treated at 60-70% confluence with either vehicle or KB2 at the respective ½IC_{50} and IC_{50} concentrations for 24 and 48 hours. Protein was harvested at the appropriate time points. Briefly, the medium was collected, and cells were washed twice with trypsin/EDTA. The trypsin/EDTA was collected, together with the cells and medium and spun down at 2500rpm for 2 minutes. The supernatant was then removed by aspiration and the pellet was resuspended in 1ml of 1xPBS solution. In order to remove any residual medium, cells were spun down again and the supernatant was removed by aspiration. The pellet was once again resuspended in 1xPBS solution, spun down and the supernatant removed. Thereafter, 70-100µl of 2x sample loading buffer (also known as buffer or boiling blue) **(appendix 1.1.1)** was added to the pellet depending on its size. The samples were then heated at 100°C for 10 minutes in order to denature the protein. Protein was stored at -20°C for no longer than 2 weeks prior to use.

2.12.2 Sodium dodecyl sulphate-polyacrylamide gel electrophoresis (SDS-PAGE)

Proteins were resolved by size using SDS-PAGE gels. The SDS-PAGE gels were cast in 1.5mm (thick) plates using a Bio-Rad Mini PROTEAN® 3 system apparatus according to manufacturer's instructions. Resolving gels were cast as 8-15% depending on the sizes of the proteins of interest, whereas the stacking gels were cast at 4% **(appendix 1.1.4 and appendix 1.1.5)**. Gels were run in a Bio-Rad running tank filled with 1x running buffer **(appendix 1.1.2)**. Protein samples were loaded equally (7-10µl) per lane alongside the PageRuler™ pre-stained protein ladder (Fermentas, Massachusetts, USA) in order to determine the degree of protein separation and ensure that the proteins of interest do not

run off the gels. The gel electrophoresis was performed at room temperature and run at 100V until adequate protein separation had occurred.

2.12.3 Protein transfer onto a nitrocellulose membrane

After electrophoresis proteins were transferred onto a Hybond ECL nitrocellulose membrane (catalogue no. GE10600008, Sigma-Aldrich, Missouri, USA). Gels were placed in a transfer 'sandwich' cassette which consisted of sponges, Whatman® filter paper, the SDS-PAGE gel and nitrocellulose membrane **(figure 2.7)**. The cassettes were then placed into the transfer unit of the Bio-Rad Mini PROTEAN® 3 transfer tank in the correct orientation. An ice pack was placed in the tank to prevent overheating and the tank was filled with 1x transfer buffer **(appendix 1.1.3)**. The transfer apparatus was connected to the Bio-Rad Powerpack 200 and the protein transfer was run at 100V for 90 minutes.

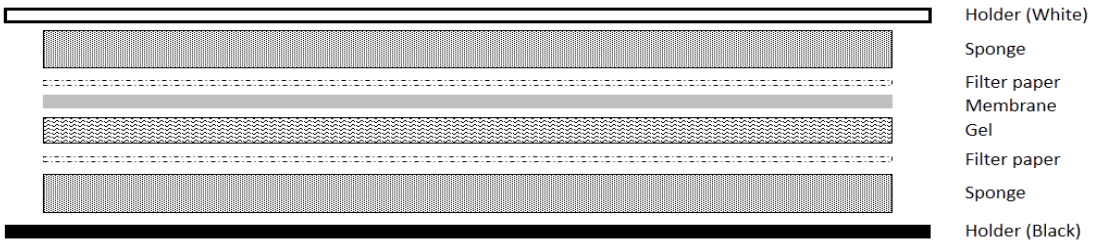

Figure 2.7: Western blotting transfer cassette setup. The components which make up the transfer 'sandwich' cassette. The direction of transfer is from the black end to the white end.

2.12.4 Western blot detection

After completion of the transfer, the nitrocellulose membrane was stained with Ponceau S (Sigma-Aldrich, Missouri, USA) in order to check if protein was indeed loaded, visualise protein bands and check the quality of the transfer. The membrane was then rinsed thrice with distilled water to remove the excess stain. The membranes were then blocked with either tris buffered saline - 0.1% Tween® 20 (TBST) or phosphate buffered saline - 0.1% Tween® 20 (PBST) in either 5% non-fat milk or 5% bovine serum albumin (BSA)

(catalogue no. 10735078001, Sigma-Aldrich, Missouri, USA) at room temperature for one hour with shaking. Thereafter the membranes were probed with the appropriate primary antibody **(table 2.1)** at 4°C overnight with gentle shaking. Total p38 was used as a loading control. After incubation with primary antibody, membranes were washed with either PBST or TBST as follows: 2 quick washes, 2x 5-minute washes and 2x 10 minute washes. Thereafter, membranes were incubated with horseradish peroxidase conjugated anti-mouse or anti-rabbit secondary antibody (1:5000) (Bio-Rad, California, USA) for one hour at room temperature. Secondary antibodies were diluted using either PBST or TBST. Membranes were then washed again as described previously prior to detection. Chemiluminescence was used to visualise protein bands. This was achieved by using either the SuperSignal West Pico Chemiluminescent Substrate Kit (Pierce Biotechnology, Massachusetts, USA) or WesternBright ECL HRP Substrate Kit (Advansta, California, USA) as per manufacturer's instructions. X-ray film (catalogue no. EWPKK, Agfa, Mortsel, Belguim) was used to capture the protein signal. Expression levels of protein were quantified by densitometry using the ImageJ software. Protein levels were normalised to the loading control, p38, and expression levels were measured relative to vehicle treated controls. The ubiquitously expressed protein p38 was used as a loading control as its expression levels are constant and independent of the cell cycle or experimental conditions (Raingeaud *et al.*, 1995).

Table 2.1: Details of primary antibodies used for western blot analyses

Primary antibody		**Manufacturer**	**Catalogue No.**	**Polyclonal or Monoclonal**	**Dilution**	**Secondary Antibody**
DNA Damage Marker	**γH2AX**	Cell signalling	#9718	Monoclonal	1:1000	GαR
Apoptosis Markers	**Caspase 3**	Cell signalling	#9662	Polyclonal	1:1000	GαR
	Cleaved Caspase 7	Cell signalling	#9491	Polyclonal	1:1000	GαR
	Caspase 8	Cell signalling	#9746	Monoclonal	1:1000	GαM
	Caspase 9	Cell signalling	#9502	Polyclonal	1:1000	GαR
	PARP	Cell signalling	#9542	Polyclonal	1:1000	GαR

Autophagy Markers	**LC3B**	Cell signalling	#2775	Polyclonal	1:1000	GαR
	p62	Cell signalling	#88588	Monoclonal	1:1000	GαM
Necroptosis Markers	**p-RIP3**	Cell signalling	#93654	Monoclonal	1:1000	GαR
	p-MLKL	Cell signalling	#91689	Monoclonal	1:1000	GαR
EMT Markers	**E-cadherin**	Cell signalling	#14472	Monoclonal	1:1000	GαM
	β-catenin	Cell signalling	#8480	Monoclonal	1:1000	GαR
	Vimentin	Cell signalling	#3932	Polyclonal	1:1000	GαR
Cell Cycle Markers	**p21**	Santa Cruz	sc-397	Polyclonal	1:1000	GαR
	p-p38	Cell signalling	#9211	Polyclonal	1:1000	GαR
	P53	Santa Cruz	sc-126	Monoclonal	1:1000	GαM
	Cyclin A	Santa Cruz	sc-751	Polyclonal	1:1000	GαR
	Cyclin B1	Cell signalling	#4135	Polyclonal	1:2000	GαM
Loading Control	**p38 MAPK**	Sigma	M0800	Polyclonal	1:5000	GαR
		Cell signalling	#9212	Polyclonal	1:5000	GαR

2.13 Immunocytochemistry

Immunocytochemistry was performed to detect the presence of LC3 punta, indicative of autophagosomes, and γH2AX, indicative of double stranded DNA breaks. Briefly, cells were seeded on glass coverslips in 35mm dishes and treated at approximately 60% confluence. Cells were treated with either vehicle or KB2 at the respective ½IC_{50} and IC_{50} concentrations for 24 or 48 hours. After treatment cells were fixed with ice cold methanol for 5 minutes at -20°C. Cells were then permeabilised and blocked using a solution of both 0.2% Triton X-100 (Sigma-Aldrich, Missouri, USA), for permeabilisation, and 5% BSA (catalogue no. 10735078001, Sigma-Aldrich, Missouri, USA), for blocking, in 1xTBS for 30 minutes at room temperature. Cells were incubated with either LC3 primary antibody (1:500 dilution) (catalogue no. #2775, Cell Signalling Technology, Massachusetts, USA) or γH2AX primary antibody (1:400 dilution) (catalogue no. #9718, Cell Signalling Technology, Massachusetts, USA) overnight at 4°C in a humidifying chamber. The following day, cells were incubated in secondary antibody (donkey anti-rabbit Cy3) in the dark for 1 hour at room temperature. Cells were stained with 1mg/ml Hoechst 33258 (Invitrogen, California, USA) for 10 minutes and mounted onto slides

using Mowial mounting medium containing n-propyl gallate (Sigma-Aldrich, Missouri, USA) to prevent the signal from fading. Images were obtained on a Carl Zeiss LSM 880 with Fast Airyscan module confocal microscope (Zeiss, Oberkochen, Germany).

2.14 Statistical analysis

All experiments were repeated in duplicate or triplicate with three technical repeats per experiment, unless stated otherwise. All statistical analyses were carried out on data pooled from all biological repeats. Significance was determined using a student t-test and taken as $P \leq 0.05$.

Chapter 3: The anti-breast cancer activity of millets

3.1 Introduction

Millets are small-seeded crops which belong to the family *Poaceae* and are farmed as a subsistence crop in parts of Africa and Asia. They are known for their antioxidant properties as well as a host of other health benefits such as lowering blood pressure and decreasing the risk of cardiovascular disease (Singh and Sarita, 2016). Coupled to this, millets are known to be a source of beneficial phytochemicals such as phenols, tannins, flavonoids and saponins. These classes of molecules are believed to be responsible for their health benefits (Mathanghi, 2012; Shay *et al.*, 2015).

In addition to their benefits to overall health, millets have also been investigated for their anti-cancer properties. Extracts derived from finger (*Eleusine coracana*) and Proso (*Panicum miliaceum*) millets have been shown to display cytotoxicity toward HepG2 liver cancer cells (Zhang, Liu and Niu, 2014; Singh *et al.*, 2015). Furthermore, both Proso and Barnyard (*Echinochloa frumentacea*) millets induce apoptosis in HT-29 human colon cancer cells (Ramadoss and Sivalingam, 2019). Interestingly, a protein (FMBP) derived from foxtail (*Setaria italica*) millet bran was also shown to exhibit anti-cancer effects against colon cancer (Shan *et al.*, 2014). Thus, there are evidence that millets exhibit anti-cancer properties.

This study focused on the anti-cancer activity of extracts derived from three varieties of indigenous African millets viz *Pennisetum glaucum* (Babala), *Sorghum bicolor* (Enforcer) and *Eragrostis tef* (Tef). While there is evidence that Enforcer exhibits anti-cancer activity, nothing is known about the cytotoxicity of Babala and Tef in cancer cells. Indeed, anthocyanins derived from Enforcer were previously shown to induce apoptosis in a single breast cancer cell line (MCF-7) but whether other components of Enforcer also have anti-cancer properties has not been reported (Suganyadevi, Saravanakumar and Mohandas, 2013).

This study aims to investigate the anti-cancer activity of Enforcer, Babalae and Tef in oestrogen receptor positive (MCF-7) and triple negative (MDA-MB-231) breast cancer cells. **Figure 3.1** shows an outline of the workflow. Briefly, extracts were obtained using either a reflux-based or cold extraction procedure and the anti-proliferative ability of the extracts were assessed using the MTT assay or Cell-Titer Glo® assays.

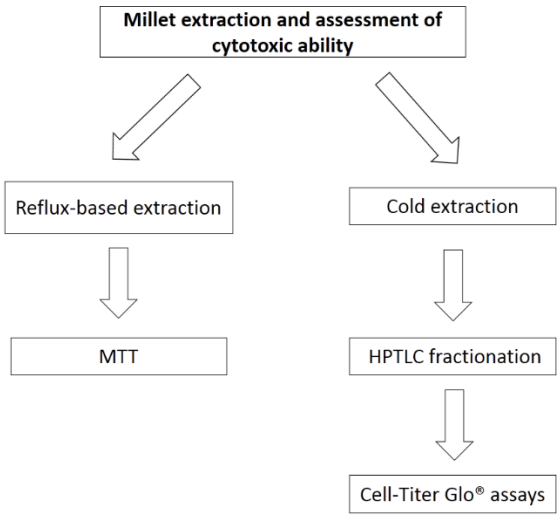

Figure 3.1: An overview of the steps followed to prepare extracts from Babala, Enforcer and Tef and to determine their anti-cancer activity. Extracts were derived from the three varieties of millets using a reflux-based and a cold extraction procedure. Whereas, the extracts derived from the reflux-based procedure were tested for their cytotoxic activity using the MTT assay, those prepared using the cold extraction procedure were subjected to an HPTLC fractionation followed by the Cell-Titer Glo® assay.

3.2 Results

3.2.1 Millet extracts derived from a reflux-based extraction procedure

3.2.1.1 Millet extracts show optimal solubility in DMSO

The reflux-based extraction procedure used in this study was adapted from Pradeep and Sreerama, 2015 and involved the use of acidified methanol. To obtain the extract, any

residual acid was neutralised using Na_2CO_3 which yielded a coloured solution (the supernatant fraction) and a precipitate (the pellet fraction). It was expected that the pellet fraction consisted mostly of salt produced during the neutralisation step and hence it was discarded, and the supernatant fraction was dried and further processed as the active fraction and will from here on be referred to as the extract.

To identify a solvent that is appropriate for use in cell culture, the solubility of the extracts was firstly tested in DMSO, PBS and ethanol. The extracts were weighed and dissolved in the three solvents and subjected to several cycles of heating and mixing. Thereafter, the solvents were removed, and the undissolved materials were pelleted, dried and weighed. To determine the solubility of the extracts in the 3 solvents, the percentage of the extract which had dissolved in the solvent was calculated by comparing the weight of the pellet after the solvent was removed to the weight of the extract before the solvent was added. As shown in **table 3.1,** DMSO displayed the greatest percentage solubility and was thus used as the solvent in all subsequent experiments.

Table 3.1: Percentage solubility of millet extracts in DMSO, PBS and ethanol

Millet Extract	Solvent								
	DMSO			PBS			Ethanol		
	Weight before (mg)	Weight After (mg)	Percentage (%) solubility	Weight before (mg)	Weight After (mg)	Percentage (%) solubility	Weight before (mg)	Weight After (mg)	Percentage (%) solubility
Enforcer	1.79	0.5	72	1.72	1.44	16	1.66	1.27	23
Babala	1.9	0.05	97	1.88	0.21	89	1.77	0.93	47
Tef	1.72	0.06	97	1.7	0.74	56	1.69	1.15	32

3.2.1.2 Millet extracts are not cytotoxic against breast cancer cells

To determine whether the millet extracts described above display short-term cytotoxic activity against MCF-7 and MDA-MB-231 breast cancer cells, MTT assays were performed. The MTT assay is a colorimetric assay which measures the activity of mitochondrial succinate dehydrogenase as a proxy for cell viability. Briefly, cells were

seeded in 96 well plates and treated with either vehicle or millet extracts for 48 hours and the MTT assay was performed. The results reveal that all three millet extracts displayed no cytotoxic effect against both MCF-7 and MDA-MB-231 breast cancer cells **(figure 3.2)**.

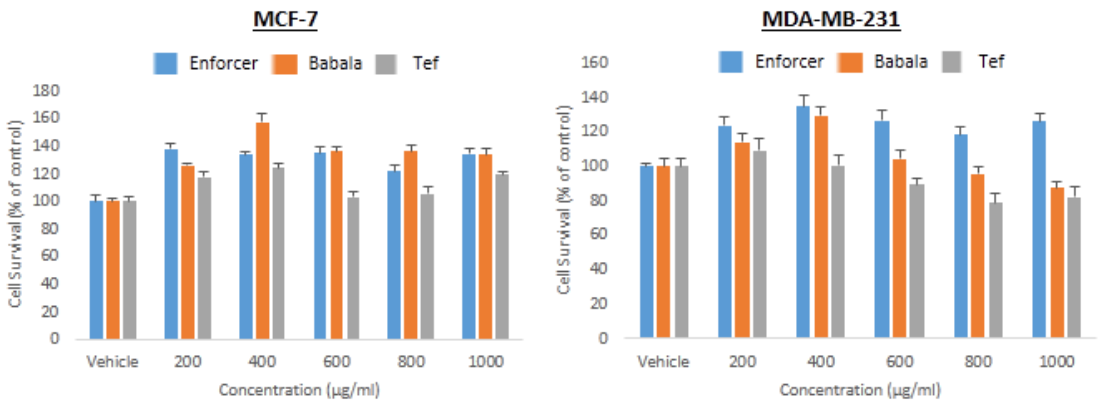

Figure 3.2: Enforcer, Babala and Tef millet extracts derived from a reflux-based extraction procedure, do not exhibit cytotoxicity against breast cancer cells. An MTT assay was carried out to determine the short-term cytotoxicity of Babala, Enforcer and Tef extracts derived from a reflux-based extraction, against MCF-7 and MDA-MB-231 breast cancer cells. Graphs show mean cell survival as a percentage of vehicle control ± SD for each concentration of millet extracts as determined from at least two independent experiments each performed in quadruplicate.

3.2.2 Millet extracts derived from cold extraction procedure

As the reflux-based extraction procedure involved the use of acid followed by neutralisation, it was postulated that the increase of the pH during the neutralisation process may have destroyed or altered any active polyphenols present in the millet extracts. To address this problem, the millet seeds were subjected to a percolation based cold extraction procedure. Briefly, millet seeds were ground, defatted, and subjected to cold extraction using methanol for approximately one week. Thereafter, the methanol containing the extract was removed, the methanol allowed to evaporate, and the extracts resuspended in methanol and subjected to HPTLC based fractionation.

3.2.2.1 HPTLC fractionation yields methanol and water fractions for Babala and Enforcer millets but only a water fraction for Tef millets

To identify fractions which could be tested for their anti-cancer activity against breast cancer cells, the millet extracts obtained above were subjected to HPTLC analyses and the constituent bands were scraped off the silica and eluted using either water or methanol. Whereas water and methanol fractions were obtained for Babala and Enforcer, only a water fraction was obtained for the Tef extract **(figure 3.3)**.

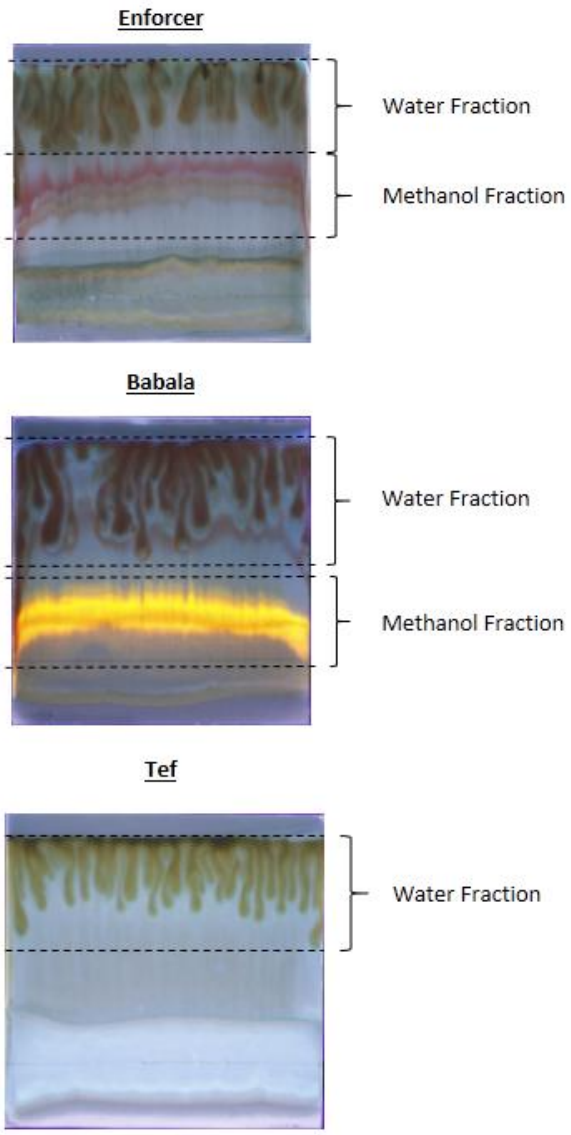

Figure 3.3: HPTLC fractionation yields methanol and water fractions for Enforcer and Babala extracts but only a water fraction for the Tef extract. To separate the extracts into its constituent fractions, HPTLC plates were adsorbed with millet extracts and developed using a mobile phase of water:methanol in a 1:1 ratio and viewed under UV light. The bands were scraped off and the compounds were extracted from the silica using either water or methanol. (a, b) Water and methanol fractions for Enforcer and Babala and (c) water fraction obtained for the Tef extract.

3.2.2.2 Methanol fractions of millet extracts show cytotoxicity against breast cancer cells

The next aim was to determine whether the fractions obtained from the HPTLC exhibit cytotoxic activity against MCF-7 and MDA-MB-231 breast cancer cells. Briefly, cells were seeded in a 96 well plate and treated with the fractions for 48 hours after which cell survival was measured using the luminescence-based Cell-Titer® Glo assay. This assay measures luminescence which results from the reaction between luciferin and luciferase and is catalysed by the ATP derived from living cells. The luminescence output is therefore a measure of viable cells. It is worth noting that the Cell-Titer® Glo assay was chosen over the more widely used MTT assay for reasons discussed later that resulted in unreliable data. The concentration of each extract used varied according to the yield obtained. The half maximal inhibitory concentration, or IC_{50}, is taken as the concentration of an extract/compound/drug required to kill 50% of cells and is a widely accepted standard for measuring cytotoxicity (He *et al.*, 2016). Thus, the IC_{50} was calculated for each fraction and is shown in **figure 3.4**. The results show that the water fractions of the Enforcer, Babala and Tef showed no cytotoxic activity in both breast cancer cell lines at the concentrations tested. The methanol fractions of Enforcer and Babala, however, showed cytotoxicity against both MCF-7 and MDA-MB-231 breast cancer cells. Indeed, the methanol fraction of Enforcer had IC_{50} values of 6.894µg/ml in MCF-7 cells and 3.94µg/ml in MDA-MB-231 cells. Similarly, the methanol fraction of Babala had IC_{50} values of 11.65µg/ml in MCF-7 cells and 9.04µg/ml in MDA-MB-231 cells. Interestingly, MDA-MB-231 cells were more sensitive than the MCF-7 cells to the methanol fractions of Enforcer and Babala. This is exciting because TN breast cancer cells are notoriously more drug resistant.

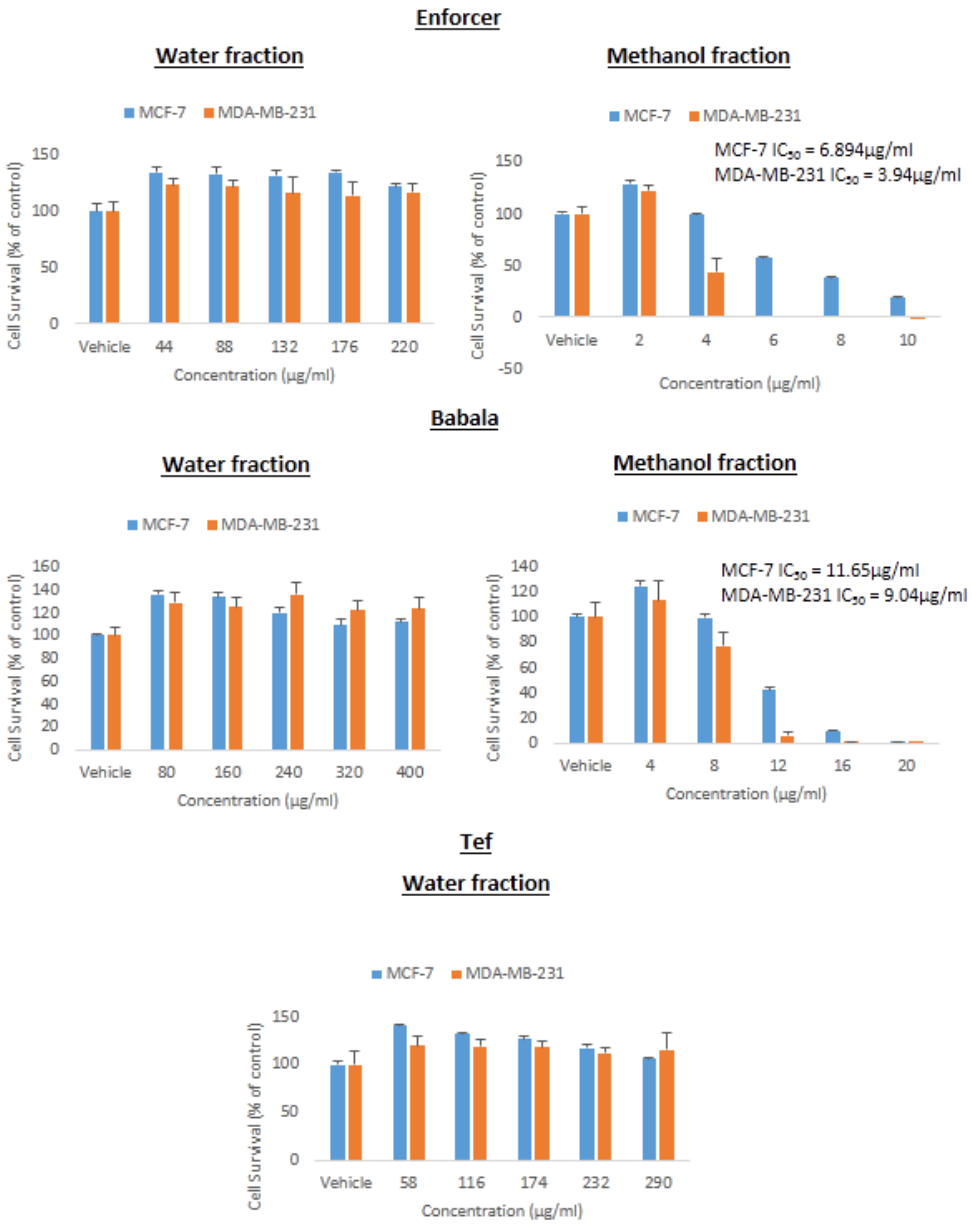

Figure 3.4: Methanol fractions of Enforcer and Babala show short-term cytotoxicity against breast cancer cells. The water and methanol fractions of millet extracts were tested against MCF-7 and MDA-MB-231 breast cancer cells using the Cell-Titer® Glo assay. The graphs represent mean cell survival as a percentage of vehicle control ± SD for each concentration of millet extract as determined from two independent experiments each performed in quadruplicate.

3.3 Discussion

Millets have long been a staple food in parts of central Africa and East Asia. In recent times millets have gained a reputation as a food which is beneficial to health. Apart from their nutritional value, millets are also a known source of anti-oxidants which have been linked to lowering blood pressure and reducing risk of cardiovascular disease, diabetes and cancer (Singh and Sarita, 2016). In addition, millets have also been shown to be a rich source of phytochemicals such as tannins, phenolic acids, anthocyanins and phytoesters which are believed to be responsible for their health benefits (Rao, Nagasampige and Ravikiran, 2011; Mathanghi, 2012). Together, this was the motivation for the current study investigating the anti-breast cancer activity of extracts derived from the African millets Babala, Enforcer and Tef. The results show that extracts derived using a reflux-based procedure exhibited no cytotoxicity against breast cancer cells. It has been reported that the polyphenol content of extracts derived from finger millets decreased with an increase in pH (Chethan and Malleshi, 2007). Therefore, it is possible that the increase of the pH during the neutralisation step in the reflux-based extraction procedure may have reduced the polyphenol content of the extracts and thus these extracts did not show any cytotoxic activity.

To overcome the problem with the reflux-based extraction procedure, extracts from the Babala, Enforcer and Tef millets were prepared using a cold extraction procedure. Furthermore, to isolate and concentrate the potential active compounds in these extracts, they were subjected to fractionation via HPTLC. This yielded methanol fractions for Enforcer and Babala and water fractions for Enforcer, Babala and Tef. This study demonstrates that the methanol fractions derived from Enforcer and Babala display cytotoxic activity against the ER+ MCF-7 and TN MDA-MB-231 breast cancer cells. Whereas this is the first study to describe anti-cancer activity for Babala, a 3-deoxyanthocyanin containing extract derived from Enforcer was previously described (Suganyadevi, Saravanakumar and Mohandas, 2013). Interestingly, while Suganyadevi et al. (2013) reported an IC_{50} of 300µg/ml for their Enforcer extract in the MCF-7 breast cancer cells, this study shows that the methanol extract of Enforcer used had a much

lower IC_{50} of 6.894µg/ml in MCF-7 cells. These results suggest that the Enforcer extract used in the current study may contain more effective compounds and this should be further explored. This study also found that the TN MDA-MB-231 cells were more sensitive than the ER+ MCF-7 cells to the methanol fractions of Enforcer and Babala. Indeed, these fractions exhibited lower IC_{50} values in MDA-MB-231 cells which is promising as TN breast cancers are known to be resistant to current chemotherapies. To explore that this is indeed the case, future studies should test the methanol fractions of Enforcer and Babala in a panel of breast cancer cell lines representative of all breast cancer subtypes.

Whereas the cytotoxicity of the extracts obtained from the reflux-based procedure was measured using the MTT assay, the Cell-Titer Glo® assay was used for extracts obtained from the cold extraction procedure. The switch to the use of the Cell-Titer Glo® assay was motivated by several inherent limitations of the MTT assay. The MTT assay is a colorimetric assay which relies on the conversion of the yellow tetrazolium salt to the purple formazan by the mitochondrial succinate dehydrogenase enzyme. However, formazan can also be formed by the culture medium or the membrane bound NADPH oxidase which impacts the colour of the reaction and is therefore likely to give rise to false positive results (Stockert *et al.*, 2018). Furthermore, the reliability of the MTT assay may depend on several factors such as the cell line being tested, the drug concentrations used, as well as the times at which the measurements were captured (Stepanenko and Dmitrenko, 2015). Indeed, when the cytotoxicity of the polyphenol (-)-epigallocatechin-3-gallate (EGCG) was tested, results from MTT assays did not correlate with the results obtained using trypan blue and Cell-Titer Glo® assays (Wang, Henning and Heber, 2010). Thus, while the MTT assay is widely used, it should be employed with caution depending on the experiments to be performed and it is recommended that it should be done in tandem with other cytotoxicity assays with microscopy still being the gold standard (Fotakis and Timbrell, 2006; Wang, Henning and Heber, 2010; Stepanenko and Dmitrenko, 2015).

It is worth noting that only the HPTLC methanol fractions of the Babala and Enforcer extracts derived from the cold extraction procedure showed short-term cytotoxicity against breast cancer cells. This suggests that the active compound(s) in these extracts is soluble in methanol which is typical of polyphenols and this should be further investigated using analytical techniques such as HPLC, NMR and LC-MS.

Chapter 4: The anti-breast cancer activity of Kraalbos

4.1 Introduction

The South African landscape is replete with indigenous plants which hold great cultural and medicinal value. An example of such a plant is *Galenia africana,* also known as Kraalbos or Geelbos, *a* perennial shrub indigenous to southern Africa. It is mainly found throughout the Namaqualand and Karoo regions (De Beer and Van Wyk, 2011). The indigenous Khoisan people and the inhabitants of the Namaqua region have long been aware of the medicinal properties of Kraalbos. Traditionally it has been used to treat a variety of ailments such as skin rashes, dandruff and dry scalp, coughs and wounds (Van Wyk, De Wet and Van Heerden, 2008; De Beer and Van Wyk, 2011). It also has known analgesic properties and has been used to treat respiratory conditions such as asthma and tuberculosis (Mativandlela *et al.*, 2008, 2009; De Beer and Van Wyk, 2011). This versatility in the traditional use of Kraalbos shows its value as a medicinal agent.

The panacea-like status of Kraalbos among the indigenous people has served as the impetus for the investigation of its medicinal properties. Several studies have demonstrated the activity of Kraalbos extracts against a broad range of biological pathogens. Elbagory *et al.* (2017) reported that gold nanoparticles encasing an aqueous Kraalbos extract showed anti-microbial properties against *Pseudomonas aeruginosa*. Kraalbos also exhibits antimycobacterial effects against both *Mycobacterium smegmatis* and *Mycobacterium tuberculosis* (Mativandlela *et al.*, 2008, 2009). Similarly, ethanolic extracts derived from the aerial parts of Kraalbos have been reported to display antifungal activity (Vries *et al.*, 2005). Thus, there is a growing pool of scientific literature that provides credibility to the anecdotal claims of Kraalbos as a medicinal agent.

Apart from its antibacterial, antimycobacterial and antifungal properties, Kraalbos extracts have also been investigated in other biological contexts. For example, a dichloromethane extract derived from the stems and leaves of Kraabos was shown inhibit human ether-a-

go-go-related gene (hERG) channel activity (Du *et al.*, 2015). Furthermore, ethanolic Kraalbos extracts have been shown to exhibit environmental toxicity and immunotoxicity (Pool, Klaasen and Shoko, 2009a, 2009b). Similarly, the acute toxicity of Kraalbos has also been investigated *in vivo* and its toxicity profile has been deemed acceptable for pharmaceutical and cosmetic applications (Ng'uni, Klaasen and Fielding, 2018).

Despite several studies that have investigated the medicinal properties of Kraalbos, the anti-cancer activity of Kraalbos has only been described in two PhD theses online (Shoko, 2010; Ng'uni, 2017). Indeed, Shoko (2010) showed that an ethanolic Kraalbos extract, prepared from leaves, showed short-term cytotoxicity against MCF-7 breast cancer cells. Similarly, Ng'uni et al. (2017) showed that an ethanolic Kraalbos extract, derived from leaves and shoots, exhibited short-term cytotoxicity against MCF-7 breast cancer cells and that it up-regulated genes involved in apoptosis and the DNA damage and repair pathways whilst down-regulating genes involved in angiogenesis and the cell cycle. This study aims to investigate the anti-cancer activity of five ethanolic Kraalbos extracts (KB1, KB2, KB3, KB4, and KB5) against ER+ MCF-7 and TN MDA-MB-231 breast cancer cells. Furthermore, the most promising of these extracts will be investigated further for its long-term cytotoxicity, specificity towards breast cancer cells, anti-migratory ability, mechanism of action (ROS generation, p38 MAPK signalling and cell cycle arrest) and modes of cell death induced (apoptosis, necroptosis and autophagy).

4.2 Results

4.2.1 Solubility of the Kraalbos extracts

During this study, the Prince laboratory received five ethanolic extracts (KB1, KB2, KB3, KB4, and KB5) derived from the Kraalbos plant using proprietary extraction methods by BioPharm (Cape Town, South Africa). Before testing the extracts for their anti-cancer activity, it was first necessary to identify a suitable solvent to dissolve them in and since KB5 was the first extract obtained these solubility studies were carried out for it.

4.2.1.1 The Kraalbos extract KB5 shows optimal solubility in DMSO

In search of a solvent that KB5 was soluble in and that was safe to use in cell culture, KB5 was dissolved in acetone, DMSO, water, ethanol and PBS and the percentage solubility in each solvent was calculated. Briefly, after solubilising KB5 in the various solvents the mass of the pellets were subtracted from the mass of the starting material and expressed as a percentage. As shown in **table 4.1**, KB5 exhibited the greatest percentage solubility in DMSO (98.44%), followed by PBS (84.29%) and water (83.82%). KB5 exhibited the poorest percentage solubility in acetone (36.50%) and ethanol (25.87%). Thus, these results revealed that KB5 displayed maximum solubility in DMSO and it was assumed that the same would hold true for the other Kraalbos extracts. DMSO was therefore used as the solvent for extracts KB1, KB2, KB3, KB4 and KB5.

Table 4.1: Percentage solubility of the Kraalbos extract KB5 in acetone, DMSO, water, ethanol and PBS

	Acetone	DMSO	Water	Ethanol	PBS
Weight before (mg)	1.37	1.28	1.36	1.43	1.40
Weight After (mg)	0.87	0.02	0.22	1.06	0.22
Percentage (%) solubility	36.50	98.44	83.82	25.87	84.29

4.2.2 KB1, KB2, KB3, KB4 and KB5 Kraalbos extracts show short-term cytotoxicity against breast cancer cells

To determine the short-term cytotoxicity of KB1, KB2, KB3, KB4 and KB5 against MCF-7 and MDA-MB-231 breast cancer cells, the cells were seeded in 96 well plates and treated with either vehicle or the respective extract at various concentrations (0 - 200µg/ml) for 48 hours. Cell lysates were subsequently prepared and subjected to the Cell-Titer® Glo assay and IC_{50} values were calculated for each extract. The results show that all 5 extracts inhibit both MCF-7 and MDA-MB-231 breast cancer cell viability in a dose

dependant manner **(figure 4.1 A)**. Importantly, the IC_{50} values for all the extracts were higher in the MDA-MB-231 cells than in the MCF-7 cells which suggests that they are less sensitive to the extracts **(figure 4.1 B)**. Furthermore, of the five extracts tested, KB2 exhibited the highest cytotoxicity, with an IC_{50} of 114µg/ml and 130.5µg/ml against MCF-7 and MDA-MB-231 cells respectively **(figure 4.1 B)**. KB2 was thus selected for further characterisation.

The next aim was to determine the effect of KB2 on the morphology of MCF-7 and MDA-MB-231 breast cancer cells using phase contrast light microscopy. Briefly, cells were seeded in 6cm dishes and treated for 48 hours with either vehicle or KB2 at their respective IC_{50} and ½IC_{50} concentrations. Treatment of both MCF-7 and MDA-MB-231 cells with KB2 resulted in reduced cell density, a change in cell morphology and an increase in rounded floating cells, indicative of dead cells **(figure 4.1 C)**.

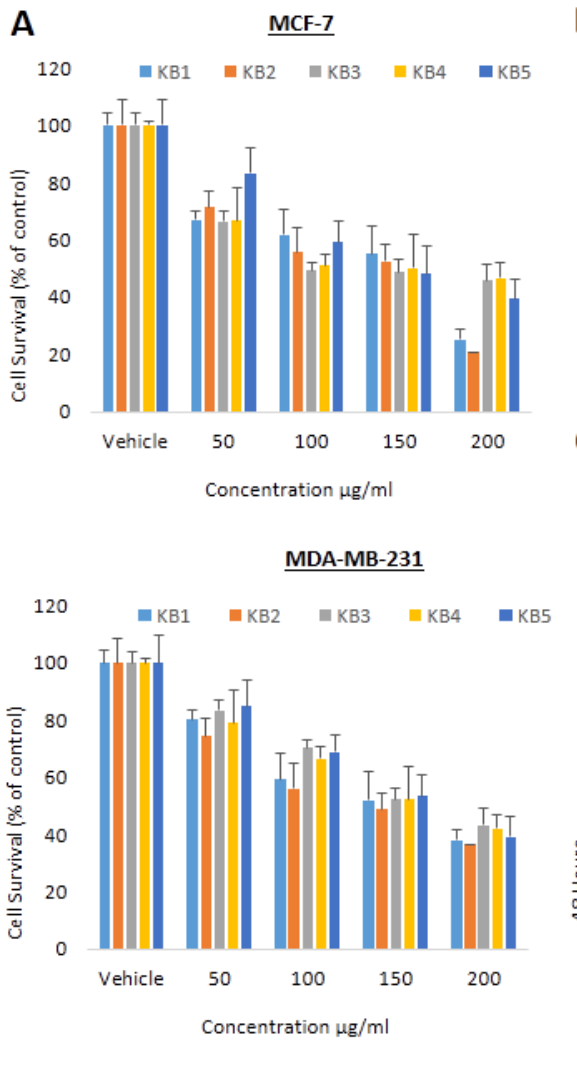

B

Extract	IC_{50} (µg/ml)	
	MCF-7	MDA-MB-231
KB1	124.2	144.2
KB2	114	130.5
KB3	132	166.3
KB4	144.1	160.8
KB5	141.6	158.4

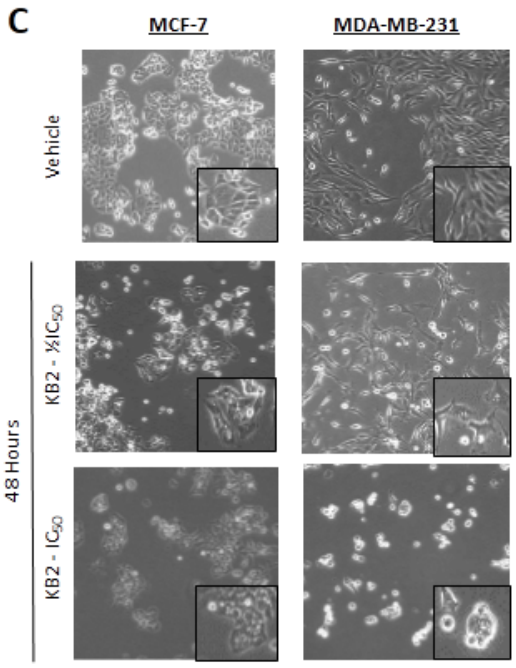

Figure 4.1: The Kraalbos extracts KB1, KB2, KB3, KB4 and KB5 show short-term cytotoxicity against breast cancer cells with KB2 showing the most potent activity. **(A)** Cell-titer Glo® short-term cytotoxicity assay of MCF-7 and MDA-MB-231 breast cancer cells treated for 48 hours with KB1, KB2, KB3, KB4 and KB5 using a range of concentrations (0 - 200µg/ml) or vehicle (DMSO). Graphs show mean cell viability as a percentage of vehicle control ± SD for each concentration of Kraalbos extract as determined from three independent experiments each performed in quadruplicate. **(B)** The IC_{50} values of KB1, KB2, KB3, KB4 and KB5 against MCF-7 and MDA-MB-231 breast cancer cells. KB2 is highlighted as it showed the most potent activity against the breast cancer cells. **(C)** Representative light microscopy images (x10; Evos® FL Core Imaging System) of MCF-7 and MDA-MB-231 cells treated for 48 hours with KB2 at their respective ½IC_{50} and IC_{50} concentrations or vehicle.

4.2.3 KB2 exhibits selectivity towards breast cancer cells in short-term cytotoxicity assays

The next aim was to establish the selectivity of KB2 towards breast cancer cells as, ideally, an anti-cancer drug should exhibit potent cytotoxicity to cancer cells with minimal cytotoxicity against non-malignant cells. To this end the IC_{50} values for KB2 in MCF-12A non-malignant breast epithelial cells and FG0 fibroblasts were established using the Cell-Titer® Glo kit as described above for the MCF-7 and MDA-MB-231 cells. The results obtained show that KB2 had IC_{50} values of 159.8µg/ml and 185.5µg/ml against MCF-12A and FG0 cells respectively **(figure 4.2 A)**. Selectivity indices (SI) for KB2 was calculated by dividing the IC_{50} value for the non-malignant cells by the IC_{50} value for the breast cancer cells. Results indicated that the breast cancer cells were slightly more sensitive than non-malignant cells with approximate SI values ranging from 1.2 to 1.6 **(figure 4.2 B)**. It is worth noting that, in general, an SI above 2.0 is considered desirable for an anti-cancer agent as it suggests that it is likely to be associated with reduced side effects (Koch *et al.*, 2005).

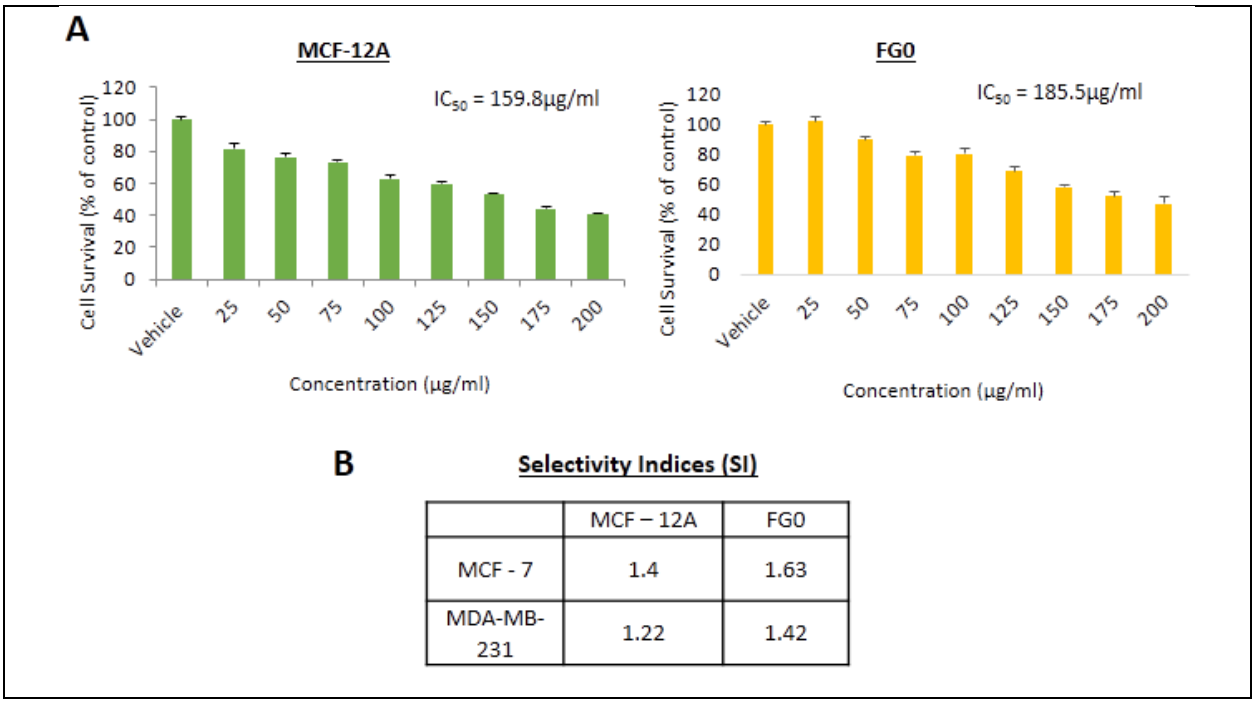

B **Selectivity Indices (SI)**

	MCF – 12A	FG0
MCF - 7	1.4	1.63
MDA-MB-231	1.22	1.42

Figure 4.2: KB2 exhibits selectivity towards breast cancer cells in short-term cytotoxicity assays. (A) Cell-titer Glo® short-term cytotoxicity assays of MCF-12A and FG0 non-malignant cells treated for 48 hours with a range of concentrations of KB2 (0 - 200µg/ml) or vehicle (DMSO). Graphs show mean cell viability as a percentage of vehicle control ± SD for each concentration of KB2 as determined from two independent experiments each performed in quadruplicate. **(B)** The selectivity indices (SI) of KB2 was determined by dividing the IC_{50} of each non-malignant cell line by the IC_{50} for each breast cancer cell line.

4.2.4 KB2 shows selectivity to breast cancer cells in long-term clonogenic assays

An effective anti-cancer drug should exhibit both short-term and long-term cytotoxicity in cancer cells. Thus, the next aim was to investigate the long-term cytotoxicity of KB2 against MCF-7 and MDA-MB-231 breast cancer cells as well as the MCF-12A non-malignant breast epithelial cells using a clonogenic survival assay. MCF-12A cells were chosen as a non-malignant cell line as they showed the greatest sensitivity to KB2 in the short-term cytotoxicity assays. The clonogenic survival assay measures the ability of single cells to survive drug treatment and grow to form new colonies. Although this assay is only an *in vitro* assay, it may give an indication of the ability of cancer cells to develop resistance to a drug (Alberts *et al.*, 1980). Briefly, cells were seeded in 6cm dishes and treated for 24 hours with either vehicle or ½IC_{50} and IC_{50} KB2 concentrations. Thereafter the cells were replated in triplicate in 35mm dishes at low densities and left to form colonies (50 or more cells per colony) in the absence of KB2 for between 7-21 days with regular media changes. Colonies were stained with crystal violet and photographed and images from three independent repeats were quantified using the ImageJ plugin ColonyArea (Guzmán et al., 2014). The results show that KB2 significantly reduces the colony forming ability of both MCF-7 and MDA-MB-231 breast cancer cells at ½IC_{50} and IC_{50} concentrations but it was more effective at inhibiting the survival of MDA-MB-231 cells **(figure 4.3)**. Interestingly, KB2 showed very little effect on the colony forming ability of MCF-12A cells at ½IC_{50} and 49.15% of colonies still survived at the IC_{50} concentration **(figure 4.3)**. Thus, it was concluded that KB2 was selectively cytotoxic to MCF-7 and MDA-MB-231 breast cancer cells in long-term cytotoxic assays.

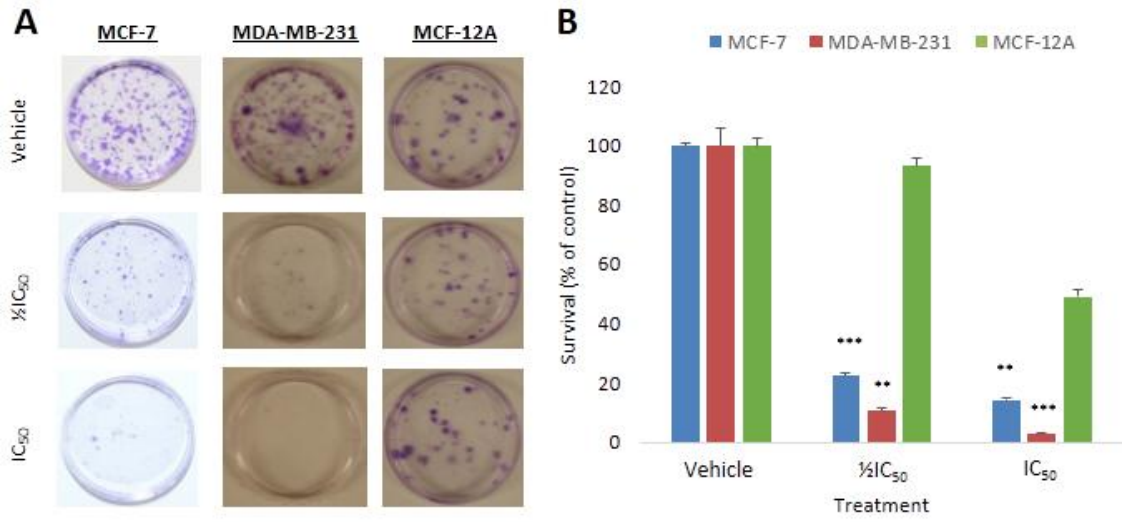

Figure 4.3: KB2 exhibits selective long-term cytotoxicity in breast cancer cells. (A) Representative photographs of MCF-7, MDA-MB-231 and MCF-12A cells treated with vehicle (DMSO) or KB2 at their respective ½IC_{50} and IC_{50} concentrations for 24 hours and then replated at low densities in KB2-free medium and left for 7-21 days for colonies to form. Colonies were stained with crystal violet. Images are representative of three independent repeats performed in triplicate. **(B)** The area covered by the colonies were measured using the ColonyArea plugin for ImageJ (Guzmán *et al.*, 2014). Graphs show cell survival as a percentage of vehicle control for each KB2 treatment condition ± SD determined from three independent experiments performed in triplicate. Data were analysed using GraphPad 6.0. Statistical significance was determined using a student *t*-test and taken as * $p \leq 0.05$, ** $p \leq 0.01$ and *** $p \leq 0.001$.

4.2.5 KB2 inhibits breast cancer cell migration

The ability of breast cancer cells to migrate from the primary site to form metastatic tumours in distant organs is the main cause of morbidity and mortality in breast cancer. Thus, to determine if KB2 was able to inhibit the migratory ability of MCF-7 and MDA-MB-231 breast cancer cells a scratch motility, or wound healing, assay was performed. In this assay an artificial wound is induced on a confluent monolayer of cells and the rate at which the cells migrate to close this wound is measured. Briefly, MCF-7 and MDA-MB-231 breast cancer cells were seeded in 12 well plates and allowed to reach 100% confluence. Thereafter, an artificial wound was induced using a pipette tip and the cells were then treated with either vehicle or KB2 at their respective ½IC_{50} and IC_{50}

concentrations. To ensure that the closure of the wound was only due to migration, cells were also treated with mitomycin C at this stage to prevent proliferation. The closure of the wound was photographed over a period of 24 hours and the area of the wound was analysed using the ImageJ software. MCF-7 cells treated with the IC_{50} KB2 showed a trend towards decreased migration at 3, 6 and 9 hours and after 24 hours the cells treated with both $½IC_{50}$ and IC_{50} migrated significantly slower than vehicle treated cells **(figure 4.4 A)**. MDA-MB-231 cells treated with both $½IC_{50}$ and IC_{50} KB2 for 3 hours showed a trend towards decreased migration and by 9 hours they migrated significantly slower than vehicle treated cells **(figure 4.4 A)**.

Epithelial-mesenchymal-transition (EMT) describes a process where epithelial cells lose their adhesive properties and acquire a fibroblast-like morphology and increased motility (Dongre and Weinberg, 2019). It confers upon cancer cells increased metastatic and invasive properties and greater resistance to chemotherapy and immunotherapy. Thus, targeting the EMT process is a potentially important approach for suppressing breast cancer cell metastasis. The effects of KB2 on the EMT markers E-cadherin, β-catenin and vimentin were therefore next investigated using western blotting. The ubiquitously expressed protein p38 was used as a loading control as its expression levels are constant and independent of the cell cycle or experimental conditions (Raingeaud *et al.*, 1995). The results show that KB2 reduces the expression of the mesenchymal markers β-catenin and vimentin whilst increasing the levels of the epithelial marker E-cadherin in both MCF-7 and MDA-MB-231 cells **(figure 4.4 B)**. Taken together these results show that KB2 inhibits the migratory ability of MCF-7 and MDA-MB-231 breast cancer cells.

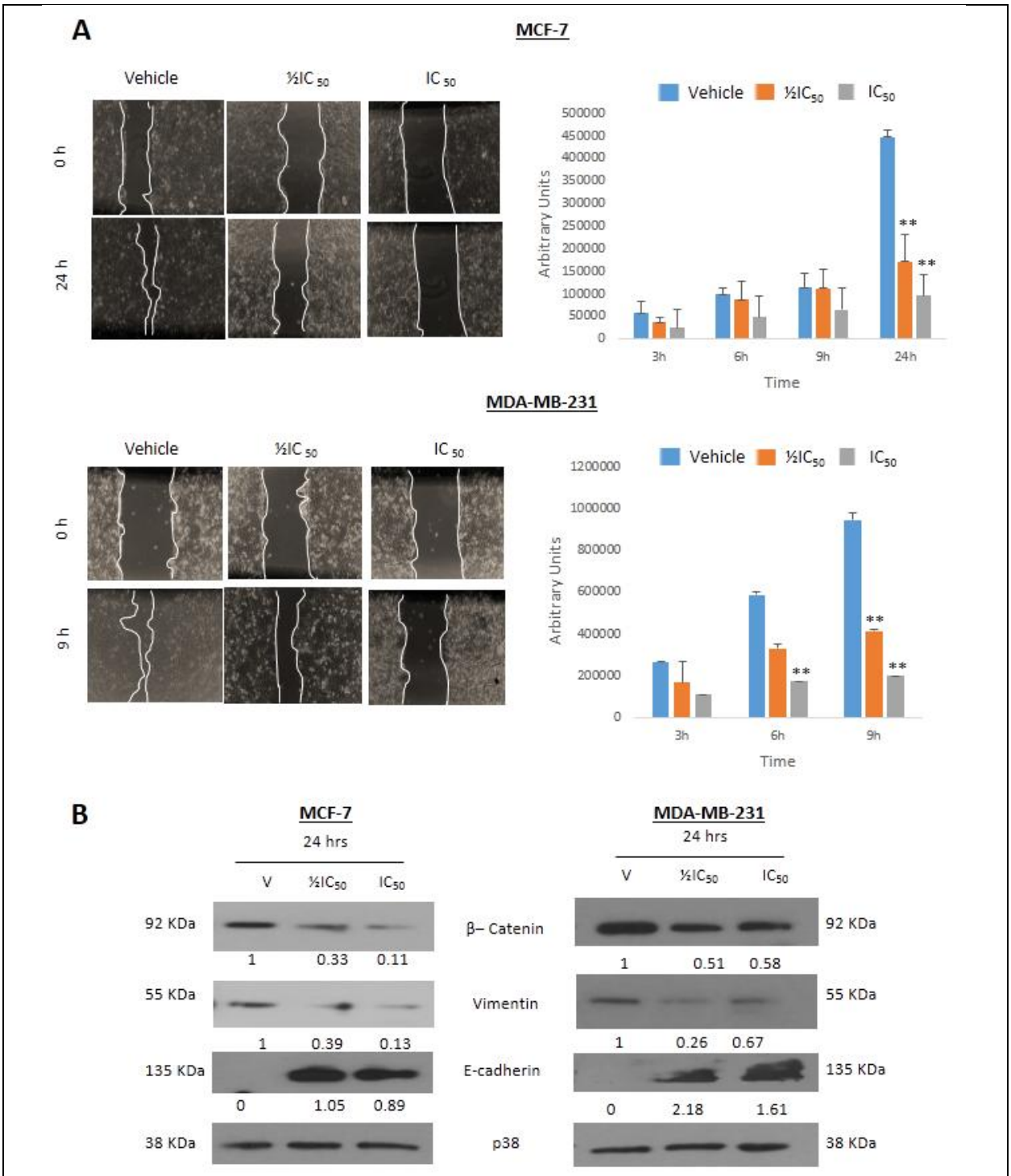

Figure 4.4: KB2 inhibits breast cancer cell migration. (A) Representative images (x10; Evos® XL Core Imaging System) of MCF-7 and MDA-MB-231 breast cancer cells treated with either ½IC_{50} or IC_{50} KB2 concentrations or vehicle (DMSO). Cells were plated and allowed to reach 100% confluence. A sterile 10µl pipette tip was used to make a linear wound in the cell

monolayer and cells were treated with KB2 or vehicle as well as mitomycin C to inhibit proliferation. Cells were imaged at the times indicated and the total area migrated was calculated by subtracting the wound area at each time point from the wound area at time 0. Graphs represent area migrated (in arbitrary units) ± SD for each treatment condition determined from three independent experiments performed in triplicate. Data were analysed using GraphPad 6.0. Statistical significance was determined using a student *t*-test and taken as * $p \leq 0.05$, ** $p \leq 0.01$ and *** $p \leq 0.001$.**(B)** Western blot analyses of protein harvested from MCF-7 and MDA-MB-231 cells treated with either vehicle (DMSO) or KB2 at their respective ½IC_{50} and IC_{50} concentrations for 24 hours. Proteins were resolved via SDS-PAGE (8-15% gels) and western blotting was performed using antibodies to the EMT markers E-cadherin, β-catenin and vimentin. Total p38 levels were used as a loading control. Densitometry readings were obtained using ImageJ and are representative of the level of the protein of interest divided by the corresponding p38 level and normalised to vehicle control sample (where possible). Blots are representative of at least two independent repeats.

4.2.6. The anti-cancer mechanism of action of KB2

To begin to elucidate the mechanism by which KB2 exhibits anti-breast cancer activity, its effect on ROS production as well as the p38 MAPK stress signalling and DNA damage pathway was next investigated.

4.2.6.1 KB2 induces ROS production in breast cancer cells

One of the mechanisms by which phytochemicals kill cancer cells is by inducing an oxidative stress through the generation of ROS which leads to a decrease in antioxidants. This imbalance is known to induce oxidative stress and apoptosis because ROS are capable of damaging DNA, RNA, protein and lipid molecules (Simon, Haj-Yehia and Levi-Schaffer, 2000; Viswesh, Gates and Sun, 2010; Vallejo, Salazar and Grijalva, 2017). It was, therefore, hypothesised that KB2 may function by inducing the production of intracellular ROS (Navaneethakrishnan, Rosales and Lee, 2019). It is important to note that the production of ROS involves the formation of different ROS species and while most of them have short half-lives, H_2O_2 has a relatively long half-life. Furthermore, many

ROS species are converted to H_2O_2 and thus it served as a good marker to measure total ROS. To investigate the impact of KB2 on the intracellular production of ROS, the levels of H_2O_2 were thus measured using the ROS-Glo™ H_2O_2 assay. This assay contains a substrate which reacts with H_2O_2 to produce a luciferin precursor which, in the presence of the ROS-Glo™ solution, is converted to luciferin which then reacts with luciferase to produce light. This luminescence output thus corresponds to the amount of H_2O_2 present. Briefly, breast cancer cells were treated with either vehicle or KB2 for 24 hours and the levels of H_2O_2 were measured using the ROS-Glo™ H_2O_2 assay. In MDA-MB-231 cells the levels of H_2O_2 increased upon treatment with IC_{50} KB2 with further increase upon $2IC_{50}$ treatment **(figure 4.5 A)**. Interestingly, in MCF-7 cells the H_2O_2 levels increased upon treatment with IC_{50} KB2 with no further increase upon $2IC_{50}$ treatment **(figure 4.5 A)**. These results suggested that KB2 induces the production of ROS in breast cancer cells.

To confirm that KB2 induces the production of ROS in MCF-7 and MDA-MB-231 breast cancer cells, the GSH-Glo™ Glutathione assay was performed. This assay is used complimentary to the ROS-Glo™ H_2O_2 assay as it measures the presence of the antioxidant glutathione, which decreases with an increase in ROS. The GSH-Glo™ Glutathione assay contains a luciferin precursor, which is converted into luciferin in the presence of glutathione and glutathione S-transferase. This luciferin then reacts with luciferase to produce light, which is measured as an output of glutathione (GSH) levels. Briefly, breast cancer cells were treated with either vehicle or KB2 for 24 hours and thereafter glutathione levels were measured using the GSH-Glo™ Glutathione assay. In KB2 treated MDA-MB-231 cells, the GSH levels decreased at the IC_{50} concentration and there was a further decrease at the $2IC_{50}$ concentration **(figure 4.5 B)**. These results were consistent with the data obtained from the ROS-Glo™ H_2O_2 assay. In MCF-7 cells treated with KB2 there was a dose dependent decrease, albeit not statistically significant, in GSH levels **(figure 4.5 B)**. The ROS-Glo™ H_2O_2 and GSH-Glo™ Glutathione assays were each only carried out once and therefore the results from these assays are only preliminary. However, taken together, they do suggest that KB2 induces oxidative stress through the production of ROS in both MCF-7 and MDA-MB-231 breast cancer cells.

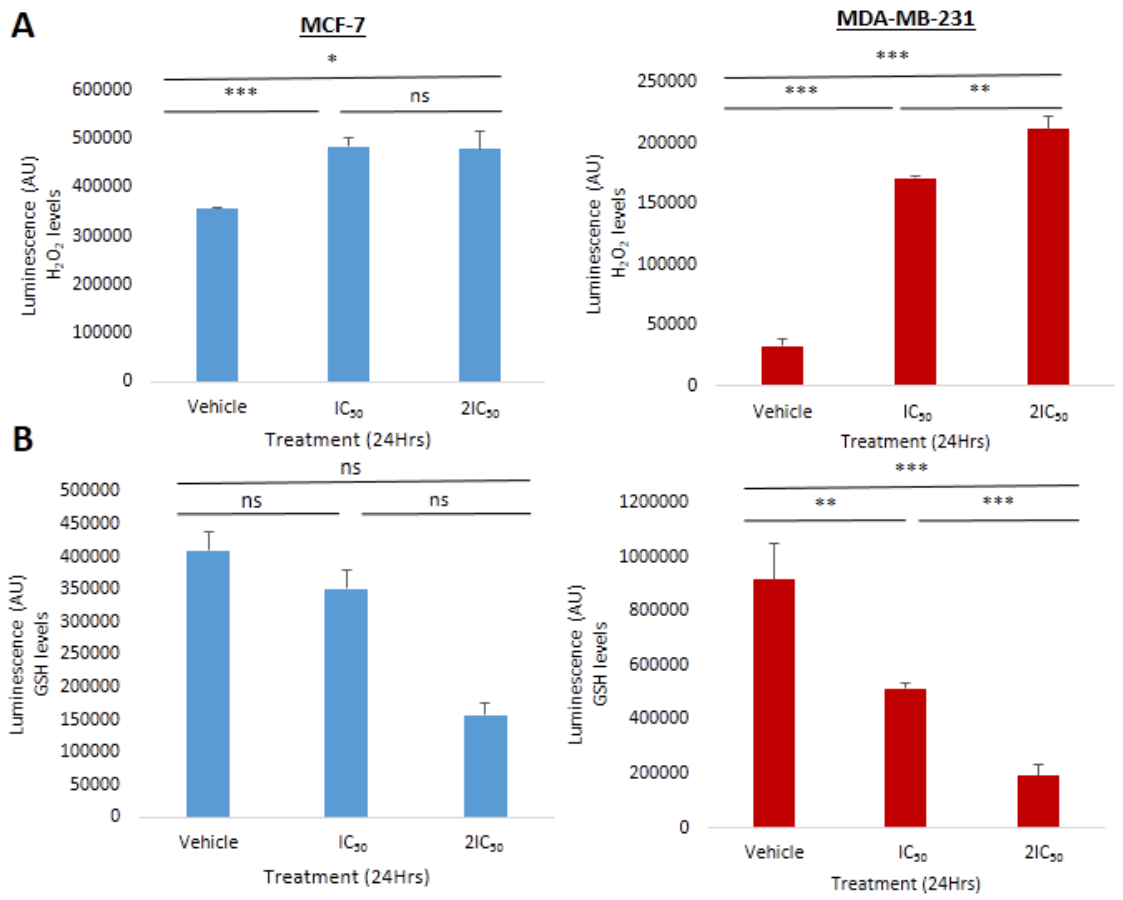

Figure 4.5: KB2 induces the production of reactive oxygen species (ROS) in breast cancer cells. (A) Peroxide levels measured using the ROS-Glo™ H_2O_2 assay in MCF-7 and MDA-MB-231 cells treated with either vehicle (DMSO) or IC_{50} or $2IC_{50}$ KB2 for 24 hours. Graphs represent luminescence, indicative of H_2O_2 levels, plotted against each treatment condition. Error bars are representative of SD. Results were obtained from one biological repeat carried out in triplicate. Data were analyzed using GraphPad Prism 6.0. Significance was determined using a student *t*-test and taken as * $p \leq 0.05$, ** $p \leq 0.01$ and *** $p \leq 0.001$. **(B)** Glutathione (GSH) levels measured using the GSH-Glo™ Glutathione assay in MCF-7 and MDA-MB-231 cells treated with either vehicle (DMSO) or IC_{50} or $2IC_{50}$ KB2 for 24 hours. Graphs represent luminescence, indicative of GSH levels, plotted against each treatment condition. Error bars are representative of SD. Results were obtained from one biological repeat carried out in triplicate. Data were analyzed using GraphPad Prism 6.0. Significance was determined using a student *t*-test and taken as * $p \leq 0.05$, ** $p \leq 0.01$ and *** $p \leq 0.001$.

4.2.6.2 KB2 induces DNA damage in breast cancer cells

The production and accumulation of intracellular ROS is known to induce double strand DNA breaks (DSBs) (Barzilai and Yamamoto, 2004). Thus, the next aim was to investigate whether KB2 induced DNA damage in MCF-7 and MDA-MB-231 breast cancer cells using western blotting and immunocytochemistry (ICC) with antibodies to γH2AX. The γH2AX protein is a phosphorylated variant of the histone H2AX and accumulates at the sites of DSBs and is considered a robust marker of DNA damage (Valdiglesias *et al.*, 2013). Western blotting revealed that the levels of γH2AX increased in MCF-7 and MDA-MB-231 cells treated with KB2 in both a time and dose dependant manner **(figure 4.6 A)**. Similarly, the results from the ICC experiments revealed the presence γH2AX puncta in the nuclei of KB2 treated MCF-7 and MDA-MB-231 cells **(figure 4.6 B)**. Furthermore, there was a dose dependent increase in γH2AX levels in KB2 treated MCF-7 and MDA-MB-231 cells **(figure 4.6 C)**. Taken together, these results indicate that KB2 induces DNA damage, in the form of DSBs, in breast cancer cells.

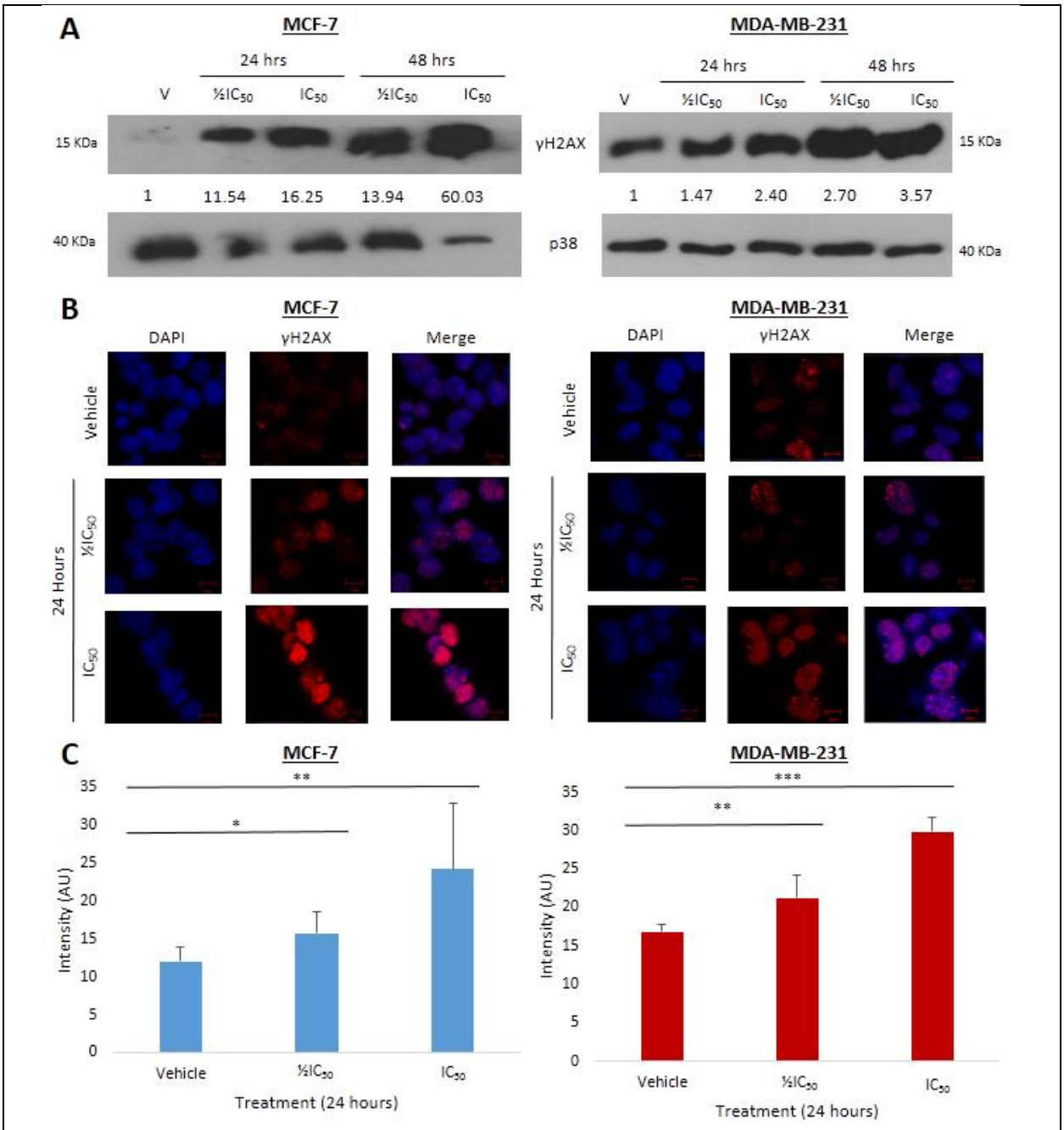

Figure 4.6: KB2 induces DNA damage in breast cancer cells. (A) Western blot analyses of protein harvested from MCF-7 and MDA-MB-231 cells treated with either vehicle (DMSO) or KB2 at their respective IC_{50} and $½IC_{50}$ concentrations for 24 and 48 hours. Proteins were resolved via SDS-PAGE (8-15% gels) and western blotting was performed using antibodies to γH2AX, a robust marker of DNA damage. Total p38 levels were used as a loading control. Densitometry readings were obtained using ImageJ and are representative of the level of the protein of interest divided by the corresponding p38 level and normalised to vehicle control

sample (where possible). Blots are representative of at least two independent repeats. **(B)** Representative confocal immunofluorescence maximum intensity projection images (63x; Carl Zeiss LSM 880) of MCF-7 and MDA-MB-231 cells treated with either vehicle (DMSO) or KB2 at their respective IC_{50} and ½IC_{50} concentrations for 24 hours and γH2AX levels detected with a flourophore-conjugated Cy3 secondary antibody. Nuclei of cells were stained with DAPI. Scale bar is 10µm. **(C)** Quantification of confocal images shown in **B** for γH2AX. Graphs are representative of the intensity of the γH2AX signal per treatment condition as mean nuclear Cy3 fluorescence across 5 or more independent fields of view. Error bars are representative of SD. Data were analyzed using GraphPad Prism 6.0. Statistical significance was determined using a student *t*-test and taken as * $p \leq 0.05$, ** $p \leq 0.01$ and *** $p \leq 0.001$.

4.2.7 KB2 induces a cell cycle arrest in both MCF-7 and MDA-MB-231 cells

The tumour suppressor protein p53 is an important mediator of cell cycle arrest and apoptosis in response to genotoxic (DSBs) and oxidative (ROS) stress. While p53 is upregulated within a few minutes of DNA damage, ROS can act as an upstream molecule to activate p53 and as a downstream factor to mediate p53 induced cell death (Lakin and Jackson, 1999). Furthermore, in response to a variety of stimuli including DNA damage, the potent cyclin dependent kinase (CDK) inhibitor, p21 (also known as p21(WAF1/Cip1)), is induced by p53-dependent and p53-independent mechanisms and it binds to and inhibits the activity of cyclin-CDK2, -CDK1, and -CDK4/6 complexes, to promote cell cycle arrest. Thus, the effects of KB2 on levels of p53, p21, cyclin A and cyclin B1 were investigated by western blotting. The results, depicted in **figure 4.7 A**, show that upon KB2 treatment p53 increased in MCF-7 cells but no increase in p53 levels were observed in MDA-MB-231 cells. This is possibly due to the expression of high levels of a mutant non-functional p53 in MDA-MB-231 cells (Gartel, Feliciano and Tyner, 2003). Interestingly, KB2 treated MDA-MB-231 cells still showed a dose dependant increase in p21 levels which suggests that its regulation is p53 independent in these cells. Similarly, p21 levels increased in KB2 treated MCF-7 cells. Furthermore, KB2 treatment resulted in a decrease in the levels of cyclin A and cyclin B1 in MCF-7 and MDA-MB-231 cells which is indicative of cell cycle arrest.

To confirm that KB2 induces cell cycle arrest, the DNA of the cells was stained with propidium iodide (PI) and the cells were subjected to flow cytometry. The amount of DNA present in cells increases as the cell cycle progresses and this results in a more intense PI fluorescent signal which can be detected by flow cytometry and used to determine the number of cells in every phase of the cell cycle. Flow cytometry analysis revealed an accumulation of MCF-7 cells in the S-phase at the expense of the G1 phase at both 24 and 48 hours of treatment **(figure 4.7 B and C)**. Interestingly, KB2 treatment of MCF-7 cells led to a decrease in G2/M cells after 24 hours but an increase in G2/M cells after 48 hours. There was an accumulation of MDA-MB-231 cells in both the S and G2/M phases at the expense of the G1 phase at both 24 and 48 hours of KB2 treatment **(figure 4.7 B and C)**. Importantly, there was a trend towards an increase in a sub-G1 peak, indicative of cell death, in MCF-7 and MDA-MB-231 cells treated with KB2. Taken together, the results showed that KB2 induced cell cycle arrests and cell death in MCF-7 and MDA-MB-231 breast cancer cells.

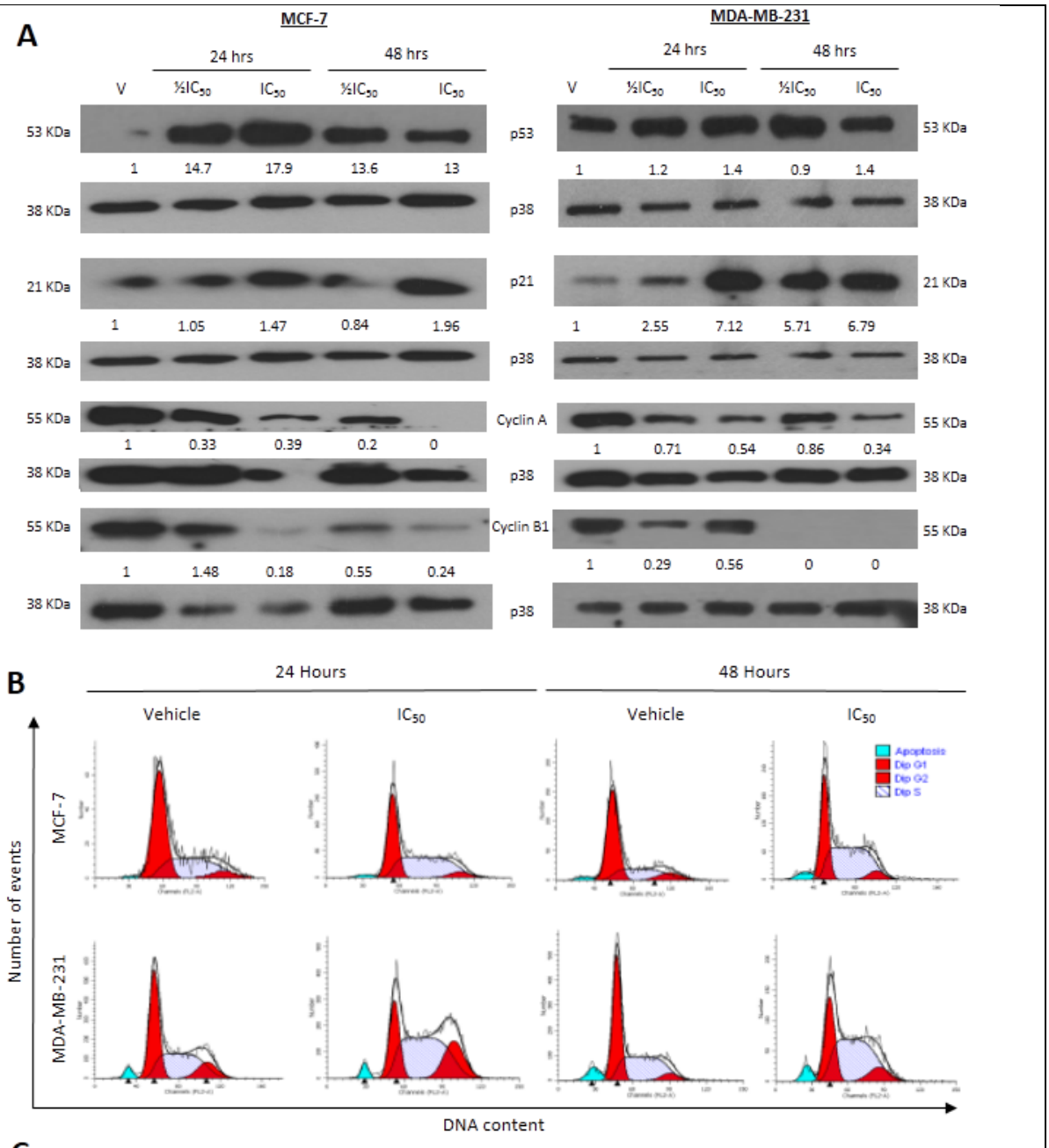

C

Cell Line	Cell Cycle Phase	24 Hours		48 Hours	
		Vehicle	IC_{50}	Vehicle	IC_{50}
MCF-7	Sub-G1	0.55 ± 0.65	1.66 ± 0.68	1.11 ± 1.63	2.42 ± 2.32
	G1	56.44 ± 7.71	50.62 ± 7.75	63.60 ± 4.51	47.59 ± 10.24
	S	33.00 ± 5.87	40.84 ± 10.47	27.97 ± 5.32	42.69 ± 13.62
	G2/M	10.23 ± 3.84	8.54 ± 2.92	8.43 ± 1.67	9.73 ± 3.38
MDA-MB-231	Sub-G1	4.05 ± 1.06	4.88 ± 2.94	6.09 ± 2.13	6.52 ± 2.57
	G1	35.52 ± 6.92	23.90 ± 1.69	43.48 ± 7.01	30.29 ± 3.22
	S	56.13 ± 11.51	60.99 ± 4.80	51.72 ± 6.04	57.51 ± 6.04
	G2/M	8.26 ± 5.59	15.11 ± 6.28	5.17 ± 1.50	12.20 ± 3.13

Figure 4.7: KB2 induces cell cycle arrests in both MCF-7 and MDA-MB-231 breast cancer cells (A) Western blot analyses of protein harvested from MCF-7 and MDA-MB-231 cells treated with either vehicle (DMSO) or KB2 at their respective ½IC_{50} and IC_{50} for 24 and 48 hours. Proteins were resolved via SDS-PAGE (8-15% gels) and western blotting was performed using antibodies to the cell cycle regulators p53, p21, cyclin A and cyclin B1. Total p38 levels were used as a loading control. Densitometry readings were obtained using ImageJ and are representative of the level of the protein of interest divided by the corresponding p38 level and normalised to vehicle control sample (where possible). Blots are representative of at least two independent repeats. **(B)** Flow cytometry analyses of MCF-7 and MDA-MB-231 cells treated with either vehicle or IC_{50} concentrations of KB2 for 24 and 48 hours. The DNA of the cells was stained with PI before flow cytometry analysis was carried out. Representative histograms show the number of cells plotted against the DNA content. Peaks are representative of the different phases of the cell cycle i.e. sub-G1, G1, S and G2/M. **(C)** The overall percentage of total cells in each phase are presented in table form. Percentages are shown together with SD. Results shown are averages across three biological repeats.

4.2.8 KB2 induces intrinsic and extrinsic apoptosis in breast cancer cells

When cells are unable to repair DNA damage, biochemical cascades are activated that lead to one or more forms of programmed cell death (PCD) such as apoptosis, programmed necrosis (necroptosis) and autophagy. Apoptotic cell death can be identified by several characteristic morphological and molecular markers. **Figure 4.8 A** shows that KB2 treatment did indeed induce several morphological features such as cell shrinkage and membrane blebbing in MCF-7 and MDA-MB-231 cells. Furthermore, when the nuclei of the cells were stained with DAPI, there was evidence of chromatin condensation, another marker of apoptosis, in the breast cancer cells treated with KB2 **(figure 4.8 A, lower panel)**.

At a molecular level, apoptosis may proceed via an intrinsic or extrinsic pathway. The extrinsic pathway is triggered by death signals originating from death receptors found on the cell membrane and it involves the initiator caspase 8. The intrinsic pathway on the other may be triggered by internal stresses such as ROS production or DNA damage and

it involves the initiator caspase 9. Both these apoptotic pathways converge on the executioner caspases 3 and 7 which cleave the DNA repair protein PARP. Therefore, to confirm that KB2 induced apoptosis in MCF-7 and MDA-MB-231 cells its impact on the levels of cleaved caspases 8, 9, 3 and 7 and cleaved PARP was investigated by western blotting. **Figure 4.8 B** shows that when comparing the levels of the initiator caspases, cleaved caspase 9 was highest at 24 hours of KB2 treatment, but levels of cleaved caspase 8 were highest at 48 hours of treatment in both breast cancer cell lines. Furthermore, compared to the vehicle treated cells, the levels of cleaved caspases 3 and 7 and PARP increased in KB2 treated MCF-7 and MDA-MB-231 cells. Together these results indicated that KB2 induced both apoptotic pathways in the breast cancer cells tested but that it triggers the intrinsic apoptotic pathway before the extrinsic apoptotic pathway.

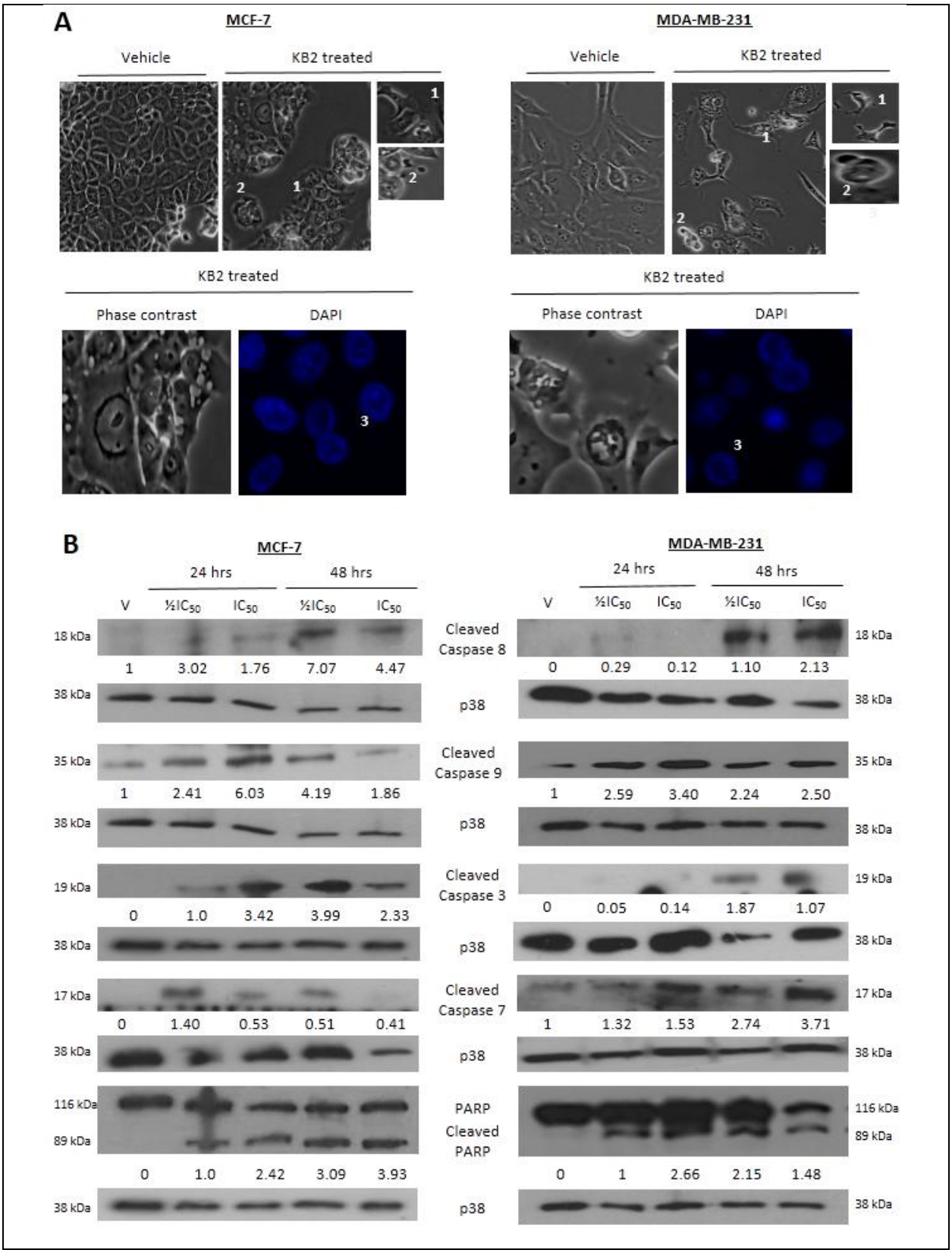
A
MCF-7
MDA-MB-231
Vehicle
KB2 treated
Vehicle
KB2 treated
1
2
1
2
1
2
1
2
KB2 treated
KB2 treated
Phase contrast
DAPI
Phase contrast
DAPI
3
3
B
MCF-7
MDA-MB-231
24 hrs
48 hrs
24 hrs
48 hrs
V
½IC50
IC50
½IC50
IC50
V
½IC50
IC50
½IC50
IC50
18 kDa
Cleaved Caspase 8
18 kDa
1
3.02
1.76
7.07
4.47
0
0.29
0.12
1.10
2.13
38 kDa
p38
38 kDa
35 kDa
Cleaved Caspase 9
35 kDa
1
2.41
6.03
4.19
1.86
1
2.59
3.40
2.24
2.50
38 kDa
p38
38 kDa
19 kDa
Cleaved Caspase 3
19 kDa
0
1.0
3.42
3.99
2.33
0
0.05
0.14
1.87
1.07
38 kDa
p38
38 kDa
17 kDa
Cleaved Caspase 7
17 kDa
0
1.40
0.53
0.51
0.41
1
1.32
1.53
2.74
3.71
38 kDa
p38
38 kDa
116 kDa
89 kDa
PARP
Cleaved PARP
116 kDa
89 kDa
0
1.0
2.42
3.09
3.93
0
1
2.66
2.15
1.48
38 kDa
p38
38 kDa

Figure 4.8: KB2 induces the intrinsic and extrinsic apoptotic pathways in breast cancer cells. (A) Representative phase contrast and fluorescent microscope images of MCF-7 and MDA-MB-231 cells treated with either vehicle (DMSO) or KB2 and in the case of the fluorescent images the nuclei of the cells were stained with DAPI. Numbers represent the morphological features of apoptosis as follows, 1: cell shrinkage, 2: membrane blebbing and 3: chromatin condensation. **(B)** Western blot analyses of proteins harvested from MCF-7 and MDA-MB-231 cells treated with either vehicle or KB2 at their respective ½IC_{50} and IC_{50} concentrations for 24 and 48 hours. Proteins were resolved via SDS-PAGE (8-15% gels) and western blotting with antibodies to caspases 8, 9, 3 and 7 and PARP. Total p38 levels were used as a loading control. Densitometry readings were obtained using ImageJ and are representative of the level of the protein of interest divided by the corresponding p38 levels and normalised to the vehicle control sample (where possible). Blots are representative of at least two independent repeats.

4.2.9 KB2 induces necroptosis in breast cancer cells

Cancer cells can often evade cell death and therefore anti-cancer drugs need to trigger multiple PCD pathways such as programmed necrosis, also called necroptosis, (PCD type III) and autophagy (PCD type II). Necroptosis proceeds via the phosphorylation of the kinase RIP3 (p-RIP3) which phosphorylates its downstream target MLKL, the executor of necroptosis (He, Huang and Shen, 2016). To investigate whether KB2 induced necroptosis in MCF-7 and MDA-MB-231 breast cancer cells, the levels of p-RIP3 and p-MLKL were therefore investigated by western blotting. The levels of p-RIP3 increased under all KB2 treatment conditions in MCF-7 cells but its levels were highest in cells treated with ½IC_{50} KB2 at both time points tested **(figure 4.9)**. Interestingly, the levels of p-MLKL increased only at 24 hours of KB2 treatment in the MCF-7 cells. This may indicate that in MCF-7 cells necroptosis may be the preferred mode of programmed cell death at lower concentrations and at shorter treatment durations. In MDA-MB-231 cells, there was an increase in the levels of p-RIP3 and p-MLKL for all KB2 treatments **(figure 4.9)**. Taken together these results show that KB2 activates necroptosis in both MCF-7 and MDA-MB-231 breast cancer cell lines.

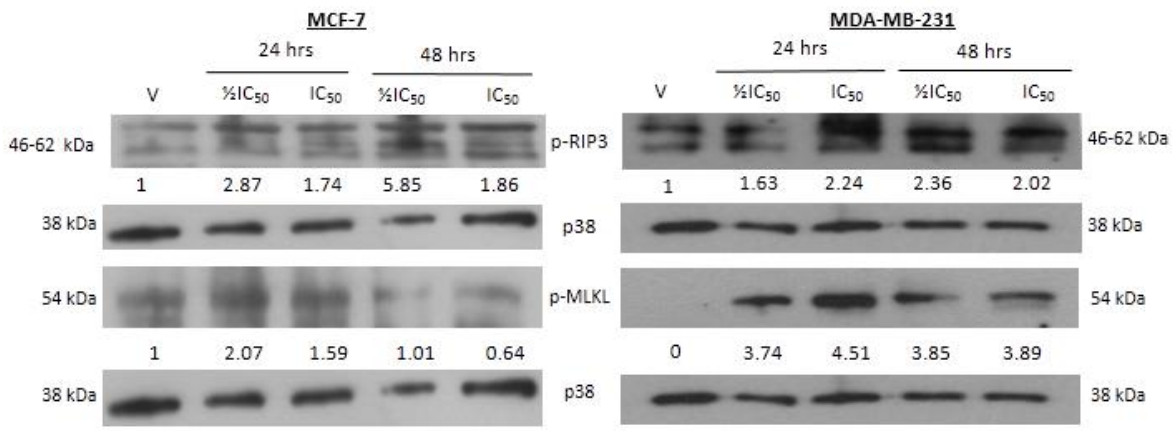

Figure 4.9: KB2 induces necroptosis in breast cancer cells. Western blot analyses of protein harvested from MCF-7 and MDA-MB-231 cells treated with either vehicle or KB2 at their respective ½IC_{50} and IC_{50} concentrations for 24 and 48 hours. Proteins were resolved on SDS-PAGE (8-15% gels) and western blotting was carried out with antibodies to p-RIP3 and p-MLKL. Total p38 levels were used as a loading control. Densitometry readings were obtained using ImageJ and are representative of the level of the protein of interest divided by the corresponding p38 levels and normalised to the vehicle control sample (where possible). Blots are representative of at least two independent repeats.

4.2.10 KB2 induces autophagy in breast cancer cells

Autophagy is a catabolic process by which cells recycle some of their contents, such as misfolded and long-lived proteins, organelles or pathogens, into reusable macromolecules. Although autophagy has a well-established role in cell survival, it is also known to function as a pro-death mechanism (PCD type II) in certain contexts (Su, Mei and Sinha, 2013; S. S. Singh *et al.*, 2017). Autophagy proceeds with the formation of a characteristic double layered membrane which encapsulates its cargo to form the autophagosome which later fuses with lysosomes to form acidic autolysosomes. Indeed, the presence of vacuoles, reminiscent of autophagic vesicles, were observed in KB2 treated MCF-7 and MDA-MB-231 cells **(figure 4.10 A)**. To confirm that KB2 induces autophagy, western blotting and immunocytochemistry (ICC) were performed with an antibody to LC3. The rationale for this is that during the formation of the autophagosome LC3 is conjugated by phosphotidylethanolamine (PE) to from LC3II, which remains bound

to the double membrane of the autophagosome. Thus, LC3II is often used as a marker of autophagy. ICC reveals a dose-dependent increase in LC3 puncta, presumed to represent LC3II aggregates conjugated to autophagosomal membranes, in both MCF-7 and MDA-MB-231 cells treated for 48 hours with KB2 **(figure 4.10 B and C)**. Similarly, western blotting revealed an increase in LC3II in MCF-7 and MDA-MB-231 cells following KB2 treatment **(figure 4.10 D)**. While these results suggested that KB2 induced autophagy in the breast cancer cells, future studies should investigate whether it is a pro-survival or pro-death mechanism.

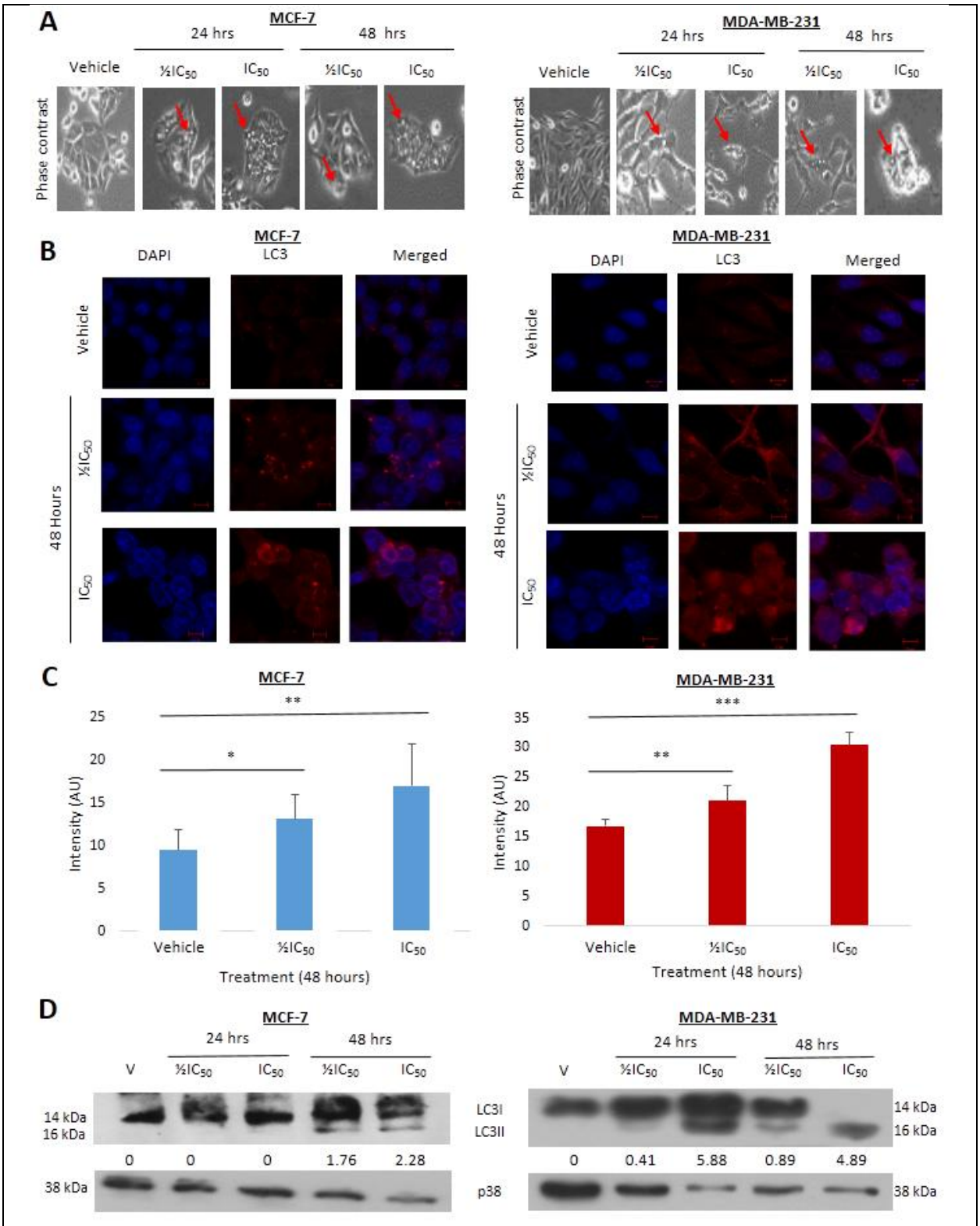

Figure 4.10: KB2 induces autophagy in breast cancer cells. (A) Phase contrast images of MCF-7 and MDA-MB-231 cells treated with either vehicle (DMSO) or KB2 for 24 and 48 hours.

Red arrows indicate the presence of vesicles reminiscent of autophagic vesicles. **(B)** Representative confocal immunofluorescence maximum intensity projection images (63x; Carl Zeiss LSM 880) of MCF-7 and MDA-MB-231 cells treated with either vehicle or KB2 at their respective ½IC_{50} and IC_{50} concentrations for 48 hours and LC3 levels detected with a fluorophore-conjugated Cy3 secondary antibody. Nuclei of cells were stained with DAPI. Scale bar is 10µm. **(C)** Quantification of confocal images shown in **(B)** for LC3. Graphs are representative of the intensity of the LC3 signal per treatment condition as mean nuclear Cy3 fluorescence across five or more independent fields of view. Error bars are representative of SD. Data were analyzed using GraphPad Prism 6.0. Significance was determined using a student *t*-test and taken as * $p \leq 0.05$, ** $p \leq 0.01$ and *** $p \leq 0.001$. **(D)** Western blot analyses of protein harvested from MCF-7 and MDA-MB-231 cells treated with either vehicle or KB2 at their respective ½IC_{50} and IC_{50} concentrations for 24 hours and 48 hours. Proteins were resolved by SDS-PAGE (8-15% gels) and western blotting was performed using antibodies to LC3 and total p38 levels were used as a loading control. Densitometry readings were obtained using ImageJ and are representative of the level of the protein of interest divided by the corresponding p38 level and normalised to vehicle control sample (where possible). Blots are representative of at least two independent repeats.

.

4.3 Discussion

Despite continuous efforts and improved methods of treatment, breast cancer remains the most common cancer and the leading cause of cancer death among women worldwide (Bray *et al.*, 2018). This is largely due to current treatments still presenting with many drawbacks. For example, common chemotherapeutics such as cisplatin, doxorubicin, trastuzumab, and tamoxifin, are associated with drug resistance and a wide range of debilitating side effects which include, but are not limited to, nausea, hair loss, fatigue, depression and cardiotoxicity (Wonders and Reigle, 2009; Astolfi *et al.*, 2013; Condorelli and Vaz-luis, 2018). In this regard, natural products have been an area of intense investigation because they are expected to be less toxic and present as a cheaper option for cancer treatments (A. K. Singh *et al.*, 2017; Banerjee *et al.*, 2018; Bonam *et al.*, 2018). Furthermore, natural products have a good track record for producing valuable medicinal drugs and are a robust source of medicinal products (Li and Vederas, 2009). This study demonstrates the anti-cancer activity of a Kraalbos extract, KB2, against the

ER+ MCF-7 and TN MDA-MB-231 breast cancer cell lines. Indeed, KB2 is shown to exert short- and long-term cytotoxicity, selectivity and anti-migratory properties in these breast cancer cells.

This is the first study to describe the anti-cancer activity of a Kraalbos extract in both ER+ and TN breast cancer cells. KB2 is an ethanolic extract derived from the leaves of the Kraalbos plant and contains, among other compounds, pinocembrin (8.4%), 7-hydroxyflavanone (3.0%), 2'4'-dihydroxychalcone (6.8%) and 2'4'-dihydroxydihydrochalcone (2.8%) **(figure 4.11)**. While the various components of KB2 were not individually tested for their anti-cancer activities it is probable that they can, at least in part, be attributed to pinocembrin and 2'4'- dihydroxychalcone. Indeed, these two compounds are thought to be responsible for the antibacterial, antimycobacterial and antifungal properties of Kraalbos (Vries *et al.*, 2005; Mativandlela *et al.*, 2009; Ticha *et al.*, 2015). Furthermore, pinocembrin has been shown to exhibit anti-cancer effects against a variety of cancers including colon cancer, prostate cancer and leukemia (Kumar *et al.*, 2007; Rasul *et al.*, 2013; Z. Chen *et al.*, 2013). To identify the most active compounds in KB2, future studies should test pinocembrin, 7-hydroxyflavanone, 2'4'-dihydroxychalcon and 2'4'-dihydroxydihydrochalcone individually and in combination for their anti-cancer properties in breast cancer cells. Furthermore, such studies should include more cell lines representative of the various breast cancer subtypes. This will be important because it could lead to the formulation of an effective anti-breast cancer drug.

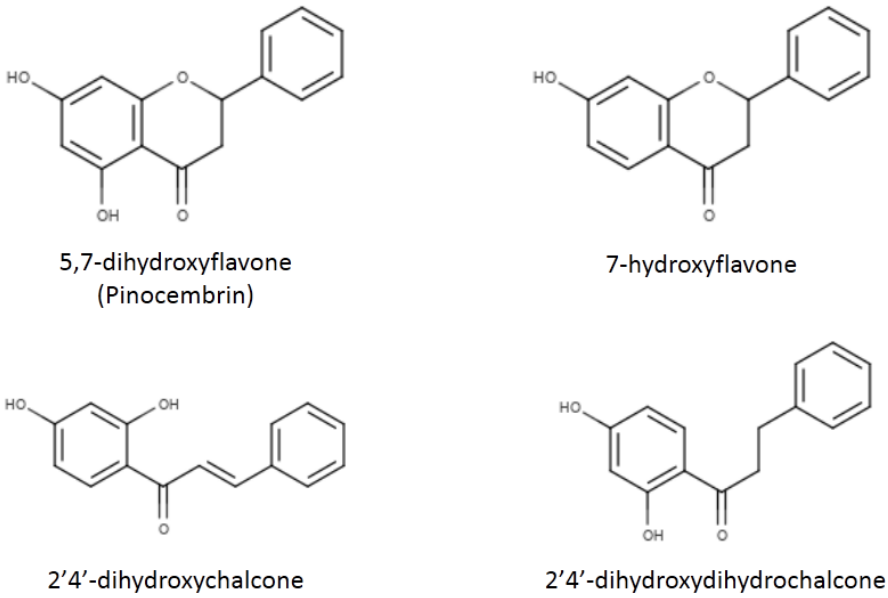

Figure 4.11: Chemical structures of compounds present in KB2

While KB2 was not convincingly selective for breast cancer cells in short-term cell viability assays, it showed promising selectivity in long-term cytotoxicity assays. Indeed, the SI values for KB2 ranged from 1.2 to 1.6 which is below the recommended SI value of 2 (Koch *et al.*, 2005). These results are however similar to results reported in the online thesis of Ng’uni (2017) for an ethanolic Kraalbos extract (prepared from leaves and shoots) in MCF-7 breast cancer cells and the KMST-6 non-malignant fibroblasts. Interestingly, while KB2 effectively inhibited the long-term survival of MCF-7 and MDA-MB-231 breast cancer cells in a clonogenic assay, it had very little effect on the survival of the MCF-12A normal breast epithelial cells. The results from the current study thus reveal that while KB2 did not demonstrate a promising SI in short-term cell viability assays, it was much more selective for the breast cancer cells in the long-term clonogenic survival assays. This suggests that KB2 may have initial side effects which fade with time as normal cells are able to recover from the effects of KB2 whilst the cancer cells are not.

The present study also showed that KB2 inhibits the migratory ability of breast cancer cells which was accompanied by an increase in the epithelial marker E-cadherin and a decrease in the mesenchymal markers B-catenin and vimentin. These results are

consistent with the results reported in the PhD thesis of Ng'uni (2017) that an ethanolic Kraalbos extract (from leaves and shoots) downregulated *CDH2,* which encodes a mesenchymal marker also known as N-cadherin, and *SNAI1*, which encodes a repressor of E-cadherin, in MCF-7 cells. This is exciting as it suggests that KB2 may be useful for treating metastatic breast cancers, for which there are limited treatment options available (Qian, Mei and Zhang, 2017). However, the present study was conducted *in vitro,* and the results should be interpreted with caution and future studies should investigate the anti-metastatic ability of KB2 *in vivo*.

This study investigated the mechanisms by which KB2 exerted its cytotoxicity in breast cancer cells. The mechanism of action is summarised in **figure 4.12**. KB2 was found to increase the production of intracellular ROS and to induce DNA damage, cell cycle arrests, apoptosis, necroptosis and autophagy in breast cancer cells. This is not surprising since one of the mechanisms by which phytochemicals kill cancer cells is by inducing an oxidative stress through the generation of ROS which leads to a decrease in anti-oxidants and apoptosis because ROS are capable of damaging DNA, RNA, protein and lipid molecules (Simon, Haj-Yehia and Levi-Schaffer, 2000; Barzilai and Yamamoto, 2004; Viswesh, Gates and Sun, 2010; Vallejo, Salazar and Grijalva, 2017; Navaneethakrishnan, Rosales and Lee, 2019). It is therefore likely that the DNA damage induced by KB2 is as a result of the increased levels of ROS. However, the possibility that compounds present in KB2 could also interact directly with DNA to cause DNA damage cannot be ruled out. This could be investigated by treating cells with KB2 in the presence of an antioxidant, such as glutathione, and investigating the levels of γH2AX in response to this treatment. If DNA damage still occurs under these conditions, then it could be concluded that KB2 may interact directly with the DNA to damage it.

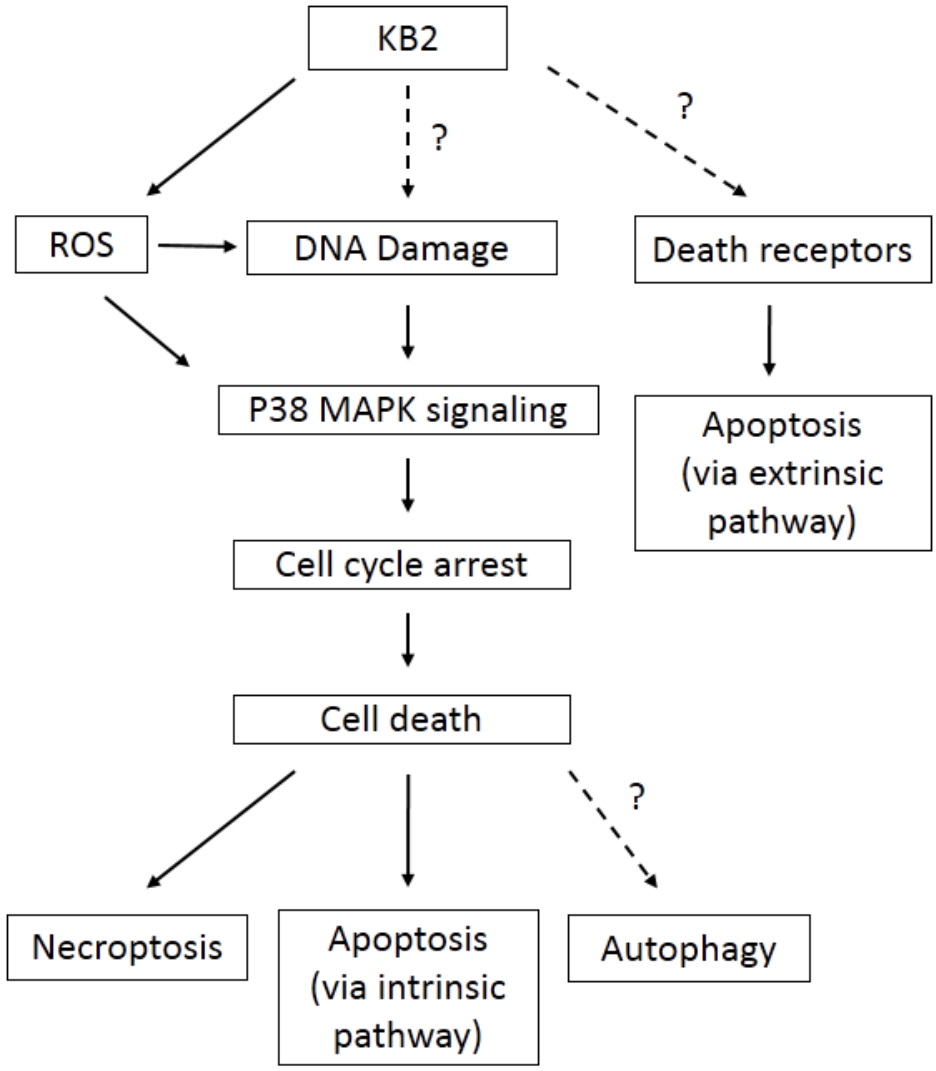

Figure 4.12: The mechanism of action of KB2 in breast cancer cells

The present study shows that KB2 treatment resulted in MCF-7 cells arresting in S phase and MDA-MB-231 cells in S and G2/M phases and this was accompanied by an increase in the potent cyclin dependent kinase (CDK) inhibitor, p21 (also known as p21 (WAF1/Cip1)) and a decrease in cyclin A and cyclin B1 levels. In addition, KB2 increased p53 levels in MCF-7 cells but not in MDA-MB-231 cells which is not surprising because MDA-MB-231 cells express high levels of a mutant p53 (Gartel, Feliciano and Tyner, 2003). Interestingly, KB2 still activated its downstream target p21 in MDA-MB-231 cells suggesting a p53 independent activation. These results are consistent with another study which demonstrated that in response to a variety of stimuli including DNA damage, p21

is induced by p53 dependent and p53 independent mechanisms and that it binds to and inhibits the activity of cyclin-CDK2, -CDK1, and -CDK4/6 complexes to promote cell cycle arrest and cell death (Russo *et al.*, 1995). Indeed, many natural products mediate their cytotoxicity through a p53 dependent or independent activation of p21. For example, the natural product CKBM, which consists of extracts derived from a variety of sources including soybean, ginseng and baker's yeast, mediates cell cycle arrests and apoptosis in gastric cancer cells in a p53 and p21 dependant manner (Luk et al., 2005). Similarly, an extract derived from *Vernonia amygdalina*, commonly known as bitter leaf, was shown to mediate its cytotoxicity in a p21 dependant manner in MCF-7 and MDA-MB-231 breast cancer cells(Choene and Motadi, 2016). Furthermore, LNCaP prostate cancer cells treated with pinocembrin arrested in S and G2/M (Z. Chen *et al.*, 2013). This suggests that pinocembrin may be responsible for the S and G2/M cell cycle arrests observed for KB2 in MDA-MB-231 breast cancer cells.

This study found that KB2 induces cell death firstly through the intrinsic apoptotic pathway followed by activation of the extrinsic apoptotic pathway in MCF-7 and MDA-MB-231 breast cancer cells. These results suggest that KB2 will have advantages over other breast cancer therapies because many cancer cells are capable of overriding the intrinsic pathway (Rebucci and Michiels, 2013). Ng'uni (2017) also reported that treatment of MCF-7 cells with an ethanolic Kraalbos extract (from leaves and shoots) led to the upregulation of caspases 2, 7 and 9 but whether this extract also activated the extrinsic apoptotic pathway was not explored. Furthermore, pinocembrin was reported to induce intrinsic and extrinsic apoptosis in HL-60 leukaemia cells, intrinsic apoptosis in HCT116 colon cancer cells and PARP cleavage in LNCaP prostate cancer cells but whether this occurred downstream of the intrinsic or extrinsic apoptotic pathway was not shown (Hsu, Yu and Yen, 2010; Kumar *et al.*, 2007; Chen *et al.*, 2013). It is important to note that cancer cells initially respond to apoptosis inducing anti-cancer drugs, but frequently they eventually develop drug resistance (Ricci and Zong, 2006; Fernald and Kurokawa, 2014; Pistritto *et al.*, 2016). The results from this study that show that KB2 also induced necroptosis in breast cancer cells is therefore important because cancer cells are less likely to develop resistance to a drug which induces multiple modes of cell death. For

example, the second mitochondrial-derived activator of caspases (SMAC) mimetic compound birinapant was found to induce both apoptosis and necroptosis in patient derived acute lymphoblastic leukaemia (ALL) cells and blocking only one PCD pathway was not sufficient to confer resistance upon these cells (Aguadé-gorgorió and Bornhauser, 2016; Mccomb *et al.*, 2016). As KB2 induces intrinsic and extrinsic apoptosis and necroptosis it could be attractive as a potential anti-cancer drug.

Autophagy has classically been considered a pro-survival mechanism and has been associated with tumour drug resistance but it is also known to play a role in cell death (Su, Mei and Sinha, 2013; S. S. Singh *et al.*, 2017). This study demonstrated that KB2 induces autophagy in breast cancer cells but did not investigate wheather it was a pro-death or pro-survival mechanism. This should be followed-up in future experiments because if the KB2 induced autophagy as a cell death mechanism then KB2 can activate three different programmed cell death pathways which provides additional credibility for its potential as an anti-breast cancer treatment. On the other hand, if the KB2 induced autophagy is found to be a cell survival mechanism then KB2 may need be administered in combination with an autophagy inhibitor. To determine whether KB2 induced autophagy is a pro-death or pro-survival mechanism would involve treating breast cancer cells with KB2 in the presence of an autophagy inhibitor, such as bafilomycin A1 or wortmannin, followed by cell viability assays. Under these conditions, an increase in cell viability would indicate that autophagy plays a pro-death role and a decrease in cell viability would indicate that autophagy plays a pro-survival role.

Chapter 5: Conclusion

Despite intense research efforts, breast cancer remains one of the leading causes of cancer deaths worldwide. Several factors related to the cancer itself as well as societal issues present challenges to the effective treatment of this cancer. Natural products have proven to be a robust source of novel anti-cancer drugs which are safe, effective and cheap. These have often been derived from plant sources, especially those used as food or medicine. Thus, this study investigated the anti-cancer effects of extracts derived from three varieties of African millets as well as from the indigenous Kraalbos plant, *Galenia africana*, against the MCF-7 oestrogen receptor positive (ER+) and the MDA-MB-231 triple negative (TN) breast cancer cell lines.

The millet extracts tested were derived from *Sorghum bicolor* (Enforcer), *Pennisetum glaucum* (Babala) and *Eragrostis tef* (Tef) using both a reflux-based extraction and a cold extraction procedure. MTT assays reveal that the millet extracts derived from the reflux-based extraction show no short-term cytotoxicity against both breast cancer cell lines. Extracts derived from the cold extraction were subjected to HPTLC fractionation and only the methanol fractions of the Babala and Enforcer millets exhibited short-term cytotoxic activity against both the ER+ MCF-7 and TN MDA-MB-231 breast cancer cell lines. These fractions exhibit cytotoxicity at relatively low concentrations, suggesting the presence of compounds with potent anti-cancer properties. The fractions should be further investigated using analytical techniques such as HPLC, NMR and LC-MS to determine its active compounds. These pure compounds should then be tested alone and in combination with each other to determine their anti-breast cancer activity. A mechanism of action, showing the pathways activated and modes of cell death induced, should then be elucidated for the compounds which display the most potent activity.

This study investigated five Kraalbos extracts (KB1, KB2, KB3, KB4 and KB5) for their short-term cytotoxicity against the ER+ MCF-7 and TN MDA-MB-231 breast cancer cell lines and found KB2 to exhibit the highest cytotoxicity. Clonogenic assays revealed that KB2 also displayed long-term cytotoxicity against breast cancer cells. Importantly, KB2

showed specificity towards breast cancer cells in long-term cytotoxicity assays. Scratch motility assays and western blotting with antibodies to the EMT markers β-catenin, vimentin and E-cadherin revealed that KB2 inhibited the migratory ability of breast cancer cells. These findings are promising as they suggest that KB2 may be used to treat drug resistant and metastatic cancers. Furthermore, this study shows that the mechanism(s) underpinning the anti-cancer activity of KB2 involves the production of ROS, the induction of double strand DNA breaks, cell cycle arrests and programmed cell death apoptosis (intrinsic and extrinsic) and necroptosis pathways. KB2 shares similarities with pinocembrin in its ability to induce S and G2/M phase arrests and apoptosis in certain cancers (Kumar *et al.*, 2007; Rasul *et al.*, 2013; Z. Chen *et al.*, 2013). As pinocembrin is a constituent of KB2 it is probable that its activity may, at least in part, be attributed to pinocembrin and future studies should investigate this further. The induction of apoptosis and necroptosis is promising as the induction of multiple modes of cell death would make it difficult for cancers to develop resistance to KB2. KB2 was also found to induce autophagy in breast cancer cells, however it was not determined whether autophagy acts as a pro-death mechanism in this context and future studies should investigate this. Furthermore, future studies should use animal models to investigate the anti-cancer activity of KB2 *in vivo* as well as its acute and sub-acute toxicity.

Taken together, this study demonstrates that extracts derived from millets and Kraalbos show anti-cancer activity against the ER+ MCF-7 and TN MDA-MB-231 breast cancer cells. Although the millet extracts show promise, they require further investigation. KB2, however, exhibits many properties which would make it a good anti-cancer drug and is worth progressing to pre-clinical studies.

References

Aguadé-gorgorió, J. and Bornhauser, B. C. (2016) 'Activation of necroptosis to overcome drug resistance in leukemia', *Receptors & Clinical Investigation*, pp. 1–7. doi: 10.14800/rci.1440.

Aiyengar, T. M., Chiranjeevi, P. and Rani, H. S. (2017) 'Role of Endothelial Nitric Oxide Synthase in Breast Cancer', in *Nitric Oxide Synthase - Simple Enzyme-Complex Roles year*, pp. 179–196.

Alberts, D. S. *et al.* (1980) 'In-vitro clonogenic assay for predicting response of ovarian cancer to chemotherapy', *The Lancet*. Elsevier, 316(8190), pp. 340–342.

Ali, S. and Coombes, R. C. (2002) 'Endocrine-responsive breast cancer and strategies for combating resistance', *Nature Reviews Cancer*, 2(February), pp. 101–112. doi: 10.1038/nrc721.

Aliwaini, S. *et al.* (2013) 'A novel binuclear palladacycle complex inhibits melanoma growth in vitro and in vivo through apoptosis and autophagy', *Biochemical Pharmacology*, 86(12), pp. 1650–1663. doi: 10.1016/j.bcp.2013.09.020.

Aliwaini, S. *et al.* (2015) 'The palladacycle, AJ-5, exhibits anti-tumour and anti-cancer stem cell activity in breast cancer cells', *Cancer Letters*. Elsevier Ireland Ltd, 357(1), pp. 206–218. doi: 10.1016/j.canlet.2014.11.027.

Amadou, I., Gounga, M. E. and Le, G. (2013) 'Millets : Nutritional composition , some health benefits and processing - A Review', *Emirites Journal of Food and Agriculture*, 25(7), pp. 501–508. doi: 10.9755/ejfa.v25i7.12045.

Anderson, K. N., Schwab, R. B. and Martinez, M. E. (2014) 'Reproductive risk factors and breast cancer subtypes : a review of the literature', *Breast Cancer Research and*

Treatment, pp. 1–10. doi: 10.1007/s10549-014-2852-7.

Astolfi, L. *et al.* (2013) 'Correlation of adverse effects of cisplatin administration in patients affected by solid tumours : A retrospective evaluation', *Oncology Reports*, 3, pp. 1285–1292. doi: 10.3892/or.2013.2279.

Aziz, M., Jacob, A. and Wang, P. (2014) 'Revisiting caspases in sepsis Revisiting caspases in sepsis'. Nature Publishing Group, 5(11), pp. e1526-12. doi: 10.1038/cddis.2014.488.

Bailly, C. (2009) 'Ready for a comeback of natural products in oncology', *Biochemical Pharmacology*, 77, pp. 1447–1457. doi: 10.1016/j.bcp.2008.12.013.

Balmana, J., Diez, O. and Castiglione, M. (2009) 'BRCA in breast cancer : ESMO Clinical Recommendations', *Annals of Oncology*, 20(Supplement 4), pp. 19–20. doi: 10.1093/annonc/mdp116.

Banerjee, J. *et al.* (2018) 'Editorial Biological Efficacy of Medicinal Plant Extracts in Preventing Oxidative Damage', *Oxidative Medicine and Cellular Longevity*, pp. 1–3.

Barzilai, A. and Yamamoto, K. (2004) 'DNA damage responses to oxidative stress', *DNA Repair*, 3, pp. 1109–1115. doi: 10.1016/j.dnarep.2004.03.002.

De Beer, J. J. J. and Van Wyk, B. (2011) 'An ethnobotanical survey of the Agter – Hantam , Northern Cape Province , South Africa', *South African Journal of Botany*. Elsevier B.V., 77(3), pp. 741–754. doi: 10.1016/j.sajb.2011.03.013.

Berghe, T. Vanden *et al.* (2014) 'Regulated necrosis: The expanding network of non-apoptotic cell death pathways', *Nature Reviews Molecular Cell Biology*. Nature Publishing Group, 15(2), pp. 135–147. doi: 10.1038/nrm3737.

Bettaieb, A. *et al.* (2017) 'Precision medicine in breast cancer : reality or utopia ?', *Journal of Translational Medicine*. BioMed Central, pp. 1–13. doi: 10.1186/s12967-017-1239-z.

Bleloch, J. (2019) *Identifying novel drugs for the treatment of rhabdomyosarcoma*.

Bonam, S. R. *et al.* (2018) 'What has come out from phytomedicines and herbal edibles for the treatment of cancer?', *ChemMedChem*, 13(18), pp. 1854–1872. doi: 10.1002/cmdc.201800343.

Bray, F. *et al.* (2018) 'Global Cancer Statistics 2018 : GLOBOCAN Estimates of Incidence and Mortality Worldwide for 36 Cancers in 185 Countries', *A Cancer Journal for Clinicians*, 68, pp. 394–424. doi: 10.3322/caac.21492.

Chan, J. J., Tan, T. J. Y. and Dent, R. A. (2019) 'Novel therapeutic avenues in triple-negative breast cancer : PI3K / AKT inhibition , androgen receptor blockade , and beyond', *Therapeutic Advances in Medical Oncology*, 11, pp. 1–11. doi: 10.1177/https.

Chandrasekara, A. and Shahidi, F. (2011a) 'Antiproliferative potential and DNA scission inhibitory activity of phenolics from whole millet grains', *Journal of Functional Foods*. Elsevier Ltd, 3(3), pp. 159–170. doi: 10.1016/j.jff.2011.03.008.

Chandrasekara, A. and Shahidi, F. (2011b) 'Bioactivities and Antiradical Properties of Millet Grains and Hulls', *Journal of Agricultural and Food Chemistry*, 59(17), pp. 9563–9571. doi: 10.1021/jf201849d.

Charlton, P. and Spicer, J. (2015) 'Targeted therapy in cancer', *Medicine*. Elsevier Ltd, 44(1), pp. 34–38. doi: 10.1016/j.mpmed.2015.10.012.

Chen, X. *et al.* (2013) 'Translocation of mixed lineage kinase domain-like protein to plasma membrane leads to necrotic cell death', *Nature Publishing Group*. Nature Publishing Group, 24, pp. 105–121. doi: 10.1038/cr.2013.171.

Chen, Z. *et al.* (2013) 'Antiproliferative and apoptotic efffects of pinocembrin in human prostate cancer cells', *Bangladesh Journal of Pharmacology*, 8(3), pp. 255–262. doi: 10.3329/bjp.v8i3.14795.

Chethan, S. and Malleshi, N. G. (2007) 'Finger millet polyphenols: Optimization of extraction and the effect of pH on their stability', *Food Chemistry*, 105(2), pp. 862–870.

doi: 10.1016/j.foodchem.2007.02.012.

Choene, M. and Motadi, L. (2016) ‘Validation of the Antiproliferative Effects of Euphorbia tirucalli Extracts in Breast Cancer Cell Lines’, *Molecular Biology*, 50(1), pp. 98–110. doi: 10.1134/S0026893316010040.

Coimbra, M. *et al.* (2011) ‘Improving solubility and chemical stability of natural compounds for medicinal use by incorporation into liposomes’, *International Journal of Pharmaceutics*. Elsevier B.V., 416(2), pp. 433–442. doi: 10.1016/j.ijpharm.2011.01.056.

Condorelli, R. and Vaz-luis, I. (2018) ‘Managing side effects in adjuvant endocrine therapy for breast cancer’, *Expert Review of Anticancer Therapy*. Taylor & Francis, pp. 1–12. doi: 10.1080/14737140.2018.1520096.

Corcelle, E. A., Puustinen, P. and Jäättelä, M. (2009) ‘Apoptosis and autophagy: Targeting autophagy signalling in cancer cells -’trick or treats’?’, *FEBS Journal*, 2009, pp. 6084–6096. doi: 10.1111/j.1742-4658.2009.07332.x.

Crown, J., O’Leary, Mi. and Ooi, W. (2004) ‘Docetaxel and Paclitaxel in the Treatment of Breast Cancer : A Review of Clinical Experience’, *The Oncologist*, 9(suppl 2), pp. 24–32.

Cuevas, C. and Francesch, A. (2009) ‘Development of Yondelis (trabectedin , ET-743). A semisynthetic process solves the supply problem’, *Natural Product Reports*, 26, pp. 322–337. doi: 10.1039/b808331m.

Dent, R. *et al.* (2007) ‘Triple-Negative Breast Cancer : Clinical Features and Patterns of Recurrence’, 13(15), pp. 4429–4435. doi: 10.1158/1078-0432.CCR-06-3045.

Dikic, I. and Elazar, Z. (2018) ‘Mechanism and medical implications of mammalian autophagy’, *Nature Reviews Molecular Cell Biology*. Springer US, 19(6), pp. 349–364. doi: 10.1038/s41580-018-0003-4.

Dongre, A. and Weinberg, R. A. (2019) ‘New insights into the mechanisms of epithelial–mesenchymal transition and implications for cancer’, *Nature Reviews Molecular Cell*

Biology. Springer US, 20(2), pp. 69–84. doi: 10.1038/s41580-018-0080-4.

Driessche, J. J. van den, Plat, J. and Mensink, R. P. (2018) 'Function E ff ects of superfoods on risk factors of metabolic syndrome : a systematic review of human', *Food and Function*. Royal Society of Chemistry, 9, pp. 1944–1966. doi: 10.1039/c7fo01792h.

Du, K. *et al.* (2015) 'HPLC-Based Activity Profiling for hERG Channel Inhibitors in the South African Medicinal Plant Galenia africana', *Planta Medica*, 81, pp. 1154–1162.

Dykes, L. and Rooney, L. W. (2007) 'Phenolic compounds in cereal grains and their health benefits', *Cereal Foods World*, 52, pp. 105–111.

Elbagory, A. M. *et al.* (2017) 'Inhibition of Bacteria Associated with Wound Infection by Biocompatible Green Synthesized Gold Nanoparticles from South African Plant Extracts'. doi: 10.3390/nano7120417.

Elmore, S. (2007) 'Apoptosis: A Review of Programmed Cell Death', *Toxicologic Pathology*, 35(4), pp. 495–516.

Ernest, N. J., Habela, C. W. and Sontheimer, H. (2009) 'Cytoplasmic condensation is both necessary and sufficient to induce apoptotic cell death', *Journal of Cell Science*, 121(Pt 3), pp. 290–297. doi: 10.1242/jcs.017343.Cytoplasmic.

Feng, Y. *et al.* (2018) 'Breast cancer development and progression : Risk factors , cancer stem cells , signaling pathways , genomics , and molecular pathogenesis', *Genes & Diseases*. Elsevier Ltd, 5(2), pp. 77–106. doi: 10.1016/j.gendis.2018.05.001.

Ferlay, J. *et al.* (2015) 'Cancer incidence and mortality worldwide : Sources , methods and major patterns in GLOBOCAN 2012', *International journal of cancer*, 386(5), pp. E359–E386. doi: 10.1002/ijc.29210.

Fernald, K. and Kurokawa, M. (2014) 'Evading apoptosis in cancer', *Trends in Cell Biology*, 23(12), pp. 620–633. doi: 10.1016/j.tcb.2013.07.006.Evading.

Fielding, B. C. *et al.* (2015) 'Testing of Eight Medicinal Plant Extracts in Combination

with Kresoxim-Methyl for Integrated Control of Botrytis cinerea in Apples', *Agriculture*, 5, pp. 400–411. doi: 10.3390/agriculture5030400.

Fotakis, G. and Timbrell, J. A. (2006) 'In vitro cytotoxicity assays: Comparison of LDH, neutral red, MTT and protein assay in hepatoma cell lines following exposure to cadmium chloride', *Toxicology Letters*, 160(2), pp. 171–177. doi: 10.1016/j.toxlet.2005.07.001.

Fulda, S. (2018) 'Repurposing anticancer drugs for targeting necroptosis', *Cell Cycle*. Taylor & Francis, 17(7), pp. 829–832. doi: 10.1080/15384101.2018.1442626.

Galluzzi, L. *et al.* (2007) 'Cell death modalities : classification and pathophysiological implications', *Cell Death and Differentiation*, 14, pp. 1237–1243. doi: 10.1038/sj.cdd.4402148.

Gartel, A. L., Feliciano, C. and Tyner, A. L. (2003) 'A new method for determining the status of p53 in tumor cell lines of different origin', *Oncol Res*, 13(6–10), pp. 405–408. doi: 10.3727/096504003108748429.

Gebremariam, M. M., Zarnkow, M. and Becker, T. (2014) 'Teff (Eragrostis tef) as a raw material for malting , brewing and manufacturing of gluten-free foods and beverages : a review', *Journal of Food Science and Technology*, 51(11), pp. 2881–2895. doi: 10.1007/s13197-012-0745-5.

Giglia-mari, G., Zotter, A. and Vermeulen, W. (2011) 'DNA Damage Response', *Cold Spring Harbour Perspectives in Biology*, 3, pp. 1–19.

Goerch, M. C. da S. *et al.* (2019) 'Nutritional composition of Eragrostis teff and its association with the observed antimutagenic effects', *RSC Advances*, 9, pp. 3764–3776. doi: 10.1039/c8ra09733j.

Grimmer, H. R., Parbhoo, V. and Mcgrath, R. M. (1992) 'Antimutagenici ty of Polyphenol-rich Fractions from Sorghum bicolor Grain', *Journal of The Science of Food and Agriculture*, 59, pp. 251–256.

Guzman, C. *et al.* (2014) 'ColonyArea : An ImageJ Plugin to Automatically Quantify Colony Formation in Clonogenic Assays', 9(3), pp. 14–17. doi: 10.1371/journal.pone.0092444.

Hanahan, D. and Weinberg, R. A. (2011) 'Review Hallmarks of Cancer : The Next Generation', *Cell*. Elsevier Inc., 144(5), pp. 646–674. doi: 10.1016/j.cell.2011.02.013.

Hansen, M. and Rubinsztein, D. C. (2018) 'Autophagy as a promoter of longevity : insights from model organisms', *Nature Reviews Molecular Cell Biology*. Springer US, 19(9), pp. 579–593. doi: 10.1038/s41580-018-0033-y.

He, S., Huang, S. and Shen, Z. (2016) 'Biomarkers for the detection of necroptosis', *Cellular and Molecular Life Sciences*. Springer International Publishing, 73(11), pp. 2177–2181. doi: 10.1007/s00018-016-2192-3.

He, Y. *et al.* (2016) 'The changing 50 % inhibitory concentration (IC 50) of cisplatin : a pilot study on the artifacts of the MTT assay and the precise measurement of density-dependent chemoresistance in ovarian cancer', *Oncotarget*, 7(43), pp. 70803–70821.

Heckmann, B. L., Tummers, B. and Green, D. R. (2019) 'Crashing the computer : apoptosis vs necroptosis in neuroinflammation', *Cell Death & Differentiation*, 26, pp. 41–52. doi: 10.1038/s41418-018-0195-3.

Hsu, C.-L., Yu, Y.-S. and Yen, G.-C. (2010) 'Anticancer Effects of Alpinia pricei Hayata Roots', *Journal of Agricultural and Food Chemistry*, 58, pp. 2201–2208. doi: 10.1021/jf9038056.

Ibidapo, O. *et al.* (2019) 'Bioactive components of malted millet (Pennisetum glaucum), Soy Residue " okara " and wheat flour and their antioxidant properties', *International Journal of Food Properties*. Taylor & Francis, 22(1), pp. 1886–1898. doi: 10.1080/10942912.2019.1689998.

Jekimovs, C. *et al.* (2014) 'Chemotherapeutic compounds targeting the DNA double-strand break repair pathways : the good , the bad , and the promising', *Frontiers in Oncology*, 4(April), pp. 1–18. doi: 10.3389/fonc.2014.00086.

Jemal, A., Bray, F. and Ferlay, J. (2011) ‘Global Cancer Statistics’, 61(2), pp. 69–90. doi: 10.3322/caac.20107.Available.

Johnson, D. G. and Walker, C. L. (1999) ‘Cyclins and Cell Cycle Checkpoints’, *Annual Review of Pharmacology and Toxicology*, 39, pp. 295–312.

de Jong, M. M. *et al.* (2002) ‘Genes other than BRCA1 and BRCA2 involved in breast cancer susceptibility’, *Journal of Medical Genetics*, 39, pp. 225–242.

Klionsky, D. J., Eskelinen, E. and Deretic, V. (2014) ‘Autophagosomes, phagosomes, autolysosomes, phagolysosomes, autophagolysosomes…Wait , I ’ m confused’, *Autophagy*, 10(April), pp. 549–551.

Koch, A. *et al.* (2005) ‘Evaluation of plants used for antimalarial treatment by the Maasai of Kenya’, *Journal of Ethnopharmacology*, 101, pp. 95–99. doi: 10.1016/j.jep.2005.03.011.

Kumar, A. (2016) ‘Vincristine and vinblastine: a review’, *International Journal of Medicine and Pharmaceutical Science*, 6(1), pp. 23–30.

Kumar, M. A. S. *et al.* (2007) ‘Pinocembrin Triggers Bax-Dependent Mitochondrial Apoptosis in Colon Cancer Cells’, *Molecular Carcinogenesis*, 46(3), pp. 231–241. doi: 10.1002/mc.

Lakin, N. D. and Jackson, S. P. (1999) ‘Regulation of p53 in response to DNA damage’, *Oncogene*, 18, pp. 7644–7655.

Li, J. W. and Vederas, J. C. (2009) ‘Drug Discovery and Natural Products : End of an Era or an Endless Frontier ?’, *Science*, 325(5937), pp. 161–166.

Li, Z. and Sheng, M. (2012) ‘Caspases in synaptic plasticity’, *Molecular Brain*. BioMed Central Ltd, 5(1). doi: 10.1186/1756-6606-5-15.

Liu, D. *et al.* (2011) ‘Inhibition of autophagy by 3-MA potentiates cisplatin-induced apoptosis in esophageal squamous cell carcinoma cells’, *Medical Oncology*, 28(1), pp.

105–111. doi: 10.1007/s12032-009-9397-3.

Lord, C. J. and Ashworth, A. (2012) ‘The DNA damage response and cancer therapy’, *Nature*, 481, pp. 287–294. doi: 10.1038/nature10760.

Majeed, W. *et al.* (2014) ‘Breast Cancer : Major Risk Factors and Recent Developments in Treatment’, *Asian Pacific Journal of Cancer Prevention*, 15, pp. 3353–3358.

Mathanghi, S. K. (2012) ‘Nutraceutical properties of Great Millet - Sorghum vulgare’, *International Journal of Food, Agriculture and Veterinary Sciences*, 2(2), pp. 40–45.

Mathiassen, S. G., Zio, D. De and Cecconi, F. (2017) ‘Autophagy and the Cell Cycle : A Complex Landscape’, *Frontiers in Oncology*, 7(51). doi: 10.3389/fonc.2017.00051.

Mativandlela, S. P. N. *et al.* (2008) ‘Activity against Mycobacterium smegmatis and M. tuberculosis by Extract of South African Medicinal Plants’, *Phytotherapy Research*, 22, pp. 841–845. doi: 10.1002/ptr.2378.

Mativandlela, S. P. N. *et al.* (2009) ‘Antimycobacterial Flavonoids from the Leaf Extract of Galenia africana’, *Journal of Natural Products*, 72, pp. 2169–2171.

Mccomb, S. *et al.* (2016) ‘Activation of concurrent apoptosis and necroptosis by SMAC mimetics for the treatment of refractory and relapsed ALL’, *Science Translational Medicine*, 8(339).

Mishra, B. K. and Parikh, P. M. (2006) ‘Targeted Therapy in Oncology’, *Medical Journal Armed Forces India*. Director General, Armed Forces Medical Services, 62(2), pp. 169–173. doi: 10.1016/S0377-1237(06)80063-8.

Moraiscardoso, L. De *et al.* (2017) ‘Sorghum (sorghum bicolor l .): Nutrients , Bioactive Compounds , and Potential Impact on Human Health’, *Critical Reviews in Food Science and Nutrition*, 57(2), pp. 372–390. doi: 10.1080/10408398.2014.887057.

Mukherjee, S. (2010) *The emperor of all maladies: a biography of cancer*. Simon and Schuster.

Nambiar, V. S. *et al.* (2011) 'Potential Functional Implications of Pearl millet (Pennisetum glaucum) in Health and Disease', *Journal of Applied Pharmaceutical Science*, 01(10), pp. 62–67.

Nambiar, V. S. *et al.* (2012) 'Flavonoids and phenolic acids from pearl millet (Pennisetum glaucum) based foods and their functional implications', *Functional Foods in Health and Disease*, 2(7), pp. 251–264.

Nani, A. *et al.* (2015) 'Effects of polyphenols and lipids from Pennisetum glaucum grains on T-cell activation : modulation of Ca 2 + and ERK1 / ERK2 signaling', *BMC Complementary and Alternative Medicine*. BMC Complementary and Alternative Medicine, 15(426), pp. 1–11. doi: 10.1186/s12906-015-0946-3.

Navaneethakrishnan, S., Rosales, J. L. and Lee, K. (2019) 'Review Article ROS-Mediated Cancer Cell Killing through Dietary Phytochemicals', *Oxidative Medicine and Cellular Longevity*.

Ng'uni, T. L. (2017) *Medicinal uses of Galenia africana: A study of the antimicrobial, antifungal and anticancer properties*. University of the Western Cape.

Ng'uni, T. L., Klaasen, J. A. and Fielding, B. C. (2018) 'Acute toxicity studies of the South African medicinal plant Galenia africana', *Toxicology Reports*. Elsevier, 5(August), pp. 813–818. doi: 10.1016/j.toxrep.2018.08.008.

Osborne, C. K. *et al.* (1980) 'The Value of Estrogen and Progesterone Receptors in the Treatment of Breast Cancer', *Cancer*, December S, pp. 2884–2888.

Ouyang, L. *et al.* (2012) 'Programmed cell death pathways in cancer : a review of apoptosis , autophagy and programmed necrosis', *Cell Proliferation*, (15), pp. 487–498. doi: 10.1111/j.1365-2184.2012.00845.x.

Parkin, D. M. *et al.* (2014) 'Cancer in Africa 2012', *American Association of Cancer Research*, pp. 953–967. doi: 10.1158/1055-9965.EPI-14-0281.

Paterson, I. and Anderson, E. A. (2005) 'The renaissance of natural products as drug

candidates', *Science*, 310(5747), pp. 451–454.

Pistritto, G. *et al.* (2016) 'Apoptosis as anticancer mechanism : function and dysfunction of its modulators and targeted therapeutic strategies', *Aging*, 8(4), pp. 603–619.

Pool, E. J., Klaasen, J. and Shoko, Y. P. (2009a) 'The environmental toxicity of Dicerothamnus rhinocerotis and Galenia africana', *African Journal of Biotechnology*, 8(18), pp. 4465–4468.

Pool, E. J., Klaasen, J. and Shoko, Y. P. (2009b) 'The immunotoxicity of Dicerothamnus rhinocerotis and Galenia africana', *African Journal of Biotechnology*, 8(16), pp. 3846–3850.

Pradeep, P. M. and Sreerama, Y. N. (2015) 'Impact of processing on the phenolic profiles of small millets: Evaluation of their antioxidant and enzyme inhibitory properties associated with hyperglycemia', *Food Chemistry*, 169(February), pp. 455–463. doi: 10.1016/j.foodchem.2014.08.010.

Qian, C. N., Mei, Y. and Zhang, J. (2017) 'Cancer metastasis : issues and challenges', *Chinese Journal of Cancer*. BioMed Central, 36(38), pp. 36–39. doi: 10.1186/s40880-017-0206-7.

Raingeaud, J. *et al.* (1995) 'Pro-inflammatory cytokines and environmental stress cause p38 mitogen-activated protein kinase activation by dual phosphorylation on tyrosine and threonine', *Journal of Biological Chemistry*. ASBMB, 270(13), pp. 7420–7426.

Ramadoss, D. P. and Sivalingam, N. (2019) 'Vanillin extracted from Proso and Barnyard millets induce apoptotic cell death in HT-29 human colon cancer cell line', *Nutrition and Cancer*. Taylor & Francis, pp. 1–16. doi: 10.1080/01635581.2019.1672763.

Rao, B. R., Nagasampige, M. H. and Ravikiran, M. (2011) 'Evaluation of nutraceutical properties of selected small millets', *Journal of Pharmacy and Bioallied Sciences*, 3(2), pp. 277–280. doi: 10.4103/0975-7406.80775.

Rao, S. *et al.* (2018) 'Chemopreventive Potential of Cereal Polyphenols', *Nutrition and*

Cancer. Taylor & Francis, 70(6), pp. 913–927. doi: 10.1080/01635581.2018.1491609.

Rasul, A. *et al.* (2013) 'Pinocembrin : A Novel Natural Compound with Versatile Pharmacological and Biological Activities', *BioMed Research International*, 2013.

Rebucci, M. and Michiels, C. (2013) 'Molecular aspects of cancer cell resistance to chemotherapy', *Biochemical Pharmacology*. Elsevier Inc., 85(9), pp. 1219–1226. doi: 10.1016/j.bcp.2013.02.017.

Reyes-aldasoro, C. C. (2017) 'The proportion of cancer-related entries in PubMed has increased considerably ; is cancer truly " The Emperor of All Maladies "?', *PLoS ONE*, 12(3), pp. 1–15. doi: 10.1371/journal.pone.0173671.

Ricci, M. S. and Zong, W.-X. (2006) 'Chemotherapeutic Approaches for Targeting Cell Death Pathways', *Oncologist*, 11(4), pp. 342–357. doi: 10.1634/theoncologist.11-4-342.Chemotherapeutic.

Rishton, G. M. (2008) 'Natural Products as a Robust Source of New Drugs and Drug Leads: Past Successes and Present Day Issues', *American Journal of Cardiology*, 101(10 SUPPL.). doi: 10.1016/j.amjcard.2008.02.007.

Russo, T. *et al.* (1995) 'A p53-independent Pathway for Activation of WAF1 / CIP1 Expression Following Oxidative Stress', *The Journal of Biological Chemistry*, 270(49), pp. 29386–29391.

Saloustros, E., Mavroudis, D. and Georgoulias, V. (2008) 'Paclitaxel and docetaxel in the treatment of breast cancer', *Expert Opinion on Pharmacotherapy*, 9(15), pp. 1–14. doi: 10.1517/14656566.9.15.2603.

Satheesh, N. and Fanta, S. W. (2018) 'Review on structural , nutritional and anti-nutritional composition of Teff (Eragrostis tef) in comparison with Quinoa (Chenopodium quinoa Willd.)', *Cogent Food & Agriculture*. Cogent, 4(1), pp. 1–27. doi: 10.1080/23311932.2018.1546942.

Shaltiel, I. A. *et al.* (2015) 'The same , only different – DNA damage checkpoints and

their reversal throughout the cell cycle', *Journal of Cell Science*, 2, pp. 607–620. doi: 10.1242/jcs.163766.

Shan, S. *et al.* (2014) 'A novel protein extracted from foxtail millet bran displays anti-carcinogenic effects in human colon cancer cells', *Toxicology Letters*. Elsevier Ireland Ltd, 227(2), pp. 129–138. doi: 10.1016/j.toxlet.2014.03.008.

Shay, J. *et al.* (2015) 'Molecular Mechanisms and Therapeutic Effects of (−) - Epicatechin and Other Polyphenols in Cancer , Inflammation , Diabetes , and Neurodegeneration', *Oxidative Medicine and Cellular Longevity*, 2015.

Shoko, Y. P. (2010) *The screening of phyto-pesticides for potential adverse effects on human health Background to Intellectual Property*.

Simon, H.-U., Haj-Yehia, A. and Levi-Schaffer, F. (2000) 'Role of reactive oxygen species (ROS) in apoptosis induction', *Apoptosis*, 5(5), pp. 415–418.

Singh, A. K. *et al.* (2017) 'Emerging importance of dietary phytochemicals in fight against cancer : Role in targeting cancer stem cells', *Critical Reviews in Food Science and Nutrition*. Taylor & Francis, 57(16), pp. 3449–3463. doi: 10.1080/10408398.2015.1129310.

Singh, E. and Sarita (2016) 'Potential of Millets : Nutrients Composition and Health Benefits', *Journal of Scientific and Innovative Research*, 5(2), pp. 46–50.

Singh, N. *et al.* (2015) 'Evaluation of antimicrobial and anticancer properties of finger millet (Eleusine coracana) and pearl millet (Pennisetum glaucum) extracts', *The Pharma Innovation Journal*, 3(11), pp. 82–86.

Singh, S. S. *et al.* (2017) 'Dual role of autophagy in hallmarks of cancer', *Oncogene*. Springer US. doi: 10.1038/s41388-017-0046-6.

Siroha, A. K. and Sandhu, K. S. (2017) 'Effect of heat processing on the antioxidant properties of pearl millet (Pennisetum glaucum L.) cultivars', *Journal of Food Measurement and Characterization*. Springer US, 11, pp. 872–878. doi:

10.1007/s11694-016-9458-1.

Skol, A. D., Sasaki, M. M. and Onel, K. (2016) ‘The genetics of breast cancer risk in the post-genome era: thoughts on study design to move past BRCA and towards clinical relevance’, *Breast Cancer Research*.

Stefan, D. C. (2015) ‘Why is cancer not a priority in South Africa ?’, *SAMJ*, 105(2), pp. 103–104. doi: 10.7196/SAMJ.9301.

Stepanenko, A. A. and Dmitrenko, V. V. (2015) ‘Pitfalls of the MTT assay: Direct and off-target effects of inhibitors can result in over/underestimation of cell viability’, *Gene*. Elsevier B.V., 574(2), pp. 193–203. doi: 10.1016/j.gene.2015.08.009.

Stockert, J. C. *et al.* (2018) ‘Tetrazolium salts and formazan products in Cell Biology: Viability assessment, fluorescence imaging, and labeling perspectives’, *Acta Histochemica*. Elsevier, 120(3), pp. 159–167. doi: 10.1016/j.acthis.2018.02.005.

Su, M., Mei, Y. and Sinha, S. (2013) ‘Role of the Crosstalk between Autophagy and Apoptosis in Cancer’, *Journal of Oncology*, 2013.

Suganyadevi, P., Saravanakumar, K. M. and Mohandas, S. (2013) ‘The antiproliferative activity of 3-deoxyanthocyanins extracted from red sorghum (Sorghum bicolor) bran through P 53 -dependent and Bcl-2 gene expression in breast cancer cell line’, *Life Sciences*. Elsevier Inc., 92(6–7), pp. 379–382. doi: 10.1016/j.lfs.2013.01.006.

Sun, Y. *et al.* (2017) ‘Risk Factors and Preventions of Breast Cancer’, 13. doi: 10.7150/ijbs.21635.

Suter, T. M., Cook-bruns, N. and Barton, C. (2004) ‘Cardiotoxicity associated with trastuzumab (Herceptin) therapy in the treatment of metastatic breast cancer $’, *The Breast*, 13, pp. 173–183. doi: 10.1016/j.breast.2003.09.002.

Suzanne, M. and Steller, H. (2013) ‘Shaping organisms with apoptosis’, *Cell Death and Differentiation*. Nature Publishing Group, 20, pp. 669–675. doi: 10.1038/cdd.2013.11.

Tan, C.-P. *et al.* (2014) 'Metallomics insights into the programmed cell death induced by metal-based anticancer compounds', *Metallomics*, 6, pp. 978–995. doi: 10.1039/c3mt00225j.

Taylor, J. R. N. and Duodu, K. G. (2015) 'Effects of processing sorghum and millets on their phenolic phytochemicals and the implications of this to the health-enhancing properties of sorghum and millet food and beverage products', *Journal of The Science of Food and Agriculture*, 95, pp. 225–237. doi: 10.1002/jsfa.6713.

Ticha, L. A. *et al.* (2015) 'Phytochemical and Antimicrobial Screening of Flavanones and Chalcones from Galenia africana and Dicerothamnus rhinocerotis', *Natural Product Communications*, 10(7), pp. 1185–1190.

Torre, L. A. *et al.* (2016) 'Global cancer incidence and mortality rates and trends - An update', *Cancer Epidemiology Biomarkers and Prevention*, pp. 16–27. doi: 10.1158/1055-9965.EPI-15-0578.

Tšuiko, O. *et al.* (2019) 'A speculative outlook on embryonic aneuploidy : Can molecular pathways be involved ?', *Developmental Biology*, 447(December 2017), pp. 3–13. doi: 10.1016/j.ydbio.2018.01.014.

Valdiglesias, V. *et al.* (2013) 'γH2AX as a marker of DNA double strand breaks and genomic instability in human population studies', *Mutation Research-Reviews in Mutation Research*. Elsevier B.V., 753(1), pp. 24–40. doi: 10.1016/j.mrrev.2013.02.001.

Vallejo, M. J., Salazar, L. and Grijalva, M. (2017) 'Oxidative Stress Modulation and ROS-Mediated Toxicity in Cancer : A Review on In Vitro Models for Plant-Derived Compounds', *Oxidative Medicine and Cellular Longevity*. doi: 10.1155/2017/4586068.

Vanderpuye, V. D. N. K. and Yarney, J. (2014) 'Cost effectiveness of cancer therapies in Africa', *Journal of Medical Diagnostic*, 3(1), pp. 10–12. doi: 10.4172/2168-9784.1000e108.

Verhoeckx, K. *et al.* (2015) *The Impact of Food Bioactives on Health In Vitro and Ex Vivo models*.

Viswesh, V., Gates, K. and Sun, D. (2010) ‘Characterization of DNA Damage Induced by a Natural Product Antitumor Antibiotic Leinamycin in Human Cancer Cells’, *Chemical Research in Toxicology*, 23(1), pp. 99–107. doi: 10.1021/tx900301r.Characterization.

Vries, F. A. *et al.* (2005) ‘An antifungal active extract from the aerial parts of Galenia africana’, in *11th NAPRECA symposium book of proceedings, Antananarivo, Madagascar*, pp. 123–131.

Waks, A. G. and Winer, E. P. (2019) ‘Breast Cancer Treatment A Review’, *Journal of American Medical Association*, 321(3). doi: 10.1001/jama.2018.19323.

Walsh, C. M. (2014) ‘Grand challenges in cell death and survival : apoptosis vs . necroptosis’, 2(February), pp. 1–4. doi: 10.3389/fcell.2014.00003.

Wang, P., Henning, S. M. and Heber, D. (2010) ‘Limitations of MTT and MTS-Based Assays for Measurement of Antiproliferative Activity of Green Tea Polyphenols’, *PLoS ONE*, 5(4). doi: 10.1371/journal.pone.0010202.

Wang, Z. *et al.* (2018) ‘Using drugs to target necroptosis: Dual roles in disease therapy’, *Histology and Histopathology*, 33(8), pp. 773–789. doi: 10.14670/HH-11-968.

Wonders, K. Y. and Reigle, B. S. (2009) ‘Trastuzumab and Doxorubicin-Related Cardiotoxicity and the Cardioprotective Role of Exercise’, *Integrative Cancer Therapies*, 1(8), pp. 17–21.

Wood, C. D. *et al.* (2009) ‘Nuclear Localization of p38 MAPK in Response to DNA Damage’, *International Journal of Biological Sciences*, 5(5), pp. 428–437.

Van Wyk, B., De Wet, H. and Van Heerden, F. R. (2008) ‘An ethnobotanical survey of medicinal plants in the southeastern Karoo , South Africa’, *South African Journal of Botany*, 74, pp. 696–704. doi: 10.1016/j.sajb.2008.05.001.

Yang, J. *et al.* (2019) ‘Development of a colorectal cancer diagnostic model and dietary risk assessment through gut microbiome analysis’, *Experimental & Molecular Medicine*. Springer US, 51(10), pp. 1–15. doi: 10.1038/s12276-019-0313-4.

Zhang, L., Liu, R. and Niu, W. (2014) ‘Phytochemical and Antiproliferative Activity of Proso’, *PLoS ONE*, 9(8). doi: 10.1371/journal.pone.0104058.

Zhang, X., Yang, H. and Zhang, R. (2019) ‘Challenges and future of precision medicine strategies for breast cancer based on a database on drug reactions’, *Bioscience Reports*, 39, pp. 4–13.

Zucca-matthes, G., Urban, C. and Vallejo, A. (2016) ‘Anatomy of the nipple and breast ducts’, *Gland Surgery*, 5(5), pp. 32–36. doi: 10.3978/j.issn.2227-684X.2015.05.10.

Appendix

1. Recipes

1.1. Western blotting

1.1.1. Laemmeli Buffer (2x boiling blue buffer)

1M Tris-Cl (pH 6.8)	1.25ml
10% SDS	4ml
B-mercaptoethanol	1ml
Glycerol (100%)	2ml
dH_2O	1.75ml
Bromophenol blue	Spatula tip

1.1.2. Running buffer (10x)

Glycine	144g
Tris base	30g
SDS	10g

Make up to 1L in dH_2O

Dilute 10x buffer stock to 1x buffer using dH_2O as follows:

10x stock	100ml
dH_2O	900ml

1.1.3. Transfer buffer

Glycine	144g
Tris base	30g

Make up to 1L in dH_2O

Dilute 10x buffer stock to 1x buffer using dH_2O

10x stock	100ml
Methanol	200ml
dH_2O	700ml

1.1.4. Resolving gels

Gel % acrylamide	**6%**		**8%**		**10%**		**12%**		**15%**	
Total volume	5ml	10ml	10ml	20ml	10ml	20ml	10ml	20ml	10ml	20ml
H_2O	2.9ml	5.8ml	5.3ml	10.6ml	4.8ml	9.6ml	4.3ml	8.6ml	3.5ml	7ml
40% acrylamide	750ul	1.5ml	2ml	4ml	2.5ml	5ml	3ml	6ml	3.8ml	7.6ml
1.5M Tris (pH 8.8)	1.25ml	2.5ml	2.5ml	5.0ml	2.5ml	5.0ml	2.5ml	5.0ml	2.5ml	5.0ml
10% SDS	50ul	100ul	100ul	200ul	100ul	200ul	100ul	200ul	100ul	200ul
10% APS	50ul	100ul	100ul	200ul	100ul	200ul	100ul	200ul	100ul	200ul
TEMED	5ul	10ul	10ul	20ul	10ul	20ul	10ul	20ul	10ul	20ul

1.1.5. Stacking gels

Gel % acrylamide	4%	
Total volume	8ml	4ml
H_2O	5.8ml	2.75ml
40% acrylamide	1ml	650ul
1.5M Tris (pH 6.8)	1ml	500ul
10% SDS	80ul	40ul
10% APS	80ul	40ul
TEMED	8ul	4ul

1.1.6. 1.5M Tris (pH 8.8) (for resolving gels)

Dissolve 181.65g tris base in 800ml dH_2O
Adjust pH to 8.8 with concentrated HCl
Fill up to 1L with dH_2O
Store at 4°C

1.1.7. 1.5M Tris (pH 6.8) (for staking gels)

Dissolve 181.65g tris base in 800ml dH_2O
Adjust pH to 6.8 with concentrated HCl
Fill up to 1L with dH_2O
Store at 4°C

1.2. MTT assay

1.2.1. MTT reagent

5mg/ml MTT in sterile filtered PBS:
Dissolve 100mg MTT in 20ml PBS
Incubate at 37°C for 15 minutes

Filter solution through 0.2µM filter
Wrap in foil and store at 4°C

1.2.2. Solubilisation buffer

10% SDS in 0.01M, non-sterile:
Dissolve 25g of SDS in 250ml dH_2O
76.6µl concentrated HCl

1.3. Mycoplasma staining

1.3.1. Mounting fluid

20mM citric acid
55mM $Na_2HPO_4 \cdot 2H_2O$
50% glycerol
pH to 5.5
Store at 4°C

1.4 Clonogenic assay

1.4.1. 0.5% Crystal violet staining solution

For 100ml:
0.5g crystal violet
100ml 100% methanol
Store at room temperature
20mM citric acid
55mM $Na_2HPO_4 \cdot 2H_2O$
50% glycerol

1.5. 10x Phosphate buffered saline (PBS)

For 2L:

160g NaCl

4g KCl

28.8g Na_2HPO_4

4g KH_2PO_4

pH to 7.4

Make up to 2L using dH_2O

For use, dilute down to 1x (100ml 10xPBS + 900ml dH_2O)

1.6. 10x Tris buffered saline (TBS)

For 1L:

60.5g Tris-base

87.6g NaCl

pH to 7.6

Make up to 1L using dH_2O

For use, dilute down to 1x (100ml 10xTBS + 900ml dH_2O)